SOLUBILIZATION OF MEDIUM-CHAINED ALCOHOLS IN SOME ENORDET^{TM} O SERIES SURFACTANTS

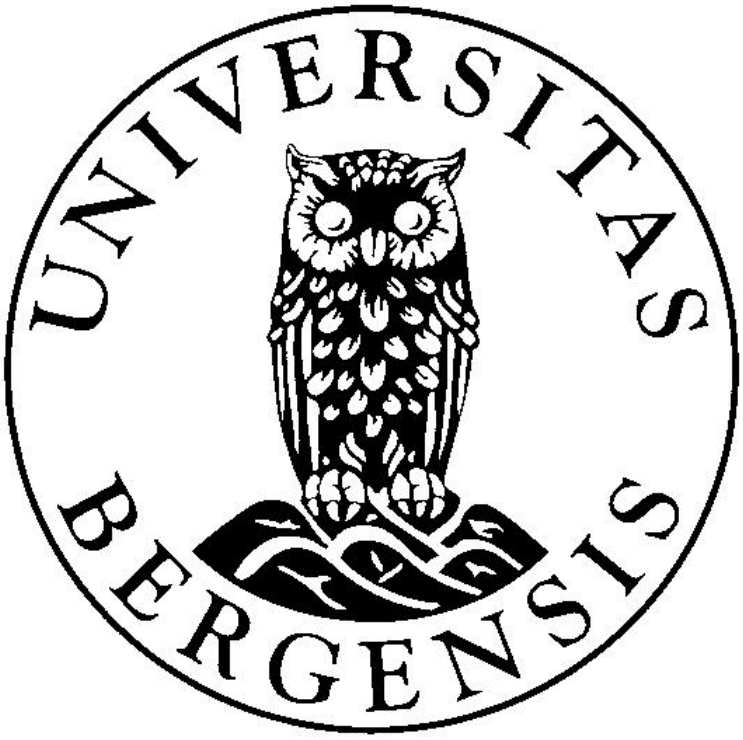

Master Thesis in Physical Chemistry

Daniel Sævland

Department of Chemistry

University of Bergen

October 2013

Acknowledgements

Bergen, 07.10.2013

Arbeidet ble påbegynt høsten 2011 ved Senter for Integrert Petroleumsforskning (Uni CIPR) ved Universitetet i Bergen, og redusert til 50 % fra vår 2013 i kombinasjon med fulltidsansettelse i M-I SWACO, Schlumberger.

Jeg vil først og fremst takke prof. dr. philos. Harald Høiland for veiledning og formelle, samt uformelle diskusjoner om fagemnet. En spesiell takk til overingeniør dr. philos. Einar Høgseth for hans tid fra pensjonisttilværelsen for bistand med ultralydapperaturen, og til de som tok seg tid til å gjennomgå- og gi verdifull tilbakemelding på det endelige utkastet. En generell takk går til forskere, phd-kandidater, masterstudenter og administrasjon ved Uni CIPR for et inspirerende og tilrettelagt arbeidsmiljø. Takk til venner og familie generelt, for støtte og inspirasjon.

Daniel Sævland

Abstract

Primary to tertiary pentanol and -hexanol in Shell Chemicals' ENORDET O series IOS 1923, and for primary pentanol in IOS 2024, have been investigated by a thermodynamic approach. Standard partial molar volume and isentropic compressibility in micellar phase, as well as mole-fraction based distribution, are determined and used for interpretation. The experimental part of this investigation include determining density and speed of sound in various concentration of alcohol and surfactant in water.

Standard partial molar properties reveal presence of mixed hydrophilic-hydrophobic interactions for alcohols in micellar phase of IOS. Distribution for alcohols is less in both IOS surfactants compared to reported values of SDS, and results suggest solubilized alcohols are on average experiencing a less hydrophobic environment in IOS 1923 compared to in SDS. The contrary is observed for 1-pentanol solubilized in IOS 2024, where the average solubilization environment seem more hydrophobic relative to in SDS. These observations may, at least in parts, be reasoned by considering the nature of the IOS surfactants.

Substituting hydroxyl group from primary to tertiary position on pentanol and on hexanol in IOS 1923 reveal some similarities with trends observed in SDS. However abnormalities are observed.

Variation in solubilization parameters among IOS 1923 and IOS 2024 does not correspond well with observations of varying surfactant chain length in model surfactants, and may be due to dissimilarities in IOS samples overriding this effect.

List of Tables

List of Figures

List of Symbols and Abbreviations

$\%H$ Relative humidity of air in %

α Fraction of additive in micellar pseudophase

α_{ma} Fraction of additive in micellar pseudophase (mass action model)

β Degree of dissociation of micellized surfactant

ΔG_t Free energy of transfer of additive from aqueous to micellar pseudophase

ΔK_2^o Transfer contribution to isentropic standard partial molar compressibility of additive from aqueous to micellar pseudophase

ΔV_2^o Transfer contribution to standard partial molar volume of additive from aqueous to micellar pseudophase

ΔY_2^o Transfer contribution to standard partial molar property of additive from aqueous to micellar pseudophase

ΔY_m Micellization property at cmc

η Number of periods

$\kappa_{S,0}$ Isentropic compressibility coefficient for pure solvent corresponding to sample

κ_S Isentropic compressibility coefficient

κ_T Isothermal compressibility coefficient

λ Fractional increase

$\mu_{2,Aq}$ Chemical potential of additive in aqueous phase

$\mu_{2,mic}$ Chemical potential of additive in micellar pseudophase

ν Degree of dissociation of unmicellized surfactant

ρ Density of sample

ρ_{air} Density of air

ρ_o Density of pure solvent corresponding to sample

τ Period of oscillation containing sample

τ_o Period of oscillation containing pure solvent corresponding to sample

A Apparatus constant (densiometry)

a Overshoot time (ultrasound velocimetry)

B Apparatus constant (densiometry)

b Regression coefficient(s)

C_P Isobaric heat capacity

D Transit distance for compression wave

E Expandability

f Frequency of oscillation

G Gibb's free energy

K Distribution coefficient (general)

k Spring constant

K^* Molar Compressibility

$K^o_{2,Aq}$ Isentropic standard partial molar compressibility of additive in aqueous phase

$K^o_{2,mic}$ Isentropic standard partial molar compressibility of additive in micellar pseudophase

K^o_2 Isentropic standard partial molar compressibility of additive

K^o_ϕ Isentropic standard apparent molar compressibility of additive

K^o_ϕ Isentropic standard apparent molar compressibility of additive

K^o_X Standard mole fraction-based distribution coefficient between aqueous and micellar pseudophase

$K^T_{2,Aq}$ Isothermal standard partial molar compressibility of additive in aqueous phase

$K^T_{2,mic}$ Isothermal standard partial molar compressibility of additive in micellar pseudophase

K^T_2 Isothermal standard partial molar compressibility of additive

K_2 Isentropic partial molar compressibility of additive

K_ϕ Isentropic apparent molar compressibility of additive

K_b Binding constant (mass action model)

K_S Setchenov's constant

K_X Mole fraction-based distribution coefficient between aqueous and micellar pseudophase

$m^*_{S,Aq}$ Molal concentration of unmicellized surfactant in absence of additive

$m_{2,Aq}$ Molal concentration of additive in aqueous phase

$m_{2,mic}$ Molal concentration of additive in micellar pseudophase

M_2 Molecular weight of additive

m_2 Molal concentration of additive

$m_{S,Aq}$ Molal concentration of unmicellized surfactant

$m_{S,mic}$ Molal concentration of micellized surfactant

m_S Molal concentration (total) of surfactant

m_w Molal concentration of water

n_1 Moles of solvent

$n_{2,Aq}$ Moles of additive in aqueous phase

$n_{2,mic}$ Moles of additive in micellar pseudophase

n_2 Moles of additive

n_i Moles of component i

$n_{S,Aq}$ Moles of unmicellized surfactant

$n_{S,mic}$ Moles of micellized surfactant

n_w Moles of water

P Pressure

R Ideal gas constant

T Temperature

t Transit time of compression wave (general)

t_w Transit time of compression wave in water

t_x Transit time of compression wave in sample

u Velocity of compression wave (general)

u_w Velocity of compression wave in water

u_x Velocity of compression wave in sample

V Volume

V^* Molar Volume

$V^o_{2,Aq}$ Standard partial molar volume of additive in aqueous phase

$V^o_{2,mic}$ Standard partial molar volume of additive in micellar pseudophase

V^o_2 Standard partial molar volume of additive

V^o_ϕ Standard apparent molar volume of additive

$V_{2,Aq}$ Partial molar volume of additive in aqueous phase

$V_{2,mic}$ Partial molar volume of additive in micellar pseudophase

V_2 Partial molar volume of additive

V_ϕ Apparent molar volume of additive

w Mass of hollow tube

$X_{2,Aq}$ Mole fraction of additive in aqueous phase

$X_{2,mic}$ Mole fraction of additive in micellar pseudophase

Y Overall property of system

Y^* Molar Property

Y^*_1 Molar property of pure solvent

$Y^o_{2,Aq}$ Standard partial molar property of additive in aqueous phase

$Y^o_{2,mic}$ Standard partial molar property of additive in micellar pseudophase

$Y^o_{2,w}$ Standard partial molar property of additive in pure water

Y^o_{2-1} Additive-solvent interaction contribution to standard partial molar property of additive

Y^o_2 Standard partial molar property of additive

$Y_{1,int}$ Intrinsic contribution from solvent to overall molar property

$Y_{2,Aq}$ Partial molar property of additive in aqueous phase

$Y_{2,int}$ Intrinsic contribution to partial molar property of additive

$Y_{2,mic}$ Partial molar property of additive in micellar pseudophase

$Y_{2,w}$ Partial molar property of additive in pure water

$Y_{2/1}$ Additive-solvent interaction parameter (McMillan-Meyer)

Y_2 Partial molar property of additive

Y_ϕ Apparent molar property of additive

$Y_{i,int}$ Intrinsic contribution from component i to overall molar property

Y_{i-j} Interaction contribution between components i and j to overall molar property

Y_i Partial molar property of component i

$Y_{S,Aq}$ Partial molar property of unmicellized surfactant

$Y_{S,mic}$ Partial molar property of micellized surfactant

cmc Critical micelle concentration

CTAB Cetyltrimethylammonium bromide

DeTAB Decyltrimethylammonium bromide

DTAB Dodecyltrimethylammonium bromide

ENORDET Enhanced Oil Recovery Detergents

IFT Interfacial Tension

IOS Internal Olefin Sulfonates

IUPAC International Union of Pure and Applied Chemistry

LC-MS Liquid Chromatography - Mass Spectrometry

NMR Nuclear Magnetic Resonance

OABr Octylammonium hydrobromide

PEO Pulse-Echo-Overlap

SANS Small Angle Neutron Scattering

SDS Sodium dodecyl sulfate

TTAB Tetradecyltrimethylammonium bromide

UV/VIS Ultraviolet/Visible

Contents

1 Introduction

1.1 Project Aim

This study was initiated in attempt to get a better understanding of the solubilization properties of the ENORDET^{TM} O Series internal olefin sulfonate (IOS) 1923 and IOS 2024 surfactants, with a focus on medium-chained alcohols (pentanols and hexanols) as solubilizates. Solubilization of these additives (solubilizates) is well described in model surfactant systems, meaning systems where the surfactant species exhibit the traditional ≪tadpole≫ structure. Much less is however documented on solubilization in commercial surfactant systems, which are often incompletely refined in order to remain profitable, constituted of a diversity of surfactant species and containing impurities. This is contrary to model surfactants, which are often highly refined by the manufacturer, and can be distributed in almost pure grade.

A thermodynamic approach presented here is somewhat simplified compared to the one described in papers by De Lisi et al. [1, 2]. For the interested reader, important simplifications and distinctions between the two approaches have been briefly summarized in Appendix A. Standard partial molar volume and isentropic compressibility in the micellar environment, as well as the distribution of additive, have all been determined simultaneously by applying densiometry, ultrasound velocimetry, and treatment of those data. All investigations have been performed at 25 ^oC and under atmospheric pressure. Transfer contribution to standard partial molar properties for each individual alcohol from pure water to micellar pseudophase have also been evaluated and presented, allowing further insight into the solubilization processes in aqueous surfactant solutions.

Regarding the additive, structural variation of alcohol have been of primary interest. Implications of both variation in the alkyl chain length (pentanols and hexanols) and location of the hydroxyl group (primary to tertiary) have been investigated in IOS 1923. Investigation was also performed regarding 1-pentanol in IOS 2024, mainly to observe implications of varying surfactant chain length of IOS[1]. To treat the additive-surfactant-water ternary system and its distribution of additive, a phase separation model is introduced, in which the micellar interior is treated as a separate phase complementary to the aqueous phase. This micellar pseudophase have properties similar to a macroscopic bulk phase.

There is an issue regarding distribution, as the molecular weight of the surfactant is not known

[1]IOS 2024 are specified with longer olefin chains (on average), see section 1.2 for details.

for the specific batches which have undergone investigation. Distribution will be presented on molecular weight basis by using average molecular weight of the surfactant, specified in paper by Barnes et al. [3]. This basis is necessary for direct comparison of distribution in similar additive-surfactant-water systems. An attempt will be made to evaluate the effect of the average molecular weight of surfactant being subjected to ambiguity.

1.2 Shell ENORDET ™ O Internal Olefin Sulphonates (IOS)

Shell Chemicals have developed and distributes a series of internal olefin sulfonates (IOS) to be used for enhanced oil recovery. These are marketed under the trade name ENORDET ™ O, ENORDET being short for ENhanced Oil Recovery DETergents [4], and «O» specifying the group of internal olefin sulfonates. The product series are results of sulfonation, neutralisation and hydrolysis with high molecular weight internal olefins and gaseous sulfonate as main reagents [3]. Detailed description of the reaction scheme and manufacturing process is presented in paper by Barnes et al. [3]. The internal olefin where sulfonation occurs is randomly positioned on the alkyl chain. This, in combination with the numerous different reactions involved in the three-step manufacturing process, results in a complex mixture of varying species of twin-tailed surfactants [3]. The main generic structures of these mixtures are presented in Figure 1.1 [5]. Zhao et al. [6] have also provided space filling molecular structures of $C15$ alkene sulfonate and hydroxyalkane sulfonate in their approximate proper (twin-tailed) configurations, using energy minimization software. The models are presented in Figure 1.2 [6].

A categorisation within the IOS series, and also the determining factors for the end composition, can be based on two main groups of variables; feedstock properties and sulfonation (or process) conditions [3]. The former group include relative branching and approximate carbon number range of olefin chains and average molecular weight of surfactant. The latter group include SO_3 to olefin ratio and temperature of «cooling water» used during the manufacturing. Products are made with four different olefin cuts, with approximate carbon number ranges C15-18, C19-23, C20-24 and C24-28 [3]. This is specified in the 4-digit number following «IOS». Thus, IOS 1923 and IOS 2024 have approximate carbon number ranges 19 to 23 and 20 to 24, respectively. The remaining variables, except for molecular weight, are specified with one of either two settings, namely high and low. The resulting composition for each of the individual

batches, having been characterised from liquid chromatography coupled with mass spectrometry (LC-MS), is specified in relative abundance of hydroxyalkane sulfonate, alkene sulfonate and di-sulfonate [3]. On average, IOS have a typical composition of $50 - 80$ % hydroxyalkane sulfonates, $15 - 50$ % alkene sulfonates and ca. $1 - 7$ % disulfonate species [3]. Sodium sulfite and «free oil» are also identified and specified as impurities [3]. Included in the term «free oil» is unreacted olefin due to decomposition of intermediate β-sultone, resulting from lack of mass transfer in the neutralisation step in the manufacturing. Sodium sulfite is also a result of decomposition reactions [3].

All these results of pilot scale IOS samples are summarised in Figure 1.3 [3]. Notice that $wt\%$ free oil and sodium sulfite in Figure 1.3 are given relative to 100 % active surfactant.

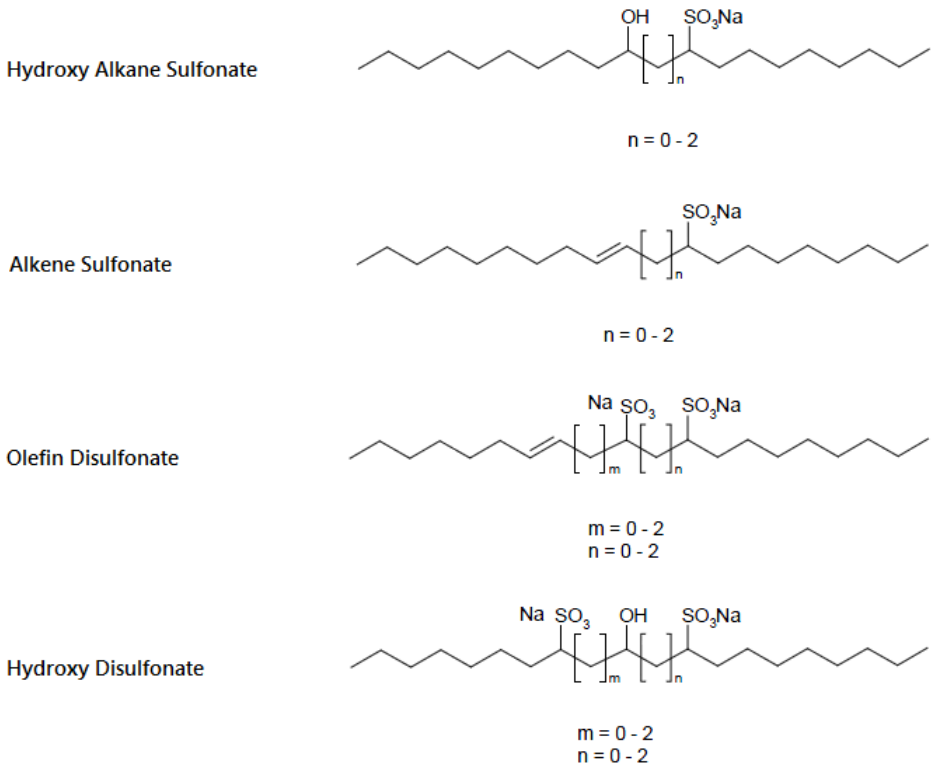

Figure 1.1: Main generic structures of internal olefin sulfonates (IOS), taken from Barnes et al. [5]. Notice the twin-tailed structure of the internal olefin sulfonates, and also the presence of hydroxyl group on hydroxyalkane sulfonate and hydroxydisulfonate. The possibility to vary m and n provide additional freedom for generating a diverse mixture of surfactant species.

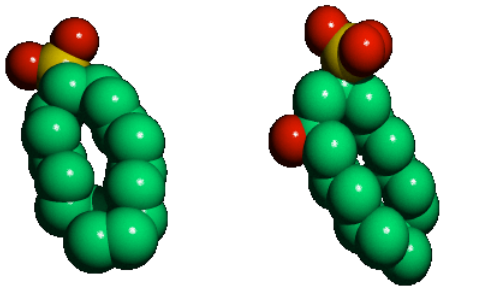

Figure 1.2: Space filling-model of IOS C15 alkene sulfonate (left) and hydroxyalkane sulfonate (right) from Zhao et al. [6]. The configurations have been obtained by energy minimization software. Hydrogen is not represented, while green, yellow and red corresponds to carbon, sulphur and oxygen, respectively.

	IOS 15-18 (Low SO3)	IOS 20-24 (Low SO3)	IOS 20-24 (High SO3)	IOS 19-23 (Low SO3)	IOS 19-23 (High SO3)	IOS 24-28 (Low SO3)
Feedstock:						
Carbon Number Range (approximate)	15-18	20-24	20-24	19-23	19-23	24-28
Molecular Weight (average)	232	287	287	295	295	378
Realtive branched content	low	low	low	high	high	high
Sulfonation conditions:						
Molar ratio SO3/olefin	low	low	high	low	high	low
Cooling water temp. (°C)	low	low	low	low	low	high
Properties#:						
Free Oil (%w)	3.1	11.2	5.9	11.4	8.4	13.0
Na_2SO_4 (%w)	3.1	5.5	7.4	8.2	11.2	9.1
% Active (%w)	33.4	28.3	31.4	33.1	36.3	28.3
Composition by LC-MS:						
Hydroxyalkane sulphonate (% abundance)	81	75	73	64	56	51
Alkene sulphonate (% abundance)	18	24	26	32	37	47
Di-sulphonates (% abundance)	0.5	0.3	0.7	4.0	7.0	1.8

#Free Oil and Na_2SO_4 are reported relative to 100% active surfactant

Figure 1.3: Properties of pilot scale IOS samples, taken from Barnes et al. [3]. Relative branching is determined by ^{13}C nuclear magnetic resonance (NMR) spectroscopy [3]. Notice that $wt\%$ free oil and Na_2SO_3 are given relative to 100 % active surfactant.

Some important criteria for selecting a commercial surfactant include low retention, compatibility with polymer to be used and with hard water, thermal and hydrolytic stability, acceptable cost/performance relationship, environmental friendliness and commercial availability in sufficient quantities (with consistent properties) [5]. The primary criteria however, is to provide ultra low interfacial tension (IFT) for maximizing recovery [5]. For optimum performance, the surfactant needs to be tailored to meet specific, and more frequently in recent years, difficult reservoir conditions. In other words, the surfactant should be applicable over different temperatures, salinities and crude oil compositions, which are characteristic properties of any

given reservoir. The freedom to vary olefin length, SO_3 to olefin ratio and degree of branching provide means for choosing a unique mixture for ultra low IFT under various conditions [5]. Phase behaviour tests with different IOS types confirm their applicability over a wide range of salinities and give high oil solubilization at optimal salinity [5]. The thermal stability of the sulfonate group make the series promising for very high-temperature reservoirs (up to 150 ^oC) [5], and a small temperature sensitivity on solubilization can be considered a positive feature for reservoirs with temperature gradients [5]. More molecular flexibility is allowed compared to many other surfactants, as the twin-tailed structure and the diversity of surfactant species give a lesser tendency to form ordered liquid crystal structures and gels [5, 6]. This ordering would result in unfavourable viscous phases, hindering effective transport of surfactant flood and oil bank through the reservoir [6, 7]. The great diversity of IOS species have also shown to increase solubilizing capacity of complex crude compositions, and high molecular weight IOS aid in excellent performance with high viscous, high wax content crude oils, as well as with light oils [6]. High molecular weight IOS also exhibited good performance at low concentrations and are shown well compatible with both alkali such as sodium carbonate and polymers when used with appropriate co-solvents [6]. Shell Chemicals have shown to further optimalise IFT and phase behaviour performance by combining IOS products with differing olefin intervals (mixture of IOS 1518, IOS 2024 and IOS 2428) [5].

Co-surfactants can be combined with IOS to further alternate optimal salinity and performance of the surfactant slug [6]. The surfactant need to remain as a single phase and not exhibit significant precipitation over time, which can prove difficult for IOS which are highly hydrophobic, and especially in high salinity reservoirs [5]. This can however be resolved in various extent by adding co-surfactants, which aid in keeping the IOS soluble at these conditions [5]. Co-solvents/co-surfactants are also combined with IOS to increase aqueous solubility, prevent or reduce formation of gel, liquid crystals and macroemulsions, and to promote rapid phase equilibration [5, 6, 7, 8]. Co-surfactants also generally aid in limiting adsorption of surfactant on the reservoir rock, thus reducing retention and, therefore, total amount of surfactant required [8] to flood the reservoir section(s). The transport and handling at well site is also eased by lowering viscosity and pour point [3].

1.3 Solubilization

One of the early definitions of solubilization was given by Merrill and McBain in 1942 as the spontaneous passage of insoluble matter into a thermodynamically stable solution [9, 10, 11, 12,

13]. This definition is general and just as applicable today. Succeeding definitions are similar but may specify the presence of micelles or other types of aggregates, including compounds which already have a significant solubility in water [9, 11, 14]. The International Union of Pure and Applied Chemistry, more commonly known as IUPAC, presents the following definition of micellar solubilization: "In a system formed by a solvent, an association colloid and at least one other component (the solubilizate), the incorporation of this other component into or on the micelles is called micellar solubilization, or, briefly, solubilization" [15]. The importance of solubilization can be seen in its many commercial applications, in addition to enhanced oil recovery, including pharmaceuticals, detergency, cosmetics and micellar catalysis, just to name a few [1, 9, 16].

This subsection is devoted to give a very brief and broad overview of preceding work and current knowledge of the field, with a special focus on medium-chained alcohols (butanol to octanol) as the solubilizate (additive) in micellar solution. It should be highlighted that the process of solubilization is neither confined to micelles or just one type of additive present in the system. The systems concerned contains three components; water, surfactant(s) and additive(s), and are collectively termed «ternary systems». Solubilization in reversed micelles where the continuous phase is apolar will not be concerned here, although given significant attention in the literature.

1.3.1 History

Solubilization is the pioneering subject within the empirical facts of colloid science [17]. References of observations that can clearly be recognised as solubilization dates as far back as the second half of the 19th century [11, 17] when Persoz observed increased solubility of partially soluble compounds in soap solution [9, 11]. Many of these studies were indeed focused on the solubilizing power of soap solutions [17]. Engler et al. made several important discoveries by studying solubility of paraffins in water and the effects of adding phenol and aromatic compounds [17]. Even though they relied on visual observation, they determined that solvent action was enhanced by (1) increasing chain length of the paraffin, (2) addition of corresponding acid, and that solvent action was decreased by (3) addition of excess alkali or carbonate [17]. Solubilizing agents were well known in the commercial world at the beginning of the 20th century, even though the mechanisms were not yet understood [17]. McBain, Beedle and Bolam and Smith suggested some sort of a sorptive process [17]. Pickering explained the solvency of soap solutions as a complex formation reaction [17].

Results from McBain and McBain obtained in 1936 lead to the important conclusion that the components of the solution are in a thermodynamically stable equilibrium and are reproducible and independent of previous history [17]. McBain and Woo also pointed out that solubilization is a unique process, distinct from related processes such as peptization, protective action and hydrotropy [17].

Microscopic characterisation of organised micelles were revealed by x-ray experiments on concentrated soap solutions [9, 17]. Hartley had already suggested incorporation in spherical, prolate or rod-like micelles where the polar head groups are exposed to surrounding solution, but this idea was opposed by McBain in support of lamellar micelles or "sandwich" structures[2] [9, 10, 17, 18]. Two solubilization regions can be recognised from the micelle, namely the inner core and the outer palisade layer. Extensive x-ray studies showed that apolar compounds like alkanes reside in the micellar core and polar compounds like alcohols reside in the palisade layer of the micelle [10, 17]. The studies also revealed the presence of water in the micellar interior [17]. Interior regions, including the micellar surface, are illustrated in Figure 1.4 [19].

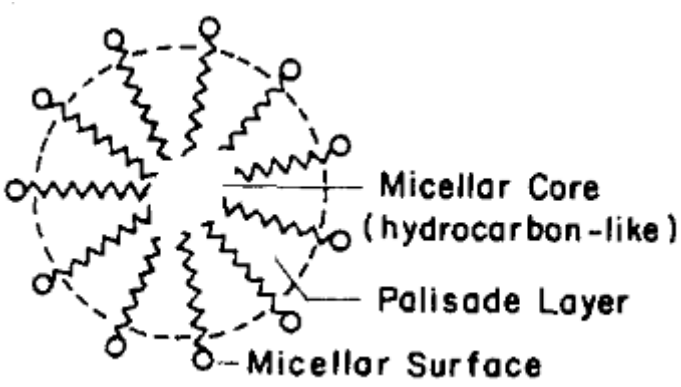

Figure 1.4: Regions recognised in the interior of micelles, being the micellar core region and the surrounding palisade layer. The micellar surface is also highlighted in the figure. The figure is taken from Valsaraj et al. [19] and is edited by author.

Early studies of solubilization have been reviewed [9, 11, 20] extensively in the mid 20th century in papers by McBain and by Klevens (1950) [10], as well as in books by McBain and Hutchinson (1955) [17] and by Elworthy, Florence and Macfarlane (1968) [21]. These papers and books give a detailed description of effect on solubilization with both varying nature and structure of additive and surfactant, temperature and presence of additives such as electrolytes [9, 10]. Although, there still seem to be debate regarding the mechanism of solubilization in these reviews [10, 17]. It is recognised that factors affecting solubilization include type and

[2]Very short lamellar sheet which have same order of dimensions both vertically and horizontally

nature of solubilizer (chain length, substitution, location- and type of hydrophilic group), type and nature of additive (chain length, cyclisation, unsaturation, branching, molar volume, polarity), temperature and presence of different types of additives, including polar compounds and electrolytes [10, 17]. Many of the systems investigated are dyes in soap solutions [10, 17] studied by methods including opacity, spectral methods, vapour pressure, x-ray diffraction and light scattering [9, 10, 12, 17]. McBain and Hutchinson [17] argues issues with these studies, including impurities of chemicals resulting in problems with reproducibility. They also critique the lack of focus on establishing true equilibrium in the systems [17].

By the 1950 and 1960, a general molecular picture of micelles and their solubilizates were emerging [9]. More recently, physical investigations such as small angle neutron scattering (SANS) and fluorescence probe methods have enriched our understanding of the dominating forces and sites of solubilization within different surfactant aggregates [9].

More modern reviews are given in the book by Christian and Schamehorn (1995) [22], and in papers by Høiland and Blokhus (2008) [11] and Miller (2008) [20]. Systems beyond the traditional and application of new methods for investigation, are some of the topics of interest in these reviews. King [23] present studies on solubilization of gases and vapours in micellar solutions. Nishikido [24] investigates solubilization in mixed micelles, i.e. micelles which are composed of more than one type of surfactant. Abe [25] extends the solubilizing medium to include vesicles. Hurter et al. [26] investigates solubilization in solution of block copolymers. Numerous methods of study are summarised and compared in papers by Marangoni et al. [16] and Høiland et al. [11]. These methods include thermodynamic methods, spectroscopic methods, Krafft point depression, vapour pressure method, total solubility method and ultrafiltration [11, 16]. Ward [27] and Miller [20] shifts focus towards kinetics of solubilization rather than only concerning equilibrium conditions.

A literature search[3] for papers concerning solubilization published after 2010 reveals topics such as drug and protein solubilization including solubilization of biomolecules, vesicles, dendrimers, polyaromatic hydrocarbons, nanomaterials, fluorinated surfactants and more. Solubilizers go well beyond regular single-chained surfactants to include systems of mixed surfactants, gemini surfactants and block copolymers, to name some. More or less sophisticated methods of study are applied, some of which are nuclear magnetic resonance (NMR) spectroscopy, SANS, fluorescent methods and ultraviolet/visible (UV/VIS) photospectrometry.

[3]Primo Ex-Libris: *http://primo-service.hosted.exlibrisgroup.com.* Search phrase ≪Solubilization≫

1.3.2 Medium-Chained Alcohols as Solubilizates in Micellar Solution

While hydrophilic alcohols mainly affect the additive-surfactant-water ternary system by modifying properties of the surrounding aqueous solution, more hydrophobic alcohols will associate with the micellar structure [28, 29, 30]. Medium-chained linear or substituted alcohols as solubilizates are good representations of polar additives. Due to their amphiphilic character, these species will generally solubilize in the palisade layer of the micelle with the polar part associated with the micellar surface and the apolar part oriented towards the micellar core [11, 16, 29, 31, 32, 33], creating mixed micelles [34, 35]. At least this is the common view at low additive concentrations [16]. Exhibiting this nature, alcohols are termed co-surfactants, which lack enough amphiphilic character to form micelles themselves[4], but may take the role of a non-ionic surfactant in a micelle [29, 36], thus reducing the critical micelle concentration (cmc) of the system [30, 36, 37]. This cmc reduction mainly is due to two effects [29, 33]: (1) An increase in system entropy upon incorporation of alcohols, due to dehydration of surfactant alkyl chains. (2) As alcohol generally reside between the surfactant monomers, screening of unfavourable electrostatic repulsion between (ionic) surfactant head groups promote micellization. The latter effect result in more dense packing of amphiphiles in the micelles [9]. The polar head groups can be viewed as anchored to the micellar surface [9, 11, 33], although the degree of anchoring is limited for alcohols [11]. Lianos et al. suggests about 2.4 anchored alcohols per surfactant molecule [11]. However, solubility measurements have shown that this amount can be significantly higher [11].

It is argued that solubilization sites for polar additives are dependent on additive concentration. Some authors reason alcohol-swollen micelles, with an alcohol-rich core, to explain a high degree of solubilization at larger concentrations of alcohol [16]. Peculiarities in experimental data at a certain threshold concentration of alcohol may be attributed to a shift in solubilization environment with more hydrocarbon-like properties, which may well be the micellar core [11]. An alternative explanation is that a large amount of alcohol is suddenly solubilized at this alcohol concentration [11]. Høiland et al. [11] base these reasoning on an abrupt change in electrical conductivity and compressibility at a given additive concentration, in addition to large gradient of compressibility at the same alcohol concentration. An initial decrease in distribution towards micelles when introducing polar additives in the system, may be explained in terms of competition for adsorption sites in the palisade layer, even competition with surfactant monomers [9, 11, 38]. This is in turn expected to result in reduced interfacial concentration of

[4] Although alcohols don't form micelles in a strict sense, some invoke the presence of associated alcoholic microaggregates or clusters in water [1, 29], sometimes to explain peculiarities in experimental data [1].

surfactant per unit surface area [38].

Anything regarding the structure of the alcohol that increases the compatibility with oil is expected to increase degree of solubilization as well. This is reasonable since the inner part of micelles can be considered liquid-like with many similarities to bulk hydrocarbon solution [9, 13, 16, 33, 39, 40], which medium to long-chained alcohols have greater affinity for than water. Increasing the chain length of a homologous series, the affinity for oil increases while the affinity for water remains constant [38]. It is likely that this results in an increased degree of penetration into the palisade layer and greater partitioning of the alcohol in the micellar core region [32, 41]. Longer-chained alcohols may extend all the way to the core region of the micelle [11, 29]. Beyond some undetermined chain length, the alcohol exhibits almost fully hydrophobic character [1, 38].

The extent of solubilization is found to increase exponentially with chain length of alcohol [29, 40]. Distribution averaged from different experimental methods show indeed an exponential increase in degree of solubilization going from 1-propanol to 1-heptanol in SDS[5] and going from 1-propanol to 1-hexanol in DTAB[6] [16]. It is also worthwhile to note the large differences in distribution obtained by different methods for the same ternary system, varying almost 10-fold [11, 16]. Among these methods, thermodynamic data generally yield higher values [11, 16]. It has been argued by Marangoni et al. [16] that it is necessary to examine error limits and model assumptions for each individual method in order to explain this scatter of distribution values.

Concerning the location of the hydroxyl group on the alcohol with respect to effects on solubilization, a decrease in solubilization is generally observed for non-terminal alcohols compared to their respective terminal alcohols [11]. Steric effects with respect to incorporation into micelle are likely to contribute to more ineffective packing for non-terminal alcohols compared to their respective terminal analogues.

Physiochemical properties of the micelle (size, shape[7], aggregation number, degree of ionisation) may be affected by the solubilization of a third component. At low additive, surfactant and electrolyte concentrations, the micelle remains nearly spherical [1, 33]. Within this geometry, the solubilized alcohol distributes uniformly in the palisade layer [29]. Increasing the concentration of these components promotes a shape transition to more elongated forms, in which the solubilized alcohol may no longer be uniformly distributed [11, 29, 33]. The elongation of

[5]SDS - Sodium dodecyl sulfate.

[6]DTAB - Dodecyltrimethylammonium bromide.

[7]It is important to beware that micelles are dynamic entities and that general pictures of micelles having well-defined geometrical shapes are to be limited [30].

the micelle is also expected to cause a shift in solubilization by normally causing a decrease in solubilization of polar additives [9, 11, 33]. In addition, the surfactant head groups are expected to pack more densely [9]. Subjected to large degree of solubilization of nonionic additives, the micellar phase may become unstable and a phase transition may result [33]. Concerning the degree of ionisation of ionic surfactants, it is expected to increase with the solubilization of a third component [29, 42]. Zana [29] explains this in terms of reduced surface charge density of the micelle [29], thus releasing ions associated with the micellar surface due to reduced binding capacity. The degree of ionisation is most commonly determined as the ratio of the slope of the conductivity versus additive concentration below and above cmc [43].

The size of the micelle is to a large extent determined by the length of surfactant alkyl chain [44]. When micelles swell upon incorporation, their size may increase an order in magnitude up to 100 nm or more [45]. This high degree of swelling is often facilitated by the incorporation of medium-chain-length alcohols [45]. Fluorescence probe studies by Lianos et al. [46] suggest that the micellar aggregation number is strongly dependent on both the alcohol chain length and branching of alcohols. An increase in aggregation number is generally observed with increasing chain length of alcohol [46]. Also, terminal alcohol generally exhibit larger increase in aggregation number compared to the respective non-terminal analogues [46].

2 Experimental

The apparatuses utilised in this study and their principles of operation are described briefly in this section, alongside with chemicals and preparation of solutions.

2.1 Chemicals & Solutions

The surfactant samples having undergone investigation are labelled ≪ENORDET O342 (Drum # E)≫ and ≪ENORDET O242 AKZOB≫ for the IOS 1923 and IOS 2024 surfactant, respectively. Both were investigated as they were received, without any further purification or processing. Their coincidental composition due to the nature of the manufacturing process makes the batch unique, and it is believed that only this batch is truly representative of the results derived from it. This limits the extent of the investigation to the amount of sample available at hand, because obtaining and investigating a new sample would likely yield results unrepresentative of results obtained from the previous sample.
Useful information concerning the specific IOS samples at hand is limited to percentage active matter (i.e active surfactant) and the approximate carbon number range. In lack of details regarding properties of the two IOS samples, properties are primarily guided by what is reported by Barnes et al. [3] in Figure 1.3. It is obvious however, that this guidance should be followed carefully, and that the specifications presented should be taken as ambiguous as they are.

An analysis set for an individual alcohol in either of IOS surfactants consisted of 4 surfactant-water binary solutions, from which 6 alcohol-surfactant-water ternary solutions were derived. This gives a total of 24 solutions to be investigated for each individual ternary system. IOS 1923 binary solutions were prepared with approximate surfactant concentrations 0.06, 0.12, 0.18 and 0.24 m. Determining sound velocity in solutions containing 0.24 m IOS 2024 revealed peculiar and inconsistent results. It is suggested that this is related to instrument limitations for handling such high concentrations of IOS 2024. A more narrow approximate concentration range was therefore selected for the IOS 2024 binary solutions; 0.06, 0.11, 0.15 and 0.18 m. The 6 additive-surfactant-water ternary solutions were prepared with alcohol concentration in the approximate range 0.05 - 0.25 m.
Prior to preparation, containers were thoroughly washed and successively flushed with distilled water before dried in a heating cabinet. All solutions were prepared on weight basis using deionised and filtrated grade 1+ water from ONDEO Puri1te ® Select, and chemicals

without further purification or processing. All weightings were performed with Mettler Toledo AX205/AE240 analytical balances[8] and Kern EW 1500-2M precision balance to ensure satisfactory accuracy. Both analytical balances were supported on vibration-resistant material to prevent disturbance from the surrounding environment, and were preferred over the precision balance whenever feasible. This meant when performing weightings where the total mass (container + solution) did not exceed the maximum reading of the analytical balances. The total mass was below this limit in all instances, except when adding water in binary solutions. Relevant specifications concerning the balances and chemicals are given in Table 2.1 [47, 48, 49] and Table 2.2, respectively.

Both surfactant samples in their original container segregated over time. IOS 1923 was quite viscous in its original form and were stirred and mildly heated to re-homogenise before transferring to containers. IOS 2024 was relatively non-viscous and was shaken rigorously prior to transferring to containers. When diluting the surfactant, a great amount of foam was created. Destabilisation of this foam was awaited prior to proceeding, and care was taken to minimize degree of refoaming from thereon, especially before actually performing the measurement. Some segregation of solutions of IOS 1923 still occurred in the fully prepared ternary solutions, and these were gently stirred prior to introducing sample to measuring cells.

Table 2.1: Properties of electronic balances. Specifications include maximum reading, readability, repeatability and linearity. These are given among other parameters by the respective manufacturer of the balance [47, 48, 49].

	Mettler Toledo AX205 Analytical Balance	Mettler Toledo AE240 Analytical Balance	Kern EW 1500-2M Precision Balance
Max Reading	220 g	205 g	1500 g
Readability	0.0001 g	0.0001 g	0.01 g
Repeatability	0.00004 g	0.0001 g	0.01 g
Linearity	$\pm$ 0.00015 g	$\pm$ 0.0002 g	$\pm$ 0.02 g

[8]The AX205 and AE240 models were used in preparing solutions of IOS 1923 and IOS 2024, respectively

Table 2.2: Details regarding chemicals, including molecular weight, the name of supplier and the specified purity. Molecular weight of IOS surfactants are given as an average parameter and are specified in paper by Barnes et al. [3].

Species	Molecular Weight $gmol^{-1}$	Supplier	Specified Purity
IOS 1923	295^a	Shell Chemicals	33 wt%
IOS 2024	287^a	Shell Chemicals	23 wt%
1-Pentanol	88.151_8	Sigma-Aldrich	$\geq$ 99 %
2-Pentanol	88.151_8	Sigma-Aldrich	98 %
3-Pentanol	88.151_8	Sigma-Aldrich	98 %
1-Hexanol	102.177_7	Sigma-Aldrich	$\geq$ 99 %
2-Hexanol	102.177_7	Sigma-Aldrich	99 %
3-Hexanol	102.177_7	Sigma-Aldrich	97 %

a - (average), Barnes et al. [3]

2.2 Oscillating-Tube Densiometry

Oscillation type densiometers are one of the most versatile and accurate methods for determining density of fluids [50]. These are highly applicable in our investigation as high accuracy is required for satisfactory determination of partial molar volume and isentropic compressibility. Other advantages of these type of densiometers include short response time, ease of use and only a small amount of sample required to perform the measurement [51, 52, 53]. Density measurements are not provided directly and require regular calibration with density-known fluids, which can be considered one of its disadvantages. Other disadvantages include sensitivity to outer vibrational forces and requirement of fluids to be clean and fairly non-viscous [54].

All density measurements were performed with Anton Paar DMA 602 measuring cell and Anton Paar DMA 60 processing unit. A comprehensive description of the apparatus and principle of operation is given in the operating instructions [55] provided by the distributor. The measuring cell is coupled with a Hetofrig (Heto Birkerød) constant temperature circulator, and the temperature in the measuring cell is measured indirectly from the bath by ASL F250 MKII digital precision thermometer. Sample introduced manually to the measuring cell via syringe to an inlet connected to the lower leg of a hollow u-shaped dual walled glass tube. An outlet is connected to the other leg of the u-tube, providing a continuous path for fluid between the

measuring cell and its surroundings. Illustrations of the measuring cell (right) and processing unit (left) is presented in Figure 2.1 [56]. The in- and outlet where sample is introduced and discharged is shown on the right hand side of the measuring cell in the Figure 2.1.

Figure 2.1: DMA 60 processing unit (left) and DMA 602 measuring cell (right) [56]. The in- and outlet where sample is introduced and discharged is shown on the right hand side of the measuring cell. A constant temperature circulator is connected to the measuring cell (not shown), providing continuous flow of thermostatted water surrounding the u-tube.

The principle of operation is based on the law of harmonic oscillation [51]. This involves measuring the period or frequency of the u-tube. The length of the tube is usually approximately 20 times the tube diameter and contains a middle chamber located between the sample region and the surrounding thermostated jacket of circulating water [54, 55]. This chamber is filled with gas having high thermal conductivity to ensure rapid thermal equilibration between sample and thermostatted water [55]. An additional shorter capillary tube is present inside the measuring cell for accurate determination of the cell temperature by means of a temperature sensor[9] [55]. The two legs of the tube constitute the elastic elements or springs of the oscillator itself, which are electromagnetically exited to vibrate at their natural frequency while the end of the legs are rigidly held in place by the apparatus. As the analytical balances are, the measuring cell is also supported on vibration-resistant material to prevent disturbance from the surrounding environment. A constant volume of 0.7 mL of sample [55] is confined inside the oscillating region of the tubes, however the applied volume is in fact higher due to overfilling in the inlet- and outlet nozzles. The natural frequency of vibration is a function of the body's mass [51]. With a confined volume of sample within the oscillating region and constant mass of the tubes, the frequency is a function of the density of the sample [51]. Introduction of sample will therefore change the system's natural frequency, which is detected electronically with great precision [57]. The remaining instrumentation consists of a system of electronic excitation and electrical components that provide a signal transmission of the period to the processing unit

[9]Not put to use. Temperature was measured indirectly from bath of the constant temperature circulator.

[51]. Schematics of the principle of operation is presented in Figure 2.2 [51].

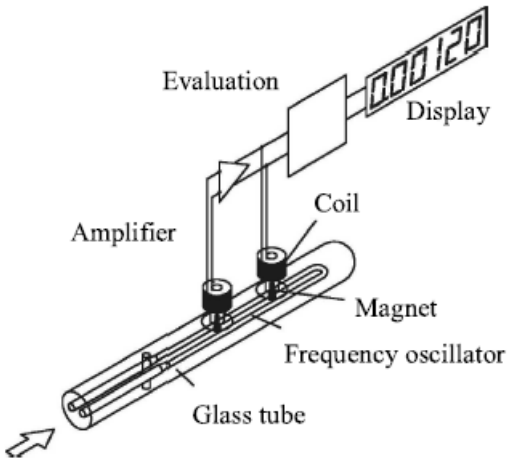

Figure 2.2: Schematics of oscillating-tube density meters [51]. The sample is introduced in a oscillating glass tube, changing the systems natural frequency. The oscillations of the tube are detected electronically with great precision and displayed at the processing unit.

Considering an equivalent system of a hollow body suspended on a spring, the total mass of the vibrating body is given the sum of the mass of the tube and its containing fluid. The natural frequency f is expressed in Equation 2.1, under the assumption of no vibration (i.e. infinite mass) in the object complementary to which the tube is connected to [55].

$$f = \frac{1}{2\pi}\sqrt{\frac{k}{w + \rho V}} \tag{2.1}$$

where k is the spring constant based on Hooke's law, w is the mass of the tube, ρ and V is the density and volume of the sample, respectively. The measured output of the instrumentation is the period of oscillation τ and is given the inverse of the systems natural frequency,

$$\tau = f^{-1} = 2\pi\sqrt{\frac{w + \rho V}{k}} \tag{2.2}$$

The squared of Equation 2.2 is a linear relationship between the period of oscillation and density of sample, where constants A and B are characteristic of the apparatus, introduced for clarification,

$$\tau^2 = A\rho + B \tag{2.3}$$

$$A = \frac{4\pi^2 V}{k} \tag{2.4}$$

$$B = \frac{4\pi^2 w}{k} \tag{2.5}$$

A is determined by measuring the period for two samples with known density (in our case air and distilled water), in which B is eliminated upon differentiation,

$$\rho - \rho_o = A^{-1}(\tau^2 - \tau_o^2) \tag{2.6}$$

When A is known, Equation 2.6 is reapplied with ρ and τ referring to the sample to be investigated, and τ_o and ρ_o referring to a known fluid as reference. Vacuum or dry air could be used as reference. Instead, an alternative approach is taken where atmospheric air is measured, and density is calculated by measuring pressure P, relative humidity $\%H$ and temperature T [58],

$$\rho_{air} = \left(0.46464\ \frac{P - 0.08987 \cdot \%H}{T}\right) \cdot 10^{-3} \tag{2.7}$$

where P, T and ρ_{air} are in units of $mmHg$, K, and gcm^{-3}, respectively.

A is dependent on temperature and slightly dependent on pressure [52], and is not stable over time. The parameter should be adjusted and checked regularly to ensure validity in the determined densities.

The density of fluids is highly dependent on temperature, which should be confined within an interval of $\pm 0.01\ ^oC$ to ensure satisfactory precision [55]. The bath circulator have a estimated maximum temperature deviation of $\pm 0.007\ ^oC$ around 25 ^oC, assuming no error in readings from the digital thermometer. It is therefore believed not to be any additional loss of precision in the obtained densities based on fluctuating temperature. A precision of $\pm 3 \cdot 10^{-6}\ gcm^{-3}$ is induced under this confinement, according to instrument specifications [55]. However, improper filling, inhomogeneities and contamination in sample, instrument drift and general replication error are some of the factors that may results in a larger practical error. $\pm 5 \cdot 10^{-6}\ gcm^{-3}$ is assumed a fair estimate. The fact that the temperature is measured indirectly in the heat bath is not believed to contribute to any loss of accuracy.

The period displayed on the processing unit is determined based on 10000 oscillations which is chosen on the processing unit as one among 6 settings between 1000 and 50000 oscillations. At least 5000 oscillations are believed necessary for satisfactory accuracy in this investigation. The two lesser options available on the processing unit are 2000 and 1000 oscillations.
It is of high importance that the sample is introduced in the tube slowly and continuously to completely wet the glass surface of the tube. Failure to do so may result in trapping of microscopic or macroscopic bubbles resulting in erroneous measurement. This can however be uncovered by the failure of the displayed output period to converge after the sample confined in the u-tube has been properly thermostatted.

The applied procedure for performing density measurements is described in detail in appendix B.1.

2.3 Pulse-Echo-Overlap Ultrasound Velocimetry

All sound velocity measurements were performed with an in-house built combination of various instrumentation to resemble the pulse-echo-overlap (PEO) method for determination of speed of sound in fluids [59]. A detailed description of the instrumentation and PEO method are given in paper by Høgseth et al. [59] and Papadakis [60], respectively. The instrumentation consists of a Parametrics 5053A ultrasonic time intervalometer, ICS Electronics 4864 GPIB relay interface, LeCroy 9386TM 1 GHz oscilloscope, Efratom Division FRK-LN 10 Mhz rubidium oscillator and GW Instek GPS 3030D and LTRONIX B300D power supplies. Measurement input and output are given by and received to the user via the UltraXP6 (computer)software. The rubidium oscillator, with its long-term stability, high precision and sensitivity, is added to the instrumentation to serve as a precision time scale, on which the main time determination is made [59]. Sound velocity in fluids is highly dependent on temperature, and a high precision thermostatting system is required for accurate measurements. The cell is submerged and thermostatted in a LKB Bromma 7600 Precision Thermostat connected to a Hetofig (Heto Birkerød) constant temperature circulator, ensuring temperature deviation within estimated 25.000 ± 0.002^oC. The temperature is measured indirectly from the bath by the same ASL F250 MKII digital precision thermometer used in the densiometer instrumentation. A gold-coated measuring cell of brass, designed by E. Høgseth, is connected to the instrumentation via the ultrasonic time intervalometer. The major components of the cell are a 10 MHz piezo-ceramic transducer, a reflector, a sample chamber and a flexible transparent silicon tube. An

illustration of the measuring cell is presented in Figure 2.3 [61]. The main function of the flexible silicon tube is to equilibrate any excess pressure created during assembly of the cell. The distance between the transducer and reflector is approximately 40 mm [59, 62], and no more than 8 mL of sample is required to properly fill the cell [63]. Block schematics of the instrumental setup of the ultrasound velocimeter is presented in Figure 2.4 [59].

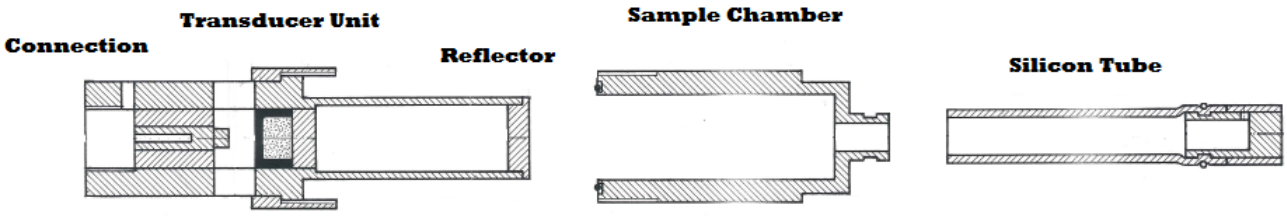

Figure 2.3: Schematics of gold-coated brass cell for measuring sound velocity in fluids [61]. The major components of the cell are a 10 MHz piezoceramic transducer, a reflector, a sample chamber and a flexible transparent silicon tube. The figure is edited by author.

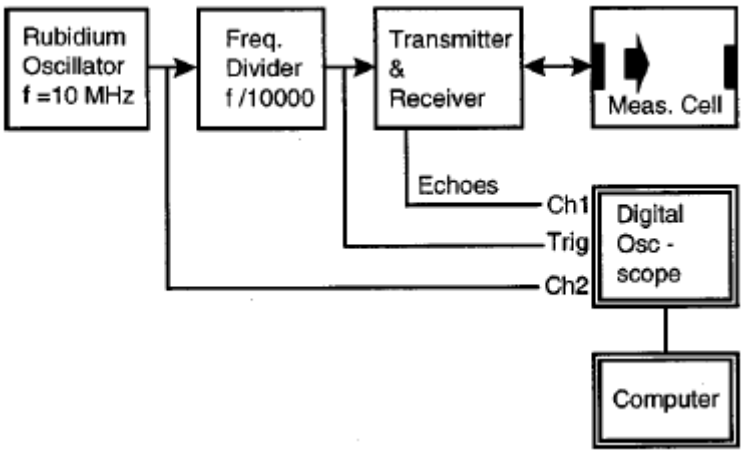

Figure 2.4: Block schematics of instrumental setup of the rubidium clock sound velocity meter [59]. The measuring cell is connected via the ultrasonic time intervallometer. Measurement input and output are given by and received to the user via the UltraXP6 software. The rubidium oscillator is added to the instrumentation to serve as a precision time scale, on which the main time determination is made.

When supplied with electric voltage, a short sound pulse is generated from the transducer [64]. The frequency of this pulse is as high as 5 Mhz and lies in the ultrasonic region of the

acoustic spectrum [61]. The generated pulse propagate back and forth between transducer and reflector is repeated as a series of diminishing echoes, and is both transmitted and received at the transducer, making the flight distance two times the distance between the transducer and reflector [59, 64]. Transit time t can be expressed as the product of number of periods η and the period of the sound wave τ, plus an overshoot time a due to electronic delay within the instrumentation [59],

$$t = \eta\tau + a \tag{2.8}$$

Høgseth et al. [59] presents the maximum overshoot time as 100 ns and an average transit time between successive echoes of typically around 50 μs, making the overshoot time in order of $1 : 500$. The transit time in a fluid is determined as the time between subsequent echoes of the ith and $(i+1)$th pulse, which equals the two way propagation time,

$$t = (\eta_i\tau + a_i) - (\eta_{(i+1)}\tau + a_{(i+1)}) \tag{2.9}$$

Numerous pulses act to give proper time estimations based on replicate measurements and can be selected in the UltraXP6 software as any integer.

As the transit time through a sample is given as output, only the path length D is required for velocity determination. Calibration measurements of pure water, to which known sound velocities exists [65], are performed to obtain a proper estimation of the path length D. The path length is given as the product of sound velocity in water u_w and the measured transit time t_w,

$$D = u_w t_w \tag{2.10}$$

The sound velocity in the sample fluid is then readily expressed relative to calibration results,

$$u_x = \frac{D}{t_x} = \frac{u_w t_w}{t_x} \tag{2.11}$$

where u_x and t_x refers to sound velocity and transit time of sample to be investigated.

It is of high importance that the cell is properly thermostatted prior to reading measurements. This can be ensured by lack of drift in transit time when performing replicate measurements. Reis et al. [63] measured the transit time in surfactant solutions at 25 ^oC after 20 minutes and again after another 10 minutes, and found no significant drift in values between the two replicates. This is for the same instrumentation used in this investigation. This suggests that 20 minutes of thermostatting is sufficient for proper equilibration between heat bath and sample. Høgseth et al. [59] have empirically estimated the precision of u to be within $\pm 0.005\ ms^{-1}$ for dilute aqueous solution of triglycine, pentaglycine and pure water [59]. This will be dependent of both instrumentation as well as type of sample, and other factors. In our case, the precision will probably depend on surfactant and alcohol concentrations as well. Precision is experimentally estimated to be $\pm 0.03\ ms^{-1}$ throughout this investigation.

The applied procedure for performing sound velocity measurements is described in detail in appendix B.2.

3 Methods

3.1 Phase Separation Model (Pseudophase Model) for Treating Solubilization

There is no doubt that ternary systems containing additive(s), surfactant(s) and water are highly complex. However, simple thermodynamic models can give less refined treatment of systems, but can be applied with minor effort and in some instances provide analytical results [66]. The simplest model for treating distribution of additive in micellar solution is the phase separation model, also commonly termed the pseudophase model [16]. Confined under this model, the micellar environment is treated as a separate phase in equilibrium with the enveloping aqueous phase. This treatment of micelles is equivalent to a regular bulk solution approximation, where surface effects are masked. Neither knowledge of number of monomers constituting micelles or constants for stepwise distribution is required.

One of the empirical bases for introducing this model is that several physical properties, including osmotic pressure, surface tension and equivalent conductivity, exhibit an abrupt change in concentration dependence around cmc [67]. An illustration is given in Figure 3.1 [67] for the above physical properties in SDS-water binary system, where properties are plotted against surfactant concentration. This type of behaviour around cmc is what is generally observed for a transition into a two-phase system [67].

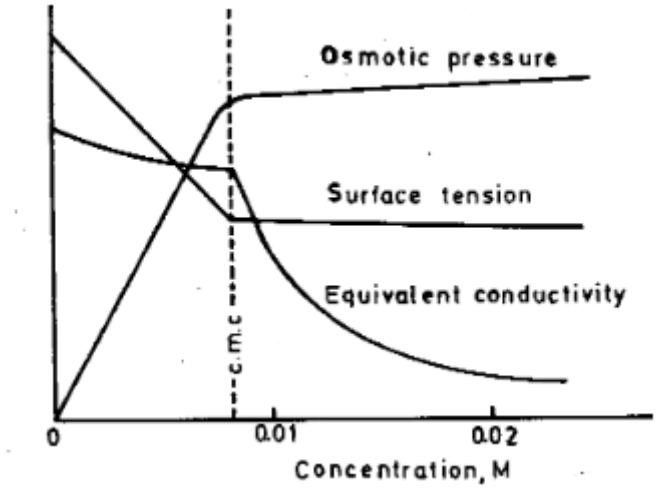

Figure 3.1: Plot of some physical properties (osmotic pressure, surface tension and equivalent conductivity) as function of concentration SDS. All properties show abrupt changes in concentration dependence around cmc. This very much what is observed for transition into a two-phase system, providing an empirical basis for the phase separation model for treating micellar solutions.

Consequent of the model, the additive[10] (2) will distribute between the two phases in a system reaching chemical equilibrium [11, 16],

$$\mu_{2,mic} = \mu_{2,Aq} \tag{3.1}$$

where $\mu_{2,mic}$ and $\mu_{2,Aq}$ represents the chemical potential of additive in micellar pseudophase and aqueous phase, respectively.

Neglecting activities and using mole fractions, the free energy of transfer ΔG_t from aqueous to micellar phase can be expressed directly by the mole-fraction based distribution coefficient K_X,

$$\Delta G_t = \mu_{2,mic} - \mu_{2,Aq} = -RTlnK_x = -RTln\frac{X_{2,mic}}{X_{2,Aq}} \tag{3.2}$$

where R is the ideal gas constant and $X_{2,Aq}$ and $X_{2,mic}$ represent mole fraction of alcohol solubilized in aqueous and micellar pseudophase, respectively.

Equation 3.2 is technically valid for any (pseudo)equilibrium coefficient. Several bases for partitioning have been proposed in the literature [9, 11]. An alternative which is frequently presented is molar concentration-based distribution [9, 11, 16, 67], being in better accordance with the mass action model [9].

[10]Additive and solvent is in thermodynamic relations denoted 2 and 1, respectively.

Bulk phases are homogeneous and large in size, which is very unlike the nature of micelles [68]. This brings to question the applicability of the model. While it is clear that micelles do not constitute a thermodynamic phase themselves, they do mimic phase-like behaviour in the sense that they can act as both a source and a sink for surfactant monomers in solution [69]. An immediate result of applying the model is resignation from description of micellar size and shape [67] as the colloid nature of micelles is excluded. The micellar phase is treated as uncharged and to be confined to a constant aggregation number, the latter taken to approach infinity [16, 70, 71]. All these are in fact real-world variables that will be affected by solubilization of a third component.

Consequent of the model, the cmc of the surfactant is (re)defined at the surfactant concentration in which the first phase separation occurs [67]. Equivalently, it can be defined as the maximum saturation point for surfactant monomers in the aqueous phase [67, 71]. If these definitions were indeed correct, the mean value of any molecular property (including partial molar properties), as well as the solubility of additives, should all change linearly with surfactant concentration above cmc [67]. (Slight) deviation from this linear relationship is observed however, mainly because of two reasons [67, 72]: (1) There is in fact no true phase change, as properties changes continuously around cmc, and not at a truly critical concentration. (2) Concentration of unmicellized (monomeric) surfactant in the aqueous phase is not constant above cmc, as assumed in the model.

Some of the great advantages of the pseudophase model is its simplicity and the fact that same formalism can be applied to different kinds of experiments and can be used to compare individual techniques or methods of approach [66]. The model is usually applicable when the aggregation number in the micelles is greater than 50, which is usually the case for commercial surfactants [70, 73].

3.2 Partial and Apparent Molar Properties

Overall properties of a mixture are not necessarily additive with respect to the individual components constituting the mixture. This is a result of non-ideal mixing, due to restructuring taking place within the system when adding more component, which in turn is result of an altered set of intermolecular interactions between the components constituting the mixture. It is desirable to relate the property of each individual component to the overall property of the mixture, which is the basis for introducing partial molar properties. This concept can be

extended to any extensive state function as its corresponding intensive property [74]. Partial molar properties are proven useful to study intermolecular interactions, because overall system properties, being readily measurable, are highly sensitive to small structural changes within the system. Another strength of this type of approach is that these structural changes can be observed continuously as the composition or nature of species, or external factors like pressure and temperature, varies [75]. Applying partial molar properties is therefore ideal for studying solubilization environment in micellar solution. Properties which have been commonly utilised for this kind of study include volume, enthalpy, heat capacity and compressibility [1, 11].

An important characteristic of extensive properties, which is directly related to the derivation of partial molar properties, is that they satisfy Euler's theorem for homogeneous functions. For a m component mixture at constant temperature and pressure, a fractional increase λ in each individual component will increase the overall property Y by the exact same amount,

$$Y(\lambda n_1, \lambda n_2, ..., \lambda n_m) = \lambda Y \qquad , P, T = const. \tag{3.3}$$

It then follows that the given thermodynamic property of the system is additive with respect to individual contributions from each component constituting the mixture,

$$Y = \sum_{i=1}^{m} n_i Y_i \qquad , P, T = const. \tag{3.4}$$

Y will in fact be a function the composition of the m-component system, as well as temperature and pressure. A change in either of these variables will result in change in Y according to Equation 3.5 [76].

$$dY = \left(\frac{\delta Y}{\delta T}\right)_{P,n_1,n_2,...} dT + \left(\frac{\delta Y}{\delta P}\right)_{T,n_1,n_2,...} dP + \left(\frac{\delta Y}{\delta n_1}\right)_{T,P,n_2,n_3,...} dn_1 + \left(\frac{\delta Y}{\delta n_2}\right)_{T,P,n_1,n_3,...} dn_2 + ... \tag{3.5}$$

The partial molar property of a component i is given as the gradient of the extensive property of the mixture with respect to the amount of component i, under the constraint that all other parameters remain constant,

$$Y_i = \left(\frac{\delta Y}{\delta n_i}\right)_{p,T,n'}, \qquad n' = \sum_{j=1}^{m-1} n_{j \neq i} \tag{3.6}$$

Regarding investigation of the molecular environment, a highly important characteristic of the overall property of the system is the fact that it can be parted into an intrinsic part and an interaction part, for and between each components constituting the mixture [1]. This is expressed in Equation 3.7 for a mixture of m components,

$$Y = \sum_{i=1}^{m} Y_{i,int} + \frac{1}{2} \sum_{i=1}^{m} \sum_{j=1}^{m} Y_{i-j} \quad , i \neq j \tag{3.7}$$

It is in our main interest to consider a two-component system of a additive (2) dissolved in solvent (1), since dealing with alcohol solubilization in micellar solution. Equation 3.6 and Equation 3.7 is thus rewritten,

$$Y_2 = \left(\frac{\delta Y}{\delta n_2} \right)_{p,T,n_1} \tag{3.8}$$

and,

$$Y = Y_{1,int} + Y_{2,int} + Y_{2-1} = Y_{1,int} + Y_{2,int} + Y_{1-2} \tag{3.9}$$

As will be one of the main topics in the following subsection, studying partial molar properties of additive at standard condition as a function of surfactant concentration allows for direct investigation of additive-solvent interactions,

$$Y_2^o = Y_{2,int}^o + Y_{2-1}^o \tag{3.10}$$

Complementary to partial molar properties, another parameter more readily available is the apparent molar property of additive Y_ϕ[11], in which the solvent is assumed unaffected upon mixing [77]. In other words, the contribution from solvent to the overall property of the mixture is the same as if the solvent were in a pure state. Contrary to partial molar property, requiring data treatment, apparent molar property of additive is calculated directly from measurement [77]. Applying the concept of apparent molar properties in Equation 3.4 results in,

$$Y = n_1 Y_1^* + n_2 Y_\Phi \tag{3.11}$$

where $*$ denotes pure component.

[11] Read $Y_{2,\phi}$. Y_ϕ is used for clarification as there is no necessity to introduce $Y_{1,\phi}$.

The definition of apparent molar volume of additive is obvious from rearrangement,

$$Y_\Phi = \frac{Y - n_1 Y_1^*}{n_2} \tag{3.12}$$

Y_2 and Y_ϕ are closely related through [78],

$$Y_2 = Y_\Phi + m_2 \left(\frac{\delta Y_\Phi}{\delta m_2} \right) \tag{3.13}$$

and at infinite dilution the two approach each other as,

$$\lim_{m_2 \to 0} \quad m_2 \left(\frac{\delta Y_\Phi}{\delta m_2} \right) = 0 \tag{3.14}$$

3.2.1 Volume

Volume is an important property because it is readily and accurately obtained from density measurements. The formal definition of volume is the first derivative of Gibbs' free energy with respect to pressure, constrained at constant temperature,

$$V = \left(\frac{\delta G}{\delta P} \right)_T \tag{3.15}$$

The partial molar volume of additive dissolved in solvent is given on the same basis as in Equation 3.8,

$$V_2 = \left(\frac{\delta V}{\delta n_2} \right)_{p,T,n_1} \tag{3.16}$$

Experimentally observing the change in volume as a function of additive on direct measures is impractical. Therefore, an expression for V_2 as a function of density is introduced, the latter being easily and accurately obtainable,

$$V_2 = \frac{M_2}{\rho} - \frac{(10^3 + M_2 m_2)}{\rho^2} \left(\frac{\delta \rho}{\delta m_2} \right) \tag{3.17}$$

where M_2 is the molar mass of additive. V_2 is given in units of $cm^3 mol^{-1}$, assured by the factor 10^3 for input units of density in gcm^{-3}. Equation 3.17 is simplified at standard condition,

$$\lim_{m_2 \to 0} V_2 = V_2^o = \frac{M_2}{\rho_o} - \frac{10^3}{\rho_o^2}\left(\frac{\delta\rho}{\delta m_2}\right) \tag{3.18}$$

In the case for the additive-surfactant-water ternary system, ρ_0 refers to the density of the surfactant-water binary system. $(\frac{\delta\rho}{\delta m_2})$ can in many instances be adequately evaluated from a quadratic polynomial from least squares linear regression of experimental data,

$$\rho = b_0 + b_1 m_2 + b_2 m_2^2 \tag{3.19}$$

$$\left(\frac{\delta\rho}{\delta m_2}\right) = 2b_2 m_2 + b_1 \tag{3.20}$$

A similar expression to Equation 3.17 for apparent molar volume V_ϕ as function of density, is readily expressed,

$$V_\phi = \frac{10^3(\rho_0 - \rho)}{m_2 \rho \rho_0} + \frac{M_2}{\rho} \tag{3.21}$$

The factor 10^3 in this expression have the same purpose as in the expression for V_2, in Equation 3.17 and Equation 3.18.

Note that V_ϕ, contrary to V_2, is undefined at zero concentration. V_ϕ^o is therefore estimated by extrapolation of V_ϕ from a region of lower to intermediate alcohol concentrations.

3.2.2 Compressibility

Partial molar compressibility of additive is defined as the negative of the pressure derivative of the overall volume, constrained at constant temperature.

$$K_2 = -\left(\frac{\delta V_2}{\delta P}\right)_T = -\frac{1}{\delta n_2}\left(\frac{\delta V}{\delta P}\right)_T \tag{3.22}$$

This quantity can be obtained if V_2 and the isentropic (adiabatic) compressibility coefficient κ_S as a function of additive concentration is available,

$$K_2 = \frac{10^3 + M_2 m_2}{\rho}\left(\frac{\delta\kappa_S}{\delta m_2}\right) + \kappa_S V_2 \tag{3.23}$$

The expression above is simplified at standard condition,

$$\lim_{m_2 \to 0} K_2 = K_2^o = \frac{10^3}{\rho_o}\left(\frac{\delta \kappa_S}{\delta m_2}\right) + \kappa_{S,0} V_2^o \tag{3.24}$$

Just as for volume, in the case for the alcohol-surfactant-water ternary system, $\kappa_{S,0}$ refers to the isentropic compressibility coefficient of the surfactant-water binary system.

The rapid compression and rarefaction of sound waves propagating in fluids assures reversible return to equilibrium [79]. The reason for which is that heat transfer from the system have insufficient time to be initiated and constant entropy condition then follows, according to the second law of thermodynamics [79]. The isentropic compressibility coefficient is directly available from additional sound velocity measurements, via the Newton-Laplace relation,

$$\kappa_S = -\frac{1}{V}\left(\frac{\delta V}{\delta P}\right)_S = u^{-2}\rho^{-1} \tag{3.25}$$

κ_S in Equation 3.25 is given in units of $10^{-3}\ Pa^{-1}$ or $10^2\ bar^{-1}$, for input of density and sound velocity in units of gcm^{-3} and ms^{-1}, respectively. Further on, K_2 is given in units of $cm^3 mol^{-1} bar^{-1}$, given that ρ and κ_S are given in units of gcm^{-3} and bar^{-1}, respectively.

$(\frac{\delta \kappa_S}{\delta m_2})$ can in many instances be adequately evaluated from a quadratic polynomial from least squares linear regression of experimental data.

$$\kappa_S = b_0 + b_1 m_2 + b_2 m_2^2 \tag{3.26}$$

$$\left(\frac{\delta \kappa_S}{\delta m_2}\right) = 2b_2 m_2 + b_1 \tag{3.27}$$

Regression coefficients b_0, b_1 and b_2 in these two equations are different from those presented for determining $(\frac{\delta \rho}{\delta m_2})$.

The isothermal compressibility coefficient κ_T could be calculated and used for interpretation, as an alternative to κ_S. However, κ_T tends to be of low precision or is excessively tedious [79]. It can be experimentally obtained by observing change in volume from known increase in pressure, but the isothermal condition is difficult to maintain [79]. The isentropic and isothermal compressibility coefficients are however simply related through Equation 3.28 [80].

$$\kappa_T = \kappa_S + \frac{E^2 TV}{C_P} \tag{3.28}$$

where E and C_P are expandability and isobaric heat capacity, respectively.

An expression for isentropic apparent molar compressibility K_ϕ as a function of density and isentropic compressibility coefficient, can be expressed based on its definition,

$$K_\phi = -\left(\frac{\delta V_\phi}{\delta P}\right)_T = \frac{10^3(\kappa_S - \kappa_{S,0})}{m_2 \rho_0} + \kappa_S V_\phi \tag{3.29}$$

As for volume, K_ϕ^o is not defined and requires extrapolation of K_ϕ from region of lower to intermediate alcohol concentration.

3.3 Thermodynamic Approach to Treat Solubilization

By applying the pseudophase model to distribution of additive, the overall partial molar property of the additive in solution Y_2 can be expressed as a weighted average of the partial molar property of the additive in each respective phase,

$$Y_2 = \alpha Y_{2,mic} + (1 - \alpha) Y_{2,Aq} \tag{3.30}$$

where $Y_{2,mic}$ and $Y_{2,Aq}$ are partial molar property of additive in micellar and aqueous phase, respectively. α is the fraction of the total amount of additive in the system which is associated with the micellar pseudophase,

$$\alpha = \frac{n_{2,mic}}{n_2} = \frac{n_{2,mic}}{n_{2,mic} + n_{2,Aq}} \tag{3.31}$$

Equation 3.30 is in accordance with Young's general mixing rule. An increase in solubilized amount of additive will increase the contribution from $Y_{2,mic}$ to the overall partial molar property of the system Y. The relation is only strictly valid for standard properties, where the additive is in a infinitely diluted state [81],

$$Y_2^o = \alpha Y_{2,mic}^o + (1 - \alpha) Y_{2,Aq}^o \tag{3.32}$$

$Y^o_{2,Aq}$ is approximated to $Y^o_{2,w}$ (additive in pure water) as the latter is much more readily obtainable,

$$Y^o_2 = \alpha Y^o_{2,mic} + (1-\alpha) Y^o_{2,w} \tag{3.33}$$

If applied, $Y_{2,Aq}$ should ideally be obtained from a system with surfactant concentration at cmc. This is because at this concentration, the aqueous phase is most representative of the surrounding aqueous solution in a system containing micelles. $Y_{2,Aq}$ can be correlated to the corresponding property in pure water $Y_{2,w}$ through the McMillan-Mayer approach, where only the interaction parameter between additive and surfactant $Y_{2/1}$ have been considered [1],

$$Y_{2,Aq} = Y_{2,w} + 2Y_{2/1} m_{S,Aq} \tag{3.34}$$

Higher-order interaction terms can be included if necessary.
The relationship between Y^o_2 and α in Equation 3.33 is linear with a slope equal to $Y^o_{2,mic} - Y^o_{2,w}$, and intercept equal to $Y^o_{2,w}$. This becomes clear from rearrangement,

$$Y^o_2 = Y^o_{2,w} + \alpha(Y^o_{2,mic} - Y^o_{2,w}) \tag{3.35}$$

The transfer contribution to Y^o_2 of infinitely diluted additive going from pure water to micellar pseudophase, is represented by the slope in Equation 3.35. Being a state function, only knowledge of parameters in the respective solvents is required for determination,

$$\Delta Y^o_2 = Y^o_{2,mic} - Y^o_{2,w} \tag{3.36}$$

All parameters in Equation 3.35 (and Equation 3.36) can be determined experimentally. However, it is necessary to present a reasonable expression for α, since $n_{2,mic}$ is not readily obtainable, and distribution between the two phases have yet to be included. This can be resolved by concerning the equilibrium conditions between the two phases, where the mole fraction-based distribution coefficient of additive can be obtained,

$$K_X = \frac{X_{2,mic}}{X_{2,Aq}} = \frac{\frac{n_{2,mic}}{n_{2,mic}+n_{S,mic}}}{\frac{n_{2,Aq}}{n_{2,Aq}+n_{S,Aq}+n_w}} \tag{3.37}$$

where S denotes surfactant. Note that activities have been neglected. Equation 3.37 can equivalently be expressed by considering molal concentrations,

$$K_X = \frac{X_{2,mic}}{X_{2,Aq}} = \frac{\frac{m_{2,mic}}{m_{2,mic}+m_{S,mic}}}{\frac{m_{2,Aq}}{m_{2,Aq}+m_{S,Aq}+m_w}} \tag{3.38}$$

A reasonable assumption is that in the aqueous phase, the amount of additive and surfactant is negligible with respect to the amount of water, thus neglecting the presence of the two former. For 1 kg of water (55.52 mol), Equation 3.38 is rewritten,

$$K_X = \frac{\frac{m_{2,mic}}{m_{2,mic}+m_{S,mic}}}{\frac{m_{2,Aq}}{55.52}} = \frac{55.52\alpha}{(1-\alpha)(\alpha m_{2,mic} + m_{S,mic})} \tag{3.39}$$

The expression is simplified at standard condition,

$$\lim_{m_2 \to 0} K_X = K_X^o = \frac{55.52\alpha}{(1-\alpha)m_{S,mic}} \tag{3.40}$$

Rearranging Equation 3.40 with respect to α gives,

$$\alpha = \frac{K_X^o m_{S,mic}}{K_X^o m_{S,mic} + 55.52} \tag{3.41}$$

$m_{S,mic}$ is easily obtainable if the cmc of the surfactant is known. Alternatively, if the cmc is low, it can be approximated to the total surfactant concentration,

$$\alpha = \frac{K_X^o m_S}{K_X^o m_S + 55.52} \tag{3.42}$$

The variation of Y_2^o with α represents variation in the micellar environment in which the additive may reside. It is desirable to accurately model this relationship, since a combination of Equation 3.35 and Equation 3.42 can be used simultaneously as a three-parameter equation to obtain solutions to K_X^o and $Y_{2,mic}^o$. This is performed by iterating K_X^o to minimize the standard deviation in a linear model of Y_2^o versus α [1]. $Y_{2,mic}^o$ is then determined from the slope, after the appropriate value of K_X^o is chosen from the iteration.

From each surfactant concentration (equivalent to each α), a value for Y_2^o is obtained. An object at zero surfactant concentration (intercept) is also included as basis in the model, where $Y_{2,w}^o$ is either obtained experimentally or gathered from the literature. Each of these objects at different (or zero) surfactant concentrations are at standard conditions, i.e. where the additive

is infinitely diluted. These standard states are obtained by least squares fitting of experimentally obtained Y_2 as a function of additive concentration, keeping surfactant concentration constant, and by extrapolating Y_2 to infinite dilution. Some of the reasons for using standard condition include (1) obtaining a common reference state. (2) Additive-additive interactions are not present as the additive is infinitely diluted in its respective phase. (3) In this state, the additive will behave as a probe not significantly affecting physiochemical properties of the micelle [1].

Regarding investigation of the solubilization environment, isentropic partial molar compressibility is preferred for interpretation over partial molar volume. The reason for which is that the intrinsic contribution for partial molar compressibility is mostly determined by the compressibility of covalent bonds and external electron shells for low weight compounds, which can be regarded as incompressible [82]. Partial molar compressibility can therefore be considered having negligible intrinsic contribution, and can be regarded as a function of interactions only. This is contrary to partial molar volume which have a significant intrinsic contribution, mainly due to the van der Waals volume. K_X^o could be determined from either volume or compressibility. However, relative to the uncertainties in Y_2^o, the variation of Y_2^o with α is small for volume compared to compressibility [81]. A larger error is therefore induced in determining K_X^o from volume, and a more accurate estimate of K_X^o is therefore made from compressibility data.

After $Y_{2,mic}^o$ is finally determined, it can be compared to the corresponding parameters in other solvent systems. These systems typically include other additive-surfactant-water ternary systems and additive in polar and apolar solvents, such as water and liquid hydrocarbon.

De Lisi et al. [83] have shown that contribution to partial molar properties include (1) distribution of additive between the two phases, (2) additive-surfactant interactions in both micellar and aqueous phase, and (3) the additive effect on shift in micellization equilibrium [83]. The last of these three effects could be calculated, if Setchenov's salting-out constant, and degree of ionisation of micellized and monomeric surfactant were all known. However, the effect has been neglected altogether in arriving at Equation 3.35.

Another neglect in this approach is obvious from topics in De Lisi et al. [1]. For properties that are first derivative of Gibb's free energy, like volume, Equation 3.35 is valid as its stated. When concerning properties that are second derivative of Gibb's free energy, like compressibility, some additional terms are introduced as result of the second derivation. Høiland et al. [81] highlights the relaxation term ($\frac{\delta \alpha_{ma}}{\delta P}$) when for compressibility, representing pressure effects on the amount additive solubilized in micellar pseudophase. This term is difficult to calculate due

to the isentropic condition [81], and is however expected to be negligible with respect to the experimental error (along with other terms introduced from the second derivative).

4 Results & Discussions

4.1 Summary of Main Results

The main results obtained in this study are presented in Table 4.1, along with estimated uncertainties presented underneath the table. These results include mole fraction-based distribution coefficient and standard partial molar volume and isentropic compressibility in micellar pseudophase, for primary to tertiary pentanols and hexanols in IOS 1923 and 1-pentanol in IOS 2024.

Table 4.1: Distribution coefficients and standard partial molar volumes and isentropic compressibilities in micellar pseudophase for terminal and non-terminal pentanols and hexanols in IOS 1923 and IOS 2024. Partial molar volume and isentropic compressibility in micellar pseudophase are given in units of cm^3mol^{-1} and $10^4 \cdot cm^3mol^{-1}bar^{-1}$, respectively. Estimated uncertainties are presented underneath the table.

	1-PentOH	2-PentOH	3-PentOH	1-HexOH	2-HexOH	3-HexOH
IOS 1923						
K_X^o	**436**	**215**	**144**	**788**	**809**	**525**
$V_{2,mic}^o$	**104.4**	**105.2**	**102.7**	**120.8**	**120.1**	**118.3**
$K_{2,mic}^o$	**58.9**	**63.1**	**65.9**	**72.9**	**61.9**	**58.8**
IOS 2024						
K_X^o	**178**					
$V_{2,mic}^o$	**106.8**					
$K_{2,mic}^o$	**89.8**					

K_X^o ± 30, $V_{2,mic}^o$ ± 0.2, $K_{2,mic}^o$ ± 0.2

In the following section, a discussion will be given on standard partial molar volume and isentropic compressibility, from which the corresponding parameters in micellar pseudophase and distribution of alcohol between pure water and micellar pseudophase are derived. Emphasis will be given on transfer contributions to V_2^o and K_2^o for alcohol transferring from pure water to micellar pseudophase. Partial molar properties, as well as distribution, are highly sensitive to modelling of density and isentropic compressibility as function of alcohol concentration, and some highlights on the approach to this and encountered obstacles will be presented. Subsequently, our values will be compared within the IOS surfactants and also to corresponding

parameters in other solvent systems, including SDS, bulk alcohol, water and octane. The two latter solvents are representative of highly hydrophilic and hydrophobic environments, respectively. A separate discussion will be made concerning distribution, including an evaluation of using average molecular weight by Barnes et al. [3] as basis for K_X^o in alcohol-IOS-water ternary systems. Lastly, focus will be shifted towards $V_{2,mic}^o$ and $K_{2,mic}^o$.

4.2 Distribution and Standard Partial Molar Volume and Isentropic Compressibility

V_2^o in various concentrations of IOS, with that in pure water as reference, is presented in Table 4.2. The exact same data, accompanied by models of linear fit, is presented graphically in Figure 4.1 for alcohols in IOS 1923 and in Figure 4.2 for 1-pentanol in IOS 2024. Corresponding table and figures for isentropic standard partial molar compressibilities is presented in Table 4.3, and Figure 4.3 and Figure 4.4, respectively.

Table 4.2: Standard partial molar volumes of pentanols and hexanols in varying IOS concentration and in pure water. Notice the different concentration range among the IOS surfactants, and that approximate concentrations are given due to this parameter varying between individual alcohols. The reference values are excepted from the estimated uncertainties given at the end of the table.

$\approx m$	V_2^o / $cm^{-3}mol^{-1}$					
	1-PentOH	2-PentOH	3-PentOH	1-HexOH	2-HexOH	3-HexOH
IOS 1923						
0.00	102.62[a]	102.55[b]	101.24[b]	118.7[c]	118.5[c]	117.1[c]
0.06	103.4	103.0	101.4	120.1	118.8	117.4
0.12	103.8	103.3	101.9	120.3	119.6	117.9
0.18	103.6	103.8	101.9	119.8	119.8	117.7
0.24	103.5	103.7	101.5	120.2	119.8	118.0
IOS 2024						
0.00	102.62[a]					
0.06	103.1					
0.11	103.8					
0.15	103.5					
0.18	104.6					
	±0.2	±0.2	±0.2	±0.2	±0.2	±0.2

a - Vikingstad [35].

b - Høiland [84].

c - Høiland et al. [11].

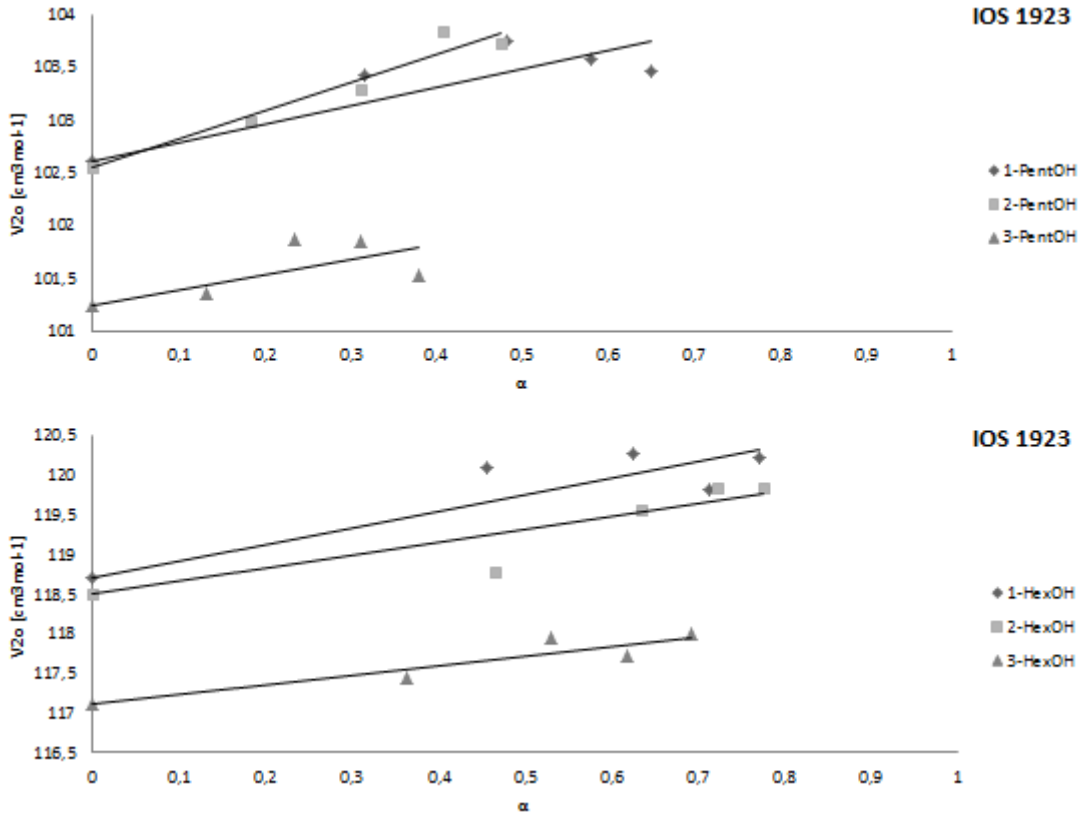

Figure 4.1: Standard partial molar volumes of pentanols (upper) and hexanols (lower) in micellar pseudophase of IOS 1923 as function of fraction alcohol solubilized in micellar pseudophase. The models are forced through the intercept in belief that reported values in water are of higher accuracy than those determined in this study.

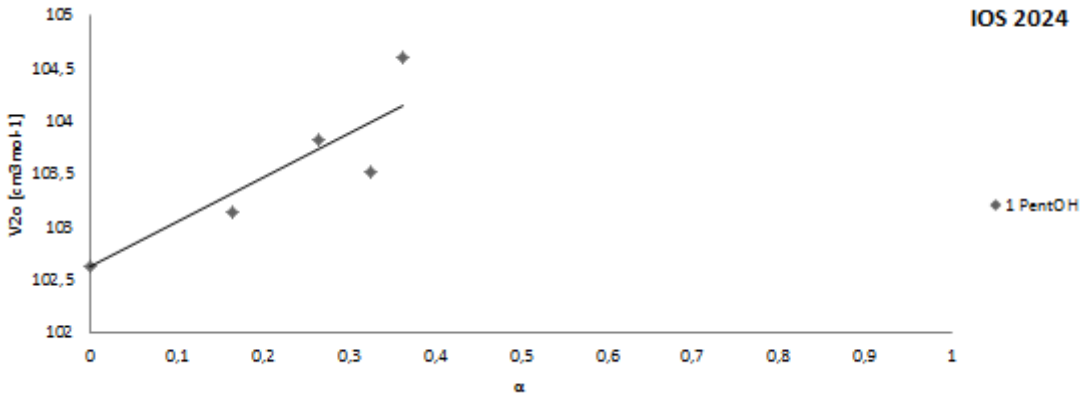

Figure 4.2: Standard partial molar volumes of 1-pentanol in micellar pseudophase of IOS 2024 as function of fraction alcohol solubilized in micellar pseudophase. The model is forced through the intercept in belief that reported values in water are of higher accuracy than those determined in this study.

Table 4.3: Isentropic standard partial molar compressibilities of pentanols and hexanols in varying IOS concentration and in pure water. Notice the different concentration range among the IOS surfactants, and that approximate concentrations are given due to this parameter varying between individual alcohols. The reference values are excepted from the estimated uncertainties given at the end of the table.

	K_2^o					
$\approx m$	$\cdot 10^4\ cm^{-3}mol^{-1}bar^{-1}$					
	1-PentOH	2-PentOH	3-PentOH	1-HexOH	2-HexOH	3-HexOH
IOS 1923						
0.00	2.3[a]	1.0[b]	-1.6_0	0.5[a]	-1.2^b	-2.7_3
0.06	20.4	12.2	7.2	34.3*	28.2	19.5
0.12	29.5	20.4	14.2	45.9	38.7	30.1
0.18	35.2	26.6	19.7	51.9	44.8	35.1
0.24	39.2	30.3	23.8	56.4	47.6	39.9
IOS 2024						
0.00	2.3[a]					
0.06	17.2					
0.11	25.4					
0.15	30.3					
0.18	34.7					
	±0.2	±0.2	±0.2	±0.2	±0.2	±0.2

a - Vikingstad [35].

b - Høiland [84].

∗ - Excluded from regression modelling.

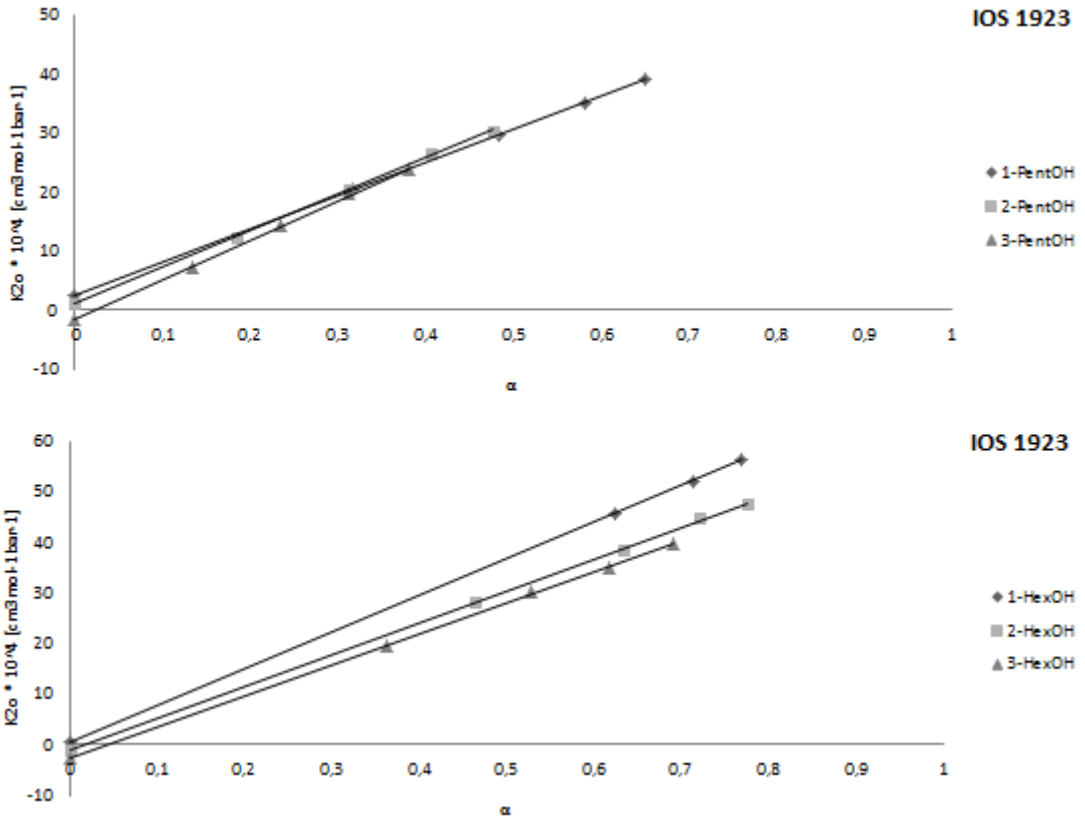

Figure 4.3: Standard isentropic partial molar compressibilities of pentanols (upper) and hexanols (lower) in micellar pseudophase of IOS 1923 as function of fraction alcohol solubilized in micellar pseudophase.

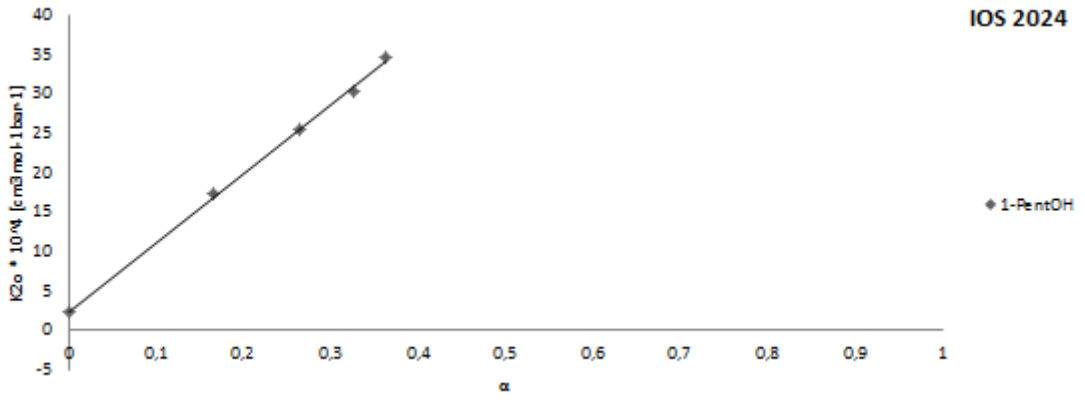

Figure 4.4: Standard isentropic partial molar compressibilities of 1-pentanol in micellar pseudophase of IOS 2024 as function of fraction alcohol solubilized in micellar pseudophase.

Relative to the estimated uncertainties (± 0.2), the greater variation of K_2^o compared to V_2^o, both with respect to α, is clearly visible from these tables and figures. K_2^o ranges beyond more than an order of magnitude, from close to zero, as far as to $56.4 \cdot 10^{-4}$ $cm^3 mol^{-1} bar^{-1}$ for 1-hexanol in approximately 0.24 m IOS 1923. The variation in V_2^o is less than 2.0 $cm^3 mol^{-1}$

for all individual alcohols in the given concentration range of IOS 1923. Observing Figure 4.1 - 4.4, the linearity principle of K_2^o versus α is adequately satisfied, meaning the linear models fit the data very well. V_2^o is expected to be submitted to the same feature, but this linear trend is likely masked by the larger relative uncertainty in the parameter. However, results and models clearly reveal positive correlation between V_2^o and α.

In gradually increasing the surfactant concentration at a fixed alcohol concentration, i.e. moving from left to right in the figures, marks the continuous extraction of alcohol into the micellar environment [1]. The reason for which is that more micelles are formed from surfactant added above cmc, thus increasing the solubilizing capacity for the system as a whole. Furthermore, the contribution from $Y_{2,mic}^o$ to the overall partial molar property of additive Y_2^o will then increasingly dominate over the contribution from $Y_{2,w}^o$, according to Equation 3.33.

Moving the opposite way, with decreasing α, the micellar pseudophase abruptly disappears at the intercept, as the ternary system is instantly transformed into the corresponding binary alcohol-water system $Y_{2,w}^o$. This is an approximation, as already mentioned, as this state will in reality contain other species, including monomeric surfactant, co- and counterions, and impurities including sodium sulfite and free oil. The modification of pure water by these compounds results in $Y_{2,Aq}^o$ not equal to $Y_{2,w}^o$, according to McMillan-Mayer (Equation 3.34). De Lisi et al. [85] found the difference $V_{2,Aq}^o - V_{2,w}^o$, representing the transfer volume of infinitely diluted additive from pure water to aqueous surfactant solution, to be positive, and also found to be less for 1-butanol (0.43 cm^3mol^{-1}) compared to 1-pentanol (0.59 cm^3mol^{-1}) in SDS. These two values are significant with respect to the estimated uncertainties in V_2^o in IOS, and suggests that $V_{2,Aq}^o$ should be preferred over $V_{2,w}^o$ in the thermodynamic approach.

Extrapolating the model of V_2^o versus α to infinite surfactant dilution (pure water) does generally not correspond very well with the reference values. This is obvious just by observing Figure 4.1 and Figure 4.2. The greatest discrepancy is observed for 1-hexanol in IOS 1923; $V_{2,w}^o$ is estimated to 118.8_7 cm^3mol^{-1} from extrapolation, compared to a reference (literature) value of 118.7 cm^3mol^{-1} [11]. In belief that reported values of $V_{2,w}^o$ are of greater accuracy than the ones obtained from extrapolation in this investigation of the ternary system, the model is forced trough the intercept. This does however not influence the estimation of K_X^o, as it is determined from K_2^o at various surfactant concentration, with pure water as reference. $K_{2,w}^o$ is taken as another object, equally leveraged as K_2^o at various IOS concentrations.

Further applying standard partial molar properties, ΔV_2^o and ΔK_2^o are determined according to Equation 3.36. These parameters are the slopes of the regression models of Y_2^o versus α, and

can be determined equally from the value of those. Results are presented in Table 4.4.

Table 4.4: Transfer contribution to standard partial molar volumes and isentropic compressibility of pentanols and hexanols from pure water to micellar pseudophase in IOS 1923 and IOS 2024. Partial molar volume and isentropic compressibility are given in units of cm^3mol^{-1} and $10^4 \cdot cm^3mol^{-1}bar^{-1}$, respectively. Estimated uncertainties are presented underneath the table.

	1-PentOH	2-PentOH	3-PentOH	1-HexOH	2-HexOH	3-HexOH
IOS 1923						
ΔV_2^o	**1.7**	**2.7**	**1.5**	**2.1**	**1.6**	**1.2**
$V_{2,mic}^o$	104.4	105.2	102.7	120.8	120.1	118.3
$V_{2,w}^o$	102.62[a]	102.55[b]	101.24[b]	118.7[c]	118.5[c]	117.1[c]
ΔK_2^o	**56.6**	**62.1**	**67.5**	**72.4**	**63.1**	**61.6**
$K_{2,mic}^o$	58.9	63.1	65.9	72.9	61.9	58.8
$K_{2,w}^o$	2.3[a]	1.0[b]	-1.6	0.5[a]	-1.2[b]	-2.7
IOS 2024						
ΔV_2^o	**4.2**					
$V_{2,mic}^o$	106.8					
$V_{2,w}^o$	102.62[c]					
ΔK_2^o	**87.5**					
$K_{2,mic}^o$	89.8					
$K_{2,w}^o$	2.3[a]					

ΔV_2^o ±0.3, ΔK_2^o ±0.3

a - Vikingstad [35].

b - Høiland [84].

c - Høiland et al. [11]

One of the most obvious features in Table 4.4 is that all transfer contributions are of positive value, which is indeed the general observation for transfer of alcohols from pure water to

micellar pseudophase in (model) surfactants [11]. These observations can be reasoned by the dehydration of alcohol molecule upon transfer, under which there is a destruction of hydrogen-bonding network between water molecules in the solvation envelope. This clathrate structure of water, enveloping the alcohol, is small in volume compared to a apolar solvation envelope, and can also be regarded as incompressible. $K^o_{2,w}$ can even be of negative values, as observed for 3-pentanol and 2-hexanol, the former and latter systems having reported values of -1.6 and $-1.2 \cdot 10^{-4}$ $cm^3mol^{-1}bar^{-1}$, respectively [11, 84]. The observation that transfer contributions have significant value, is evidence of a great change in the enveloping environment in interchanging between the two phases. In other words, the environment in micellar pseudophase of IOS is highly dissimilar to that in pure water.

One of the advantages of concerning transfer contributions to standard partial molar properties is that the intrinsic contribution is largely eliminated upon subtraction of $Y^o_{2,w}$ from $Y^o_{2,mic}$. In our case, this would be most useful concerning volume, as the intrinsic contribution from adding of a methyl group makes the comparison of $V^o_{2,mic}$ between pentanol and hexanol rather useless. ΔV^o_2 overlap to various degree accounting with the estimated limit uncertainty, comparing among 1-alcohols and among 3-alcohols in IOS 1923. Regarding 2-alcohols, ΔV^o_2 is significantly larger for 2-pentanol compared to 2-hexanol, suggesting a greater change in solvation envelope for the former alcohol transferring from pure water to micellar pseudophase. Furthermore, ΔV^o_2 is significantly larger for 2-pentanol compared to each individual alcohol in IOS 1923, being 0.6 cm^3mol^{-1} greater than the next largest value (for 1-hexanol). Similar values of ΔV^o_2, and ΔK^o_2 for that matter, suggests similar changes in solvation envelope when undergoing solubilization. Mark the word *change* in environment, since these parameters do not themselves give any description of the environment in the respective phases. The extended size of ΔV^o_2 for 2-pentanol is dominated by the relatively large value in micellar pseudophase. Indeed, the value in micellar pseudophase is generally expected dominate ΔV^o_2 and ΔK^o_2, comparing across individual alcohols and different surfactant system. The basis for this reasoning is the effect of a more diverse solubilization envelope in micellar pseudophase, where the solubilized alcohol experience different ratios of both apolar and polar components (mainly surfactant head groups, surfactant alkyl chains and water/ions). The greater variation in micellar pseudophase is especially obvious from ΔK^o_2 where values for $K^o_{2,mic}$ are in the range $58.8 - 72.9 \cdot 10^{-4}$ $cm^3mol^{-1}bar^{-1}$ among individual alcohols in IOS 1923, up to $89.8 \cdot 10^{-4}$ $cm^3mol^{-1}bar^{-1}$ for 1-pentanol in IOS 2024. On the other hand, $K^o_{2,w}$ ranges only from -2.7 to $2.3 \cdot 10^{-4}$ $cm^3mol^{-1}bar^{-1}$.

Comparing a given alcohol across different surfactant systems, the extension of the transfer contributions is completely dominated by the values of $V^o_{2,mic}$ and $K^o_{2,mic}$. This is because of the

equal reference state (the given alcohol in water). Notice from Table 4.4 that ΔV_2^o and ΔK_2^o for 1-pentanol in IOS 2024 greatly exceeds the respective parameters for each individual alcohol in IOS 1923. The latter observation suggest a greater influence on transfer contributions by interchanging surfactant system for 1-pentanol, in comparison to varying among primary to tertiary pentanols or -hexanols in IOS 1923.

4.2.1 Modelling Density and Isentropic Compressibility

It is important to highlight the large degree of ambiguity regarding the approach to model density and compressibility as function of (molal) alcohol concentration, from which solubilization parameters[12] are derived. According to Høiland et al. [81], the error in these models should be confound within $\pm 10^{-5}\ gcm^{-3}$ and $\pm 10^{-8}\ bar^{-1}$ for density and compressibility data, respectively. All models applied in this investigation were limited to polynomial(s) of second order. The main reason for which is that in applying polynomials of higher order, the region in-between the objects is likely to be overestimated. It is also in attempt to keep consistent about the modelling, by applying the same order of polynomials to each alcohol series. It could even be questioned whether the use of a second order model is in some instances an over-fitting of density data, particularity in instances where very little curving is observed, such as for some or more pentanol series. However, plotting residuals[13] between obtained density objects and the corresponding linear model, systematic trends are revealed for hexanol- and also for some pentanol series. What is more, the outermost residuals have especially large values compared to the residuals in-between these, in many of the alcohol series. These observations would support applying a non-linear approach to modelling density versus alcohol concentration.

Increasing concentration of alcohol in the ternary system, the micellar pseudophase become increasingly saturated with alcohol. What results is an increasingly dominating influence of alcohol on the ternary system, as internal rearrangement and alternation of physiochemical properties of micelles takes place. This is to more favourably accommodate the newly added alcohol. Density and compressibility data reflect the influence of alcohol, and expresses itself as more abrupt changes in the two parameters as alcohols become more abundant in the ternary system, thus making the model curve significantly in the higher concentration region. A large increase in compressibility at higher alcohol concentrations may be a result of transition of alcohols to a more hydrophobic environment, as one of two explanations suggested by Høiland

[12] The term «solubilization parameters» will collectively refer to K_X^o, $V_{2,mic}^o$ and $K_{2,mic}^o$.

[13] See appendix E, page 81.

et al. [11]. As an example for illustration, this effect is obvious for 1-pentanol in 0.1769 m IOS 1923. In this alcohol series (and others), the model includes more than one regression model for compressibility data, overlapping each other. The reason for applying two models is that, by only applying one polynomial, the result is an under-representation at lower- and an over-representation at higher alcohol concentration. The influence of alcohol on the ternary system (curving) is less pronounced for density data, but is indeed present. A graphical representation is given in Figure 4.5, where density (upper) and isentropic compressibility coefficient (lower) are modelled as function of concentration 1-pentanol,

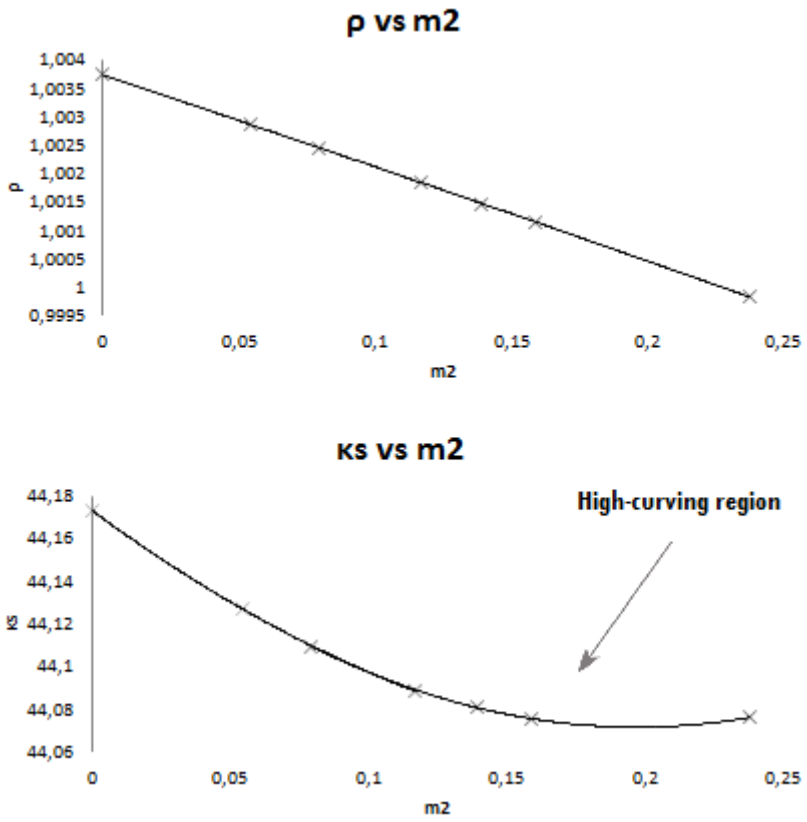

Figure 4.5: Density (upper) and isentropic compressibility (lower) as function of (molal) concentration of 1-pentanol in 0.1769 m IOS 1923. The pronounced curving at higher alcohol concentration is highlighted in the lower plot. The effect is obvious for isentropic compressibility due to the influence of alcohol on the ternary system, and is also present for density data.

The abrupt change in concentration-dependence for compressibility at higher alcohol concentration can often be more pronounced than what is observed in the lower plot of Figure 4.5. This is in several instances to such an extent where large-compressibility objects provide such a great leverage to obstruct the modelling in the lower-concentration region. To put it differently, because the model is not able to handle the abruptness in increase in compressibility (degree of

curving), the limiting region is improperly modelled. Objects at higher alcohol concentration characteristic of large compressibility, have been highlighted in other discussions [11, 81]. The observation that large-compressibility objects are generally more an issue regarding hexanols than pentanols in IOS supports the reasoning of Høiland et al. [11], as the former is expected to have a greater affinity for an environment more hydrophobic. If obstruction was indeed the observed case, these large-compressibility objects were regarded as non-representative for our purpose and were left out of the regression modelling. This was in order to maintain a representative model in the limiting region. Whether to exclude these objects or not have great implications on the determination of K_2^o at the given surfactant concentrations. As an example for illustration, 2-hexanol in 0.1193 m IOS 1923 display characteristics of what have been described. Including the (obstructing) compressibility object at highest alcohol concentration (0.2042 m 2-hexanol) changes the determination of K_2^o at the given surfactant concentration from 38.7 to $37.3 \cdot 10^{-4}$ $cm^3 mol^{-1} bar^{-1}$. This is well beyond the estimated limits of uncertainty. Particular concern has been given to 1-hexanol in 0.0592 m IOS 1923, for which the modelling κ_S versus m_2 proved some additional difficulties. K_2^o were determined from alcohol concentrations: (1) 0.0627 m, (2) 0.0709 m, (3) 0.0979 m, (4) 0.1102 m, (5) 0.1532 m, (6) 0.2228 m. Objects at (5) 0.1532 m and (6) 0.2228 m fits the description as having large-compressibility character. However, only modelling the lower region up to (4) 0.1102 m, resulted in a K_2^o deviating greatly from the linear trend of the three K_2^o at higher surfactant concentration (higher α). A satisfactory fit were observed with regards to residuals of κ_S versus m_2 and the linearity principle of K_2^o versus α, constituting a model from objects at 0 m, (3) 0.0979 m, (4) 0.1102 m, and (6) 0.2228 m. The issue here is that a relatively large number of objects have been selectively removed, and one of the remaining objects (6) have large-compressibility character. This leaves only two objects in the lower concentration region to determine K_2^o. A decision was ultimately made to exclude K_2^o at 0.0592 m IOS 1923, determining $K_{2,mic}^o$ and K_X^o based on K_2^o at the remaining three surfactant concentrations.

Complementary to issues in the higher alcohol concentration range, problems will also arise at lower alcohol concentrations, typically below 0.04 m [81], due to neglect of the micellar shift contribution. At higher alcohol concentrations, the effect becomes negligible. Only one object of the total number of objects in both IOS surfactant may fit this lower region, 2-hexanol in 0.2367 m IOS 1923 having an object at exactly 0.0400 m. Other objects are generally in the alcohol concentration region > 0.05 m. De Lisi et al. [1] highlights a lesser contribution from micellar shift (relative to distribution) for surfactants having lower cmc. It is easily imaginable that the IOS surfactants does in fact have a low cmc, due to factors expected to promote

spontaneous aggregation. Such factors include the twin tail nature, and presence of sodium sulfite, hydroxyl groups and free oil as impurities. Gilje [86] reports the cmc of IOS 1923 and IOS 2024 to be in the range $5.1 - 5.9 \cdot 10^{-5}$ m and $4.9 - 5.0 \cdot 10^{-5}$ m, respectively. This is considered very low compared to that of anionic model surfactants, which generally have cmc in the range of $10^{-3} - 10^{-2}$ M [87]. The low cmc of the two IOS surfactants is in support of the neglect of micellar shift contribution. However, the contribution should be calculated to observe if this is indeed a proper neglect, due to it being dependent on several variables. The low cmc is also in support of approximating m_S to $m_{S,mic}$, and describing α as function of the former rather than the latter parameter (i.e. applying Equation 3.42 rather than Equation 3.41) in the thermodynamic approach.

In general, suspected outlying or obstructing objects where left out of the regression analysis. These objects were primarily identified from experiments and residuals of the second order fit, and were confirmed secondarily by the attempt to satisfy the equality of partial and apparent molar quantities at infinite alcohol dilution, and to satisfy the linearity principle of Y_2^o versus α. Based on the issue of micellar shift contribution, and large-compressibility objects described, objects from the low- to intermediate concentration region is used to constitute models of density and isentropic compressibility coefficient as function of alcohol concentration. No less than 5 objects were applied to constitute any model of κ_S versus m_2 in IOS. The reader is encouraged to prepare his/her own models from the densities and isentropic compressibility coefficients obtained in this investigation, and compare to the ones presented here.

4.2.2 Comparison with Other Solvent Systems

K_X^o, $V_{2,mic}^o$ and $K_{2,mic}^o$ for pentanols and hexanols in IOS, along with corresponding partial molar properties in various solvent systems, are presented in Table 4.5. Other solvents include, in order as listed in the table: SDS, water, liquid alcohol (molar property) and octane (*oct*). All uncertainties are either left out for clarification, or are not obvious from the literature from which they are referred to.

Table 4.5: Mole fraction-based distribution coefficient and standard partial molar volume and isentropic compressibilities of pentanols and hexanols in IOS and in various solvent systems. The two latter parameters are given in units of cm^3mol^{-1} and 10^4 $cm^3mol^{-1}bar^{-1}$, respectively. The value determined in IOS surfactants are given in bold, for clarity. $*$ denotes pure component (in molar property).

	1-PentOH	2-PentOH	3-PentOH	1-HexOH	2-HexOH	3-HexOH
$K^o_X(IOS\ 1923)$	**436**	**215**	**144**	**788**	**809**	**525**
$K^o_X(IOS\ 2024)$	**178**					
$K^o_X(SDS)^a$	780	500	420	2300	1500	1030
$V^o_{2,mic}(IOS\ 1923)$	**104.4**	**105.2**	**102.7**	**120.8**	**120.1**	**118.3**
$V^o_{2,mic}(IOS\ 2024)$	**106.8**					
$V^o_{2,mic}(SDS)$	$105.3^{a,b}$			$122.2^a, 122.0^b$	121.2^a	119.6^a
$V^o_{2,w}$	$102.7^a, 102.6^{b,c}$	102.55^d	101.3, 101.3^d	$118.7^{a,b}, 118.65^c$	118.5^a	117.2, 117.1^a
V^*	$108.7^{b,c}$			125.3^b		
$V^o_{2,oct}$	115.8^b			131.9^b		
$K^o_{2,mic}(IOS\ 1923)$	**58.9**	**63.1**	**65.9**	**72.9**	**61.9**	**58.8**
$K^o_{2,mic}(IOS\ 2024)$	**89.8**					
$K^o_{2,mic}(SDS)$	67.5^a			81.4^a	69.0^a	66.5^a
$K^o_{2,w}$	$2.4^a, 4.5^b, 2.3^c$	1.0^d	-1.6, -1.6^d	$0.5^{a,c}, 5.8^b$	-1.2a	-2.7, 2.8a
K^*	$82.6^{b,c}$			$90.6^{b,c}$		
$K^o_{2,oct}$						

a - Høiland et al. [11].

b - De Lisi et al. [1].

c - Vikingstad [35].

d - Høiland [84].

4.2.3 Distribution

The estimated uncertainties (±30) in K_X^o in IOS are (1) similar to that of Høiland et al. [81] (±20) for some butanols to hexanols in SDS and some pentanols and hexanols in TTAB, determined from the thermodynamic approach. (2) Lower than those derived from other methods presented by Marangoni et al. [16], for which uncertainties are presented for 1-pentanol and 1-hexanol in both SDS and TTAB.

Evident from Table 4.5 is the decrease in K_X^o in the order 1-pentanol, 2-pentanol, 3-pentanol in IOS 1923. Replacing 1-pentanol (436) with 2-pentanol (215) halves the distribution towards the micellar pseudophase, and is furthermore less for 3-pentanol (144). Assuming the palisade layer to be the site of solubilization, terminal alcohols would align favourably parallel between micellized surfactant in the palisade layer of the micelle, with the hydroxyl group exposed to surfactant head groups and surrounding water, and the alkyl chain exposed to the hydrophobic deeper parts of the micelle. Non-terminal alcohols will be sterically hindered from the same degree of orderly alignment and is expected to pack less densely with the micellized surfactant. This is at least the common view at low concentrations of medium-chained alcohols in model surfactant systems [16]. This generalisation could reason the higher K_X^o observed for 1-pentanol, due to less rearrangement required in the palisade layer when introducing the latter. The rearrangement should be less comparing among non-terminal analogues, and hence, the difference in K_X^o should be greater comparing 1-alcohol and 2-alcohol, than comparing 2-alcohol and 3-alcohol. These observations are consistent with the observations made for pentanols in IOS 1923.

Solubilization of hexanol requires the transfer and accommodation of an additional methyl group in the micellar pseudophase, compared to pentanol. The observation that distribution towards micellar pseudophase is larger for hexanol compared to pentanol in IOS 1923, is consistent with the literature [1, 11, 29, 38, 40] and with what is reported in SDS [11]. This is mainly due to the entropy of dehydration in transfer from aqueous to micellar pseudophase, being proportional to the number of methyl groups constituting the alcohol. These observations does indeed support the importance of hydrophobic interactions in micellar pseudophase of IOS.

1-hexanol (788) and 2-hexanol (809) are indistinguishable within the estimated limits of uncertainty. However, both are certainly more extensively distributed towards micellar pseudophase of IOS 1923 than 3-hexanol (525). These observations suggests that substituting the hydroxyl group from α- to β-position does not significantly affect distribution of hexanol, and that both individual hexanols can preferably accommodate in the micellar pseudophase. Substituting the

hydroxyl group on hexanol to γ-position significantly lowers distribution to almost half the value.

K_X^o for 1-pentanol is less than half (41 %) in IOS 2024 (178) compared to in IOS 1923 (436), the former value being intermediate of those of 2-pentanol (215) and 3-pentanol (144) in IOS 1923. For polar additives solubilizing in the palisade layer, if the surface region remains the same, an extension of surfactant chain length should only slightly increase the degree of solubilization. This is at least what seems to be the general observation in model surfactant systems [11]. Under the above assumptions, K_X^o should not differ greatly for 1-pentanol interchanging between IOS 1923 and IOS 2024, due to only a small extension of approximate chain length interval in IOS 2024 compared to IOS 1923. This generalisation is however inconsistent with our observations, since by a small shift in the approximate olefin cuts towards a higher interval, distribution for 1-pentanol is greatly decreased.

Distribution is significantly less in both IOS surfactants compared to what is reported in SDS, comparing each individual alcohol in all three systems. This general observation is consistent with observations and reasoning by Gilje [86], based on conductivity measurements for primary to tertiary pentanol in IOS 1923[14]. Comparing each individual alcohol, the values obtained in IOS 1923 in our investigation are in the range $34 - 56$ % relative to values reported in SDS, and even lower (23 %) for 1-pentanol in IOS 2024 relative to in SDS. The lowest absolute values in IOS 1923 are observed for non-terminal pentanols, pointing towards a less favourable solubilization environment for the two alcohols. 3-pentanol in IOS 1923 have a K_X^o not much greater than that of 1-propanol in SDS, the values being 144 ± 30 and 105 ± 15 [11], respectively, the estimated uncertainty in both values slightly overlapping.

It is believed that the lesser distribution in IOS can partly be reasoned by the presence of sodium sulfite in IOS samples. These ions would preferably reside in the surrounding aqueous phase, and is expected to promote more elongated structures, in which the general observation is a decrease solubilization of polar additives [9, 11, 33]. The explanation presented is due to screening between sulfonate head groups, resulting in closer packing in the palisade layer [9, 32]. This in turn limits the volume available for alcohol solubilization, according to Rosen [32]. Additional screening effects may come from hydroxyl group(s), illustrated on some main generic structures of IOS (see Figure 1.1), thus introducing the idea that the IOS micelles might themselves exhibit some characteristics of a mixed anionic/non-ionic aggregate.

On the contrary, Rosen [32] suggests that introducing more than one ionic group on surfactant species will result in increased electrostatic repulsion in the surface region, and hence increase

[14]The exact same sample, «ENORDET O342 (Drum # E)»

in the volume available for alcohol solubilization. This seem balanced by other factors, likely to include the factors described above.

It would be interesting to observe how the variation of (average) molecular weight of surfactant would affect the solubilization parameters in IOS. This dependence may give insight into the reliability of using the average molecular weight by Barnes et al. [3] in the thermodynamic approach.

α is dependent on molecular weight of surfactant via m_S in Equation 3.42. However, by continuously iterating K_X^o to adjust for various inputs of molecular weight of surfactant, the slope of V_2^o/K_2^o versus α remains constant. This in turn means that $V_{2,mic}^o$ and $K_{2,mic}^o$, and therefore also ΔV_2^o and ΔK_2^o, are all independent of molecular weight of the surfactant, thus bypassing this issue concerning the ambiguity in molecular weight of surfactant.

The dependence of molecular weight of surfactant on K_X^o is on the other hand present. Using 1-pentanol in IOS 1923 as an example, a molecular weight in the range 295 $gmol^{-1}$ ± 1 %, ± 5 % and ± 10 % would give an estimate of K_X^o in the approximate range of 436 ± 5 , 436 ± 23 and 436 ± 45, respectively. Notice that the variation in molecular weight is directly proportional to the variation in K_X^o. In other words, x % variation in molecular weight results in x % variation in K_X^o. From the main results presented in Table 4.1, K_X^o is determined to 436 ± 30 in the case for 1-pentanol in IOS 1923. Variation in average molecular weight of approximately ± 7 % (range 295 ± 21 $gmol^{-1}$) would just fall outside this limit of estimated uncertainty. This unravels the small dependence of the molecular weight of surfactant on K_X^o, and may justify the interpretation of K_X^o by applying the average molecular weight of surfactant presented by Barnes et al. [3] .

4.2.4 Standard Partial Molar Volume and Isentropic Compressibility in Micellar Pseudophase

Questions were raised regarding the validity of $K_{2,w}^o$ for 3-hexanol presented in paper by Høiland et al. [11]. This value is reported as $2.8 \cdot 10^{-4}$ $cm^3 mol^{-1} bar^{-1}$, being significantly larger than that reported for 1-hexanol ($0.5 \cdot 10^{-4}$ $cm^3 mol^{-1} bar^{-1}$) and 2-hexanol ($-1.2 \cdot 10^{-4}$ $cm^3 mol^{-1} bar^{-1}$) [11]. One would initially, at least in simple terms, imagine 3-hexanol distorting the water structure to a less degree due to its more compact steric nature, and hence, be less compressible in pure water. The decreasing trend of $K_{2,w}^o$ with locating the

hydroxyl group further down the alkyl chain, is observed among primary to tertiary pentanol and -heptanol [11]. An attempt were made to give an accurate estimate of $K^o_{2,w}$ for 3-hexanol, based on the thermodynamic approach. $K^o_{2,w}$ for 3-pentanol, and $V^o_{2,w}$ for both 3-pentanol and 3-hexanol were also determined, and compared to values reported elsewhere [11, 84]. This to ensure accuracy in the obtained values. Results are presented in Table 4.6 (and also among others in Table 4.5).

Table 4.6: Standard partial molar volume and isentropic compressibility for 3-alcohols in pure water. Parameters are given in units of cm^3mol^{-1} and 10^4 $cm^3mol^{-1}bar^{-1}$, respectively. The value determined in this investigation are given in bold, for clarity.

	3-PentOH	3-HexOH
$V^o_{2,w}$	**101.3***, 101.3[a]	**117.2***, 117.1[b]
$K^o_{2,w}$	**-1.6***, −1.6[a]	**-2.7***, 2.8[b]

a - Høiland [84].

b - Høiland et al. [11].

* $\pm$ 0.2

$V^o_{2,w}$ for 3-pentanol and 3-hexanol, and $K^o_{2,w}$ for 3-pentanol, are all practically equal to their corresponding values reported elsewhere. On the other hand, a large inconsistency is observed in $K^o_{2,w}$ for 3-hexanol, where the value obtained in this investigation ($-2.7 \cdot 10^{-4}$ $cm^3mol^{-1}bar^{-1}$) is significantly less than that reported previously ($2.8 \cdot 10^{-4}$ $cm^3mol^{-1}bar^{-1}$) [11]. As already mentioned, the choice of $K^o_{2,w}$ affects $K^o_{2,mic}$ as well as K^o_X, the two latter being determined from K^o_2 versus α. Using K^o_w for 3-hexanol with value $2.8 \cdot 10^{-4}$ $cm^3mol^{-1}bar^{-1}$ results in $K^o_{2,mic}$ equal to $64.6 \cdot 10^{-4}$ $cm^3mol^{-1}bar^{-1}$ and K^o_X equal to 357. This is in comparison to respective values of $58.8 \cdot 10^{-4}$ $cm^3mol^{-1}bar^{-1}$ and 525, using $K^o_{2,w}$ for 3-hexanol obtained in this investigation.

$V^o_{2,mic}$ for 1-pentanol in IOS 1923 and in IOS 2024 and 1-hexanol in IOS 1923 are greater than $V^o_{2,w}$, and less than $V^o_{2,oct}$ (See Table 4.5). $V^o_{2,mic}$ do probably not vary significantly between terminal and non-terminal alcohol compared to the variation between the respective properties in water and octane. It is believed to be safe to claim that $V^o_{2,mic} < V^o_{2,oct}$ for non-terminal pentanols and hexanols as well. Much of the same discussion can be reasoned concerning $K^o_{2,mic}$, it being significantly greater than $K^o_{2,w}$ and likely to be less than $K^o_{2,oct}$, for all the alcohols. These observations and reasonings support the presence of both hydrophilic and hydrophobic interactions for alcohol solubilized in micellar pseudophase of IOS, and is additionally supported by values of ΔY^o_2 being positive. It could then further be reasoned that at least some part of the alcohol must be accommodated close to the micellar surface, where the concentration of

water and ionic head groups are non-negligible. An interesting observation is that $V^o_{2,mic}$ and $K^o_{2,mic}$ in IOS 1923 and in SDS are both less than the corresponding molar property Y^*. $K^o_{2,mic}$ for 1-pentanol in IOS 2024 is on the other hand not only similar, but also slightly larger than K^*. The former and latter parameter having values of 89.8 and $82.6 \cdot 10^{-4}$ $cm^3 mol^{-1} bar^{-1}$, respectively. An obvious distinction between micellar pseudophase and liquid alcohol is the more orderly arrangement in the former. Various degree of hydration in the palisade layer as well as presence of electrolytes[15] is absent in liquid alcohol, which are also distinct features between the two solvents. However, any similarity of $V^o_{2,mic}$ to V^*, and $K^o_{2,mic}$ to K^*, would be in support of the palisade layer as the solubilizing environment for the alcohols.

$V^o_{2,mic}$ and $K^o_{2,mic}$ are both less in IOS 1923 compared to what is reported in SDS, comparing each individual alcohol in each of the systems, for which values in both systems have been presented. This suggests hydrophilic interactions being more dominant for 1-pentanol and hexanols in IOS 1923 compared to SDS. On the contrary, $V^o_{2,mic}$ and $K^o_{2,mic}$ for 1-pentanol in IOS 2024 are significantly greater compared to the respective parameters in SDS.

The solubilizing environment for alcohols in IOS may again be related to the very nature of the IOS surfactant. On the basis of Figure 1.1, illustrating the main generic structures of IOS surfactants, there is more than one head group on all but one of the main generic structures. It is thus highly likely that a IOS aggregate have a large concentration of ionic head groups associated with the micellar surface, thus giving rise to additional interactions between surfactant head groups and solubilized alcohol. A more disordered packing in the palisade layer is also highly likely, due to the steric nature and mixture of various species in IOS. If n and/or $m > 0$ (Figure 1.1) for a large distribution of surfactant species constituting the micellar aggregate, the packing in the palisade layer of IOS is likely to be less dense overall. Both these observations would support reasoning a more hydrophilic solubilization environment. A disordered structure may also reason the lesser K^o_X observed in IOS due to less favourable alignment in the palisade layer. More labile micelles resulting in less distribution and lower $V^o_{2,mic}$, due to greater hydration of micelles, have been proposed by Hétu et al. [88] to explain both parameters of benzene being lower in OABr[16] compared to in SDS. It should however be noted that the structural difference between IOS and SDS is much greater than between OABr and SDS. A disordered packing and strong interaction among surfactant head groups may also allow for greater hydration in the palisade layer, although some of this water is expected to be excluded upon solubilization of alcohol. Additional hydrophilic interactions between water and alcohol will be present under

[15] and free oil in the case for IOS.

[16] OABr - Octylammonium hydrobromide.

this assumption. The difference in $V^o_{2,mic}$ and $K^o_{2,mic}$ for a given individual alcohol in IOS 1923, IOS 2024 and SDS may otherwise be reasoned if the degree of penetration in the micellar aggregates is different, as the concentration of water and ions are expected to lessen in direction towards the micellar core. On the contrary, one would initially imagine that the twin-tailed nature of the IOS surfactant would result in a more hydrophobic solubilization environment for the alcohols. Additionally, the screening of surfactant head groups by sodium sulfite and hydroxyl groups, would result in more dense packing in the palisade layer.
$V^o_{2,mic}$ and $K^o_{2,mic}$ in IOS must be a balance of several factors, which is likely to include some of all these just mentioned.

The difference between $Y^o_{2,mic}$ of any of two isomers among pentanols or hexanols, represent the change in the parameter due to the process of alcohol molecule undergoing isomerisation. This reaction involves removing the hydroxyl group from its current position and relocating it in the new position, all within the micellar pseudophase. In the same way as different isomers of an alcohol will influence the micellar pseudophase differently, the isomerisation reaction will also trigger rearrangement within the micellar pseudophase and in the ternary system in general. This rearrangement is reflected in the isomerisation contribution to $Y^o_{2,mic}$.
$K^o_{2,mic}$ is lower in IOS 1923 for both 2-hexanol and especially 3-hexanol compared to their respective individual pentanols. However, $K^o_{2,mic}$ is much larger for 1-hexanol compared to 1-pentanol. Large differences between $K^o_{2,w}$ for isomeric additives in general are not uncommon according to Hedwig et al. [89], and significant variation is present among $V^o_{2,mic}$ and $K^o_{2,mic}$ for alcohols in model surfactant systems, as well as in IOS 1923. Both $V^o_{2,mic}$ and $K^o_{2,mic}$ in IOS 1923 decrease in the order 1-hexanol, 2-hexanol, 3-hexanol, corresponding with the trend reported for hexanols in SDS. This decreasing trend is however inconsistent with the trend observed for pentanols in IOS 1923, the latter systems not even being systematic among any of the three parameters, K^o_X, $V^o_{2,mic}$ and $K^o_{2,mic}$. $K^o_{2,mic}$ decrease in the order 3-pentanol, 2-pentanol, 1-pentanol, reverse of what is initially expected and for hexanols in IOS 1923. $V^o_{2,mic}$ decrease in the order 2-pentanol, 1-pentanol, 3-pentanol. If $K^o_{2,mic}$ is regarded as a more reliable solubilization parameter than $V^o_{2,mic}$, based on its lesser error by greater relative variation and negligible intrinsic contribution, then $K^o_{2,mic}$ for pentanols is inversely proportional to K^o_X. Still discarding $V^o_{2,mic}$ for the moment, the trend of K^o_X decreasing and $K^o_{2,mic}$ increasing with substituting the hydroxyl group further down the alkyl chain of pentanol, is highly peculiar and difficult to explain. A positive correlation between K^o_X and $K^o_{2,mic}/V^o_{2,mic}$ is generally observed among terminal and non-terminal alcohol analogues in model surfactant systems [11], due to

more dense packing in the palisade layer for alcohols which are expected to align favourable in-between micellized surfactant.

What might be observed in the case for medium-chained alcohols in IOS 1923 is a transition in the nature of solubilization behaviour, going from pentanol to hexanol in IOS 1923. The extension of the region of the micelles which would be considered more "core-like" would depend on the nature of the surfactant, including type of head group and surfactant tail length, and their packing. This means that the imaginary interface separating the palisade layer from the core-region, would have a location depending on the properties of the surfactant. As reasoned previously comparing SDS and IOS, the IOS surfactant systems may have greater concentration of surfactant head groups. These would interacting more extensively with the solubilized alcohol and may allow greater hydration in the palisade layer. If this is indeed the real case, it would be reasonable that the palisade layer has a greater extension towards the inner parts of the micelle. This could also explain the lesser $V^o_{2,mic}$ and $K^o_{2,mic}$ observed in IOS. It is generally considered that, while medium-chain alcohols associate with the palisade layer, increasing the alkyl chain of alcohol results in deeper penetration and greater extension towards the core region of the micelle [32, 41]. The trend for hexanols in IOS 1923 behave corresponding to what is generally observed for model surfactants, suggesting that at least some of its alkyl chain is associated with the deeper parts of the micelle, and even into the micellar core region. It might be that pentanols in IOS are significantly less or insignificantly associated with this region.

De Lisi et al. [1] presents $V_{2,mic}$ for 0.05 m 1-pentanol in DeTAB[17] (C10) to CTAB[18] (C16) increasing in the range $107.4 - 108.0\ cm^3mol^{-1}$, while $K_{2,mic}$ in DTAB (C12) to CTAB (C16) increase in the range $67.2 - 75.7 \cdot 10^{-4}\ cm^3mol^{-1}bar^{-1}$. The narrowness of these volume- and compressibility intervals, with a relatively large variation in surfactant chain length, is not consistent with our observation comparing 1-pentanol in IOS 1923 and IOS 2024. First of all, $V^o_{2,mic}$ and $K^o_{2,mic}$ for 1-pentanol differs greatly between the two IOS surfactants, difference in values being $2.4\ cm^3mol^{-1}$ and $30.9 \cdot 10^{-4}\ cm^3mol^{-1}bar^{-1}$, respectively. Both parameters are however larger in IOS 2024, consistent with the trends reported for trimethylammonium bromides, but inconsistent with trends of trimethylammonium chlorides [1]. This comparison between IOS surfactants is in what is suppose to be a much more narrow variation of surfactant chain length, approximately C19-23 and C20-24. The large variation in values by only slightly shifting the interval of olefin cuts of IOS suggest that additional factors affect the solubilization parameters between the two systems. This may very well be dominated by differences in

[17]DeTAB - Decyltrimethylammonium bromide.
[18]CTAB - Cetyltrimethylammonium bromide.

the surface regions of the micelles of each IOS surfactant, and can in turn be reflected in the composition of various species constituting the IOS samples. From Figure 1.3, there is a significant difference in abundance of hydroxyalkane sulfonate, alkene sulfonate and disulfonate in IOS 1923 and IOS 2024, the latter having generally greater abundance of hydroxyalkane sulfonate relative to the two other groups of species. Such differences in composition is probable between our IOS samples as well. The difference in composition seems to also be reflected in the average molecular weight of the IOS samples, being slightly less for IOS 2024 (287 $gmol^{-1}$) compared to IOS 1923 (295 $gmol^{-1}$). This is opposite of what would be expected for a batch which on average contain slightly longer olefin chains. It is thus likely this variation in species discards the assumption of equal surface regions of the micelles of IOS 1923 and IOS 2024, and that differences in K_X^o and $V_{2,mic}^o/K_{2,mic}^o$ for 1-pentanol between the two surfactant systems is less significantly or insignificantly governed by shift in approximate olefin chain interval for IOS.

5 Conclusion

Investigations concerning ternary systems of primary to tertiary pentanols and hexanols in IOS 1923 and 1-pentanol in IOS 2024 have been performed.

Results reveal presence of mixed hydrophilic-hydrophobic interactions for alcohols in micellar pseudophase of IOS, based on positive ΔV_2^o and ΔK_2^o, and also from comparing $V_{2,mic}^o$ and $K_{2,mic}^o$ to corresponding parameters in other solvent systems.

K_X^o for alcohols in IOS 1923 and in IOS 2024 are all less compared to reported values in SDS, and results suggest solubilized alcohol are on average experiencing a less hydrophobic environment in IOS 1923, for which values in both IOS 1923 and SDS are presented. The contrary is observed for 1-pentanol solubilized in IOS 2024, where the average solubilization environment seem more hydrophobic relative to in SDS. These observations may, at least in parts, be reasoned by considering the nature of the IOS surfactants.

Substituting the hydroxyl group from terminal to tertiary position on pentanol and on hexanol in IOS 1923 reveal some similarities with the trends of solubilization parameters reported in SDS, for which values have been compared. However, abnormalities are observed. Especially worthy of highlighting is the trend of decrease in K_X^o and increase in $K_{2,mic}^o$ going from 1-pentanol to 3-pentanol.

Comparing parameters for 1-pentanol in IOS 1923 and IOS 2024 do not correspond well with observations of varying surfactant chain length of model surfactants, and may suggest that dissimilarities between the two IOS samples overrides the effect of slightly shifting the interval of olefin cuts.

While $V_{2,mic}^o$ and $K_{2,mic}^o$ are independent of molecular weight of surfactant, the effect on K_X^o is surprisingly small. This supports the using the average molecular weight of surfactant presented by Barnes et al. [3] for determination of K_X^o.

References

[1] R. De Lisi; S. Milioto. *Thermoynamics of Solubilization of Polar Additives in Micellar Solutions*, volume 55 of *Surfactant Science Series*, chapter 3. Marcel Dekker, Inc, 1995.

[2] R. De Lisi; S. Milioto. Thermodynamic properties of additive-surfactant-water ternary systems. *Chem. Soc. Rev.*, 23(1):67 – 73, 1994.

[3] J. R. Barnes; H. Dirkzwager; J. R. Smit; J. P. Smit; A. On; R. C. Navarrete; B. H. Ellison; M. A. Buijse, editor. *Application of Internal Olefin Sulfonates and Other Surfactants to EOR. Part 1: Structure - Performance Relationships for Selection at Different Reservoir Conditions*, SPE Improved Oil Recovery Symposium, 2010. Shell Global Solutions International/Shell Global Solutions US/Shell Exploration and Production, Society of Petroleum Engineers.

[4] Shell chemicals - enordet product overview. `http://www.shell.com/chemicals/products-services/our-products/alpha-olefins-detergent-alcohols/enordet-surfactants/product-oveview.html`, 2013.

[5] J. R. Barnes; J. P. Smit; J. R. Smit; H. Shpakoff; K. H. Raney; M. C. Puerto, editor. *Development of Surfactants for Chemical Flooding at Difficult Reservoir Conditions*, SPE Improved Oil Recovery Symposium, 2008. Shell Global Solutions International/Shell Global Solutions US/Rice University, Society of Petroleum Engineers.

[6] P. Zhao; A. C. Jackson; C. Britton; D. H. Kim; L. N. Britton; D. B. Levitt; G. A. Pope, editor. *Development of High-Performance Surfactants for Difficult Oils*, SPE Improved Oil Recovery Symposium, 2008. University of Texas, Society of Petroleum Engineers.

[7] Enordet surfactants for enhanced oil recovery. `http://www.shell.com/chemicals/products-services/our-products/alpha-olefins-detergent-alcohols/enordet-surfactants.html`, 2013.

[8] R. Zana; S. Yiv; C. Strazielle; P. Lianos. Effect of alcohol on the properties of micellar systems: I. critical micellization concentration, micelle molecular weight and ionization degree, and solubility of alcohols in micellar solutions. *J. Colloid Interface Sci.*, 80(1):208 – 223, 1981.

[9] C. S. Dunaway; S. D. Christian; J. F. Schamehorn. *Overview and History of the Study of Solubilization*, volume 55 of *Surfactant Science Series*, chapter 1. Marcel Dekker, Inc, 1995.

[10] H. B. Klevens. Solubilization. *Chem. Rev.*, pages 1–74, 1950.

[11] H. Høiland; A. M. Blokhus. Solubilization in aqueous surfactant systems. In *Handbook of Surface and Colloid Chemistry*, chapter 8, pages 379–410. 3th edition.

[12] J. C. Harris. Solubilization - a micellar phenomenon. *J. Am. Oil Chem. Soc.*, 35(8):428–435, 1958.

[13] M. Bourrel; R. S. Schechter, editor. *The R-Ratio*, volume 30 of *Surfactant Science Series*, chapter 1. Marcel Dekker, Inc, 1988.

[14] J. W. McBain; P. H. Richards. Solubilization of insoluble organic liquids by detergents. *Ind. Eng. Chem.*, 38(6):642–646, 1946.

[15] Iupac gold book online - micellar solubilization. `http://goldbook.iupac.org/M03887.html`, 2012.

[16] D. G. Marangoni; J. C. T. Kwak. *Comparison of Experimental Methods for the Determination of the Partition Coefficient of n-Alcohols in SDS and DTAB Micelles*, volume 55 of *Surfactant Science Series*, chapter 14. Marcel Dekker, Inc, 1995.

[17] M. L. McBain; E. Hutchinson. *Solubilization and Related Phenomena*. Academic Press, 1955.

[18] R. C. Merrill Jr.; J. W. McBain. Studies on solubilization. *J. Phys. Chem.*, 46(1):10–19, 1942.

[19] K. T. Valsaraj; A. Gupta; L. J. Thibodeux; D. P. Harrison. Partitioning of chloromethanes between aqueous and surfactant micellar phases. *Water Research*, 22(9):1173 – 1183, 1988.

[20] C. A. Miller. Solubilization in surfactant systems. In *Handbook of Surface and Colloid Chemistry*, chapter 9, pages 415–435. 3th edition.

[21] P. H. Elworthy; A. T. Florence; C. B. Macfarlane. *Solubilization by Surface-Active Agents and its Application*. Chapman & Hall, 1968.

[22] S. D. Christian; J. F. Scamehorn, editor. *Solubilization in Surfactant Aggregates*, volume 55 of *Surfactant Science Series*. Marcel Dekker, Inc, 1995.

[23] A. D. King. *Solubilization of Gases*, volume 55 of *Surfactant Science Series*, chapter 2. Marcel Dekker, Inc, 1995.

[24] N. Nishikido. *Solubilization in Mixed Micelles*, volume 55 of *Surfactant Science Series*, chapter 5. Marcel Dekker, Inc, 1995.

[25] M. Abe; K. Ogino. *Solubilization of Organic Compounds by Vesicles*, volume 55 of *Surfactant Science Series*, chapter 10. Marcel Dekker, Inc, 1995.

[26] P. N. Hurter; P. Alexandridis; T. A. Hatton. *Solubilization in Amphiphilic Copolymer Solution*, volume 55 of *Surfactant Science Series*, chapter 6. Marcel Dekker, Inc, 1995.

[27] A. J. Ward. *Kinetics of Solubilization in Surfactant-Based Systems*, volume 55 of *Surfactant Science Series*, chapter 7. Marcel Dekker, Inc, 1995.

[28] G. M. Førland; J. Samseth; M. I. Gjerde; H. Høiland; A. Ø. Jensen; K. Mortensen. Influence of alcohol on the behavior of sodium dodecylsulfate micelles. *J. Colloid Interface Sci.*, 203(2):328–334, 1998.

[29] R. Zana. Aqueous surfactant - alcohol systems: A review. *Adv. Colloid Interface Sci.*, 57(1):1 – 64, 1995.

[30] M. Bourrel; R. S. Schechter, editor. *Structure of Aqueous Solutions of Amphiphiles*, volume 30 of *Surfactant Science Series*, chapter 2. Marcel Dekker, Inc, 1988.

[31] R. Nagarajan. Solubilization by amphiphilar aggregates. *Curr. Opin. Colloid Interface Sci.*, 2(3):282–293, 1997.

[32] M. J. Rosen; J. T. Kunjappu. *Surfactants and Interfacial Phenomena*. Wiley, 4th edition, 2012.

[33] B. Jönsson; M. Landgren; G. Olofsson. *Solubilization of Uncharged Molecules in Ionic Micellar Solutions: Toward an Understanding at the Molecular Level*, volume 55 of *Surfactant Science Series*, chapter 4. Marcel Dekker, Inc, 1995.

[34] R. De Lisi; S. Milioto. Thermodynamic properties of pentanol in dodecyltrimethylammonium bromide aqueous solutions. *J. Colloids Surf.*, 35(2):309 – 323, 1989.

[35] E. Vikingstad. Partial molar volumes and compressibilities of n-alcohols in micellar solution of sodium alkylcarboxylates. *J. Colloid Interface Sci.*, 72(1):75 – 80, 1979.

[36] K. Hayase; S. Hayano. Effect of alcohols on the critical micelle concentration decrease in the aqueous sodium dodecyl sulfate solution. *J. Colloid Interface Sci.*, 63(3):446 – 451, 1978.

[37] P. Lianos; R. Zana. Surfactant-alcohol mixed-micelle formation: Cetyltrimethylammonium bromide-1-butanol system. *Chem. Phys. Lett.*, 72(3):171 – 175, 1980.

[38] A. Graciaa; J. Lachaise; C. Cucuphat; M. Bourrel; J. L. Salager. Improving solubilization in microemulsions with additives. 2. long chain alcohols and lipophilic linkers. *Langmuir*, 9:3371–3374, 1993.

[39] T. J. Ward; K. D. Ward. *Solubilization in Micellar Separations*, volume 55 of *Surfactant Science Series*, chapter 16. Marcel Dekker, Inc, 1995.

[40] P. Stilbs. *Solubilization, As Studied by Nuclear Spin Relaxation and NMR-Based Self-Diffusion Techniques*, volume 55 of *Surfactant Science Series*, chapter 11. Marcel Dekker, Inc, 1995.

[41] M. Bourrel; R. S. Schechter, editor. *Solubilization*, volume 30 of *Surfactant Science Series*, chapter 7, page 335 – 395. Marcel Dekker, Inc, 1988.

[42] M. S. Akhter. Effect of solubilization of alcohols on critical micelle concentration of non-aqueous micellar solutions. *Colloids Surf., A*, 157(1-3):203 – 210, 1999.

[43] C. Treiner. *The Partitioning of Neutral Solutes between Micelles and Water As Deduced from Critical Micelle Concentration Determinations*, volume 55 of *Surfactant Science Series*, chapter 12. Marcel Dekker, Inc, 1995.

[44] G. Broze. *Solubilization and Detergency*, volume 55 of *Surfactant Science Series*, chapter 15. Marcel Dekker, Inc, 1995.

[45] J. C. Berg. *An Introduction to Interfaces & Colloids - The Bridge to Nanoscience*. World Scientific, 2010.

[46] P. Lianos; J. Lang; R. Zana. Fluorescence probe study of oil-in-water microemulsions. 2. effect of the nature of the alcohol, oil, surfactant on the surfactant aggregation number in the aggregates. *J. Phys. Chem.*, 86(24):4809 – 4814, 1982.

[47] Mettler Toledo, Switzerland. *A Quantum Leap: The New Microbalances and Analytical Balances*, May 2000.

[48] Mettler Toledo, Switzerland. *Operating Instructions - Mettler Analytical Balance AE240 Dual Range Balance.*

[49] Operating instructions kern eg/ew. `http://www.direct-scale.com/fic_bdd/catalogue_fichier_en_fichier/BA_EW_gb.pdf`, 2003.

[50] I. M. S. Lampreia; C. A. Nieto de Castro. A new and reliable calibration method for vibrating tube densimeters over wide ranges of temperature and pressure. *J. Chem. Therm.*, 43(4):537 – 545, 2011.

[51] A. Furtado; E. Batista; I. Spohr; E. Filipe. *Measurement of Density Using Oscillation-Type Density Meters - Calibration, Traceability and Uncertainties.* Instituto Portugûes da Qualidade (IPQ), Portugal.

[52] L. Hnědkovský; I. Cibulka. An automated vibrating-tube densimeter for measurements of small density differences in dilute aqueous solutions. *Int. J. Thermophys.*, 25(4):1135 – 1142, 2004.

[53] S. A. Dyer, editor. *Survey of Instrumentation and Measurement.* Wiley-Interscience, 2001.

[54] S. K. Singh. *Industrial Instrumentation and Control.* Tata-McGraw-Hill, 3rd edition, 2009.

[55] WaMo a/s. *Operation Manual - Digital Precision Density Measurement System for Liquid and Gases, External Measuring Cells.*

[56] Anton Paar. *DMA 60 + DMA 602 - High-Precision Digital Density Measuring System for Liquids and Gases.*

[57] A. Cooper, editor. *Biophysical Chemistry.* Royal Society of Chemistry, 2 edition, 2011.

[58] E. Alagic. Ultralydsmålinger under høyt trykk - en undersøkelse av solubilisering av 1-heksanol i natrium dodecylsulfat som funksjon av trykk. Master's thesis, University of Bergen, 2005.

[59] E. Høgseth; G. Hedwig; H. Høiland. Rubidium clock sound velocity meter. *Rev. Sci. Instrum.*, 71(12):4679 – 4680, 2000.

[60] E. P. Papadakis. New, compact instrument for pulse-echo-overlap measurement of ultrasonic wave transit times. *Rev. Sci. Instrum.*, 47(7):806 – 813, 1976.

[61] E. Høgseth. Ultralyd tips. Unpublished - Personal notes.

[62] G. Douhhret; M. I. Davis; J. C. R. Reis; I. J. Fjellanger; M. B. Vaage; H. Høiland. Aggregative processes in aqueous solutions of isomeric 2-butoxyethanols at 298.15 k. *Phys. Chem. Chem. Phys.*, 4(24):6034–6042, 2002.

[63] J. C. R. Reis; G. Douheret; M. I. Davis; I. J. Fjellanger; H. Hoiland. Isentropic expansion and related thermodynamic properties of non-ionic amphiphile–water mixtures. *Phys. Chem. Chem. Phys.*, 10(4):561 – 573, 2008.

[64] D. Pandey; S. Pandey. *Ultrasonics: A Technique of Material Characterization*, chapter 18. Acoustic Waves. InTech, 2010.

[65] V. A. Del Grosso; C. W. Mader. Speed of sound in pure water. *J. Acoust. Soc. Am.*, 52(5B):1442–1446, 1972.

[66] C. Minero; E. Pelizzetti. The generalized pseudophase model: Treatment of multiple equilibria in micellar solutions. *Pure Appl. Chem.*, 65(12):2573 – 2582, 1993.

[67] H. Wennerström; B. Lindman. Micelles. physical chemistry of surfactant association. *Phys. Rep.*, 52(1):1 – 86, 1979.

[68] S. J. Dougherty; J. C. Berg. Distribution equilibria in micellar solutions. *J. Colloid Interface Sci.*, 48(1):110 – 121, 1974.

[69] P. M. Holland; D. N. Rubingh, editor. *Mixed Surfactant Systems - An Overwiew*, volume 501 of *Symposium Series*, chapter 1, pages 2 – 30. Am. Chem. Soc., 1992.

[70] P. M. Holland. Nonideal mixed micellar solution. *Adv. Colloid Interface Sci.*, 26:111 – 129, 1986.

[71] K. Shinoda; E. Hutchinson. Pseudo-phase separation model for thermodynamic calculations on micellar solutions. *J. Phys. Chem.*, 66(4):577 – 582, 1962.

[72] D. P. Cistola; D. M. Small. On micelle formation and phase separation. *J. Am. Chem. Soc.*, 112(18):3214 – 3215, 1990.

[73] J. F. Scamehorn, editor. *An Overview of Phenomena Involving Surfactant Mixtures*, volume 311 of *Symposium Series*, chapter 1, pages 1 – 27. Am. Chem. Soc., 1986.

[74] P. Atkins; J. De Paula. *Atkins' Physical Chemistry*. Oxford University Press, 8th edition, 2006.

[75] G. A. Krestov. Thermodynamics and structure of solutions. *J. Struct. Chem.*, 25(2):252–258, 1984.

[76] M. Asif. Notes - thermodynamics. Govt. College Sahiwal, Pakistan, 2011.

[77] M. I. Davis; G. Douheret; J. C. R. Reis; M. J. Blandamer. Apparent and partial ideal molar isentropic compressibilities of binary liquid mixtures. *Phys. Chem. Chem. Phys.*, 3(20):4555 – 4559, 2001.

[78] J. C. R. Reis. New thermodynamic relations concerning apparent molar isentropic compression and apparent and partial isentropic compressibilities. *J. Chem. Soc. Faraday Trans.*, 94(16):2385–2388, 1998.

[79] G. Douheret; M. I. Davis; J. C. R. Reis; M. J. Blandamer. Isentropic compressibility - experimental origin and the quest for their rigorous estimation in thermodynamically ideal liquid mixtures. *Chem. Phys. Phys. Chem.*, 2(3):148 – 161, 2001.

[80] M. J. Blandamer; M. I. Davis; G. Douheret; J. C. R. Reis. Apparent molar isentropic compressions and expansions of solutions. *Chem. Soc. Rev.*, 30(1):8 – 15, 2001.

[81] H. Høiland; M. I. Gjerde; C. Mo; E. Lie. Solubilization of alcohols in sds and ttab from isentropic partial molar compressibilities and solubilities. *Colloids Surf.*, 183 - 185:651–660, 2001.

[82] T. V. Chalikian; A. P. Sarvazyan; K. J. Breslauer. Partial molar volumes, expansibilities, and compressibilities of α,ω-aminocarboxylic acids in aqueous solutions between 18 and 55 deg c. *J. Phys. Chem.*, 97(49):13017 – 13026, 1993.

[83] R. De Lisi; S. Milioto. Excess enthalpies of solution of some primary and secondary alcohols in sodium dodecylsulfate micellar solutions. *J. Sol. Chem.*, 17(3):245 – 265, 1988.

[84] H. Høiland. Unpublished - Personal Notes.

[85] R. De Lisi; C. Genova; R. Testa; V. T. Liveri. Thermodynamic properties of alcohols in a micellar phase. binding constants and partial molar volumes of pentanol in sodium dodecylsulfate micelles at 15, 25, and 35 deg.c. *J. Sol. Chem.*, 13(2):121 – 150, 1984.

[86] T. Gilje. Surface tension and counterion binding of micellar systems - comparison of sds and commercial surfactants. Master's thesis, Centre for Integrated Petroleum Research/University of Bergen, 2013.

[87] R. J. Farn, editor. *Chemistry and Technology of Surfactants*. Blackwell Publishing, 2006.

[88] D. Hétu; A. H. Roux; J. E. Desnoyers. Application of a chemical equilibrium model to the volumes and heat capacities of transfer of benzene from water to aqueous solutions of surfactants. *J. Colloid Interface Sci.*, 122(2):418 – 429, 1988.

[89] G. R. Hedwig; H. Høiland. Thermodynamic properties of peptide solutions. part 11. partial molar isentropic pressure coefficients in aqueous solutions of some tripeptides that model protein side-chains. *J. Sol. Chem.*, 49(2):175 – 181, 1994.

[90] R. De Lisi; A. Lizzio; S. Milioto; V. T. Liveri. Binding constants and partial molar volumes of primary alcohols in sodium dodecylsulfate micelles. *J. Sol. Chem.*, 15(8):623 – 648, 1986.

[91] S. Milioto; R. Crisantino; R. De Lisi. Thermodynamics of solubilization of pentanol in sodium dodecyl sulfate-dodecyldimethylamine oxide mixed micelles. *J. Colloid Interface Sci.*, 66(2):356–362, 1994.

A Comparison with De Lisi et al.

It could be of interest to highlight the simplifications made compared to the approach by De Lisi et al. [1, 2]. Only a brief summary is presented here, and the reader is referred to [1] for a detailed description.

The final expression presented by the authors is one similar to Equation 3.35, although slightly more accurate [81]. They have shown that contribution to partial molar properties include (1) distribution of additive between the two phases, (2) additive-surfactant interactions in both micellar and aqueous phase, and (3) the additive effect on shift in micellization equilibrium [83]. The latter of the three effects is a result of additives acting as co-surfactants, thus reducing the cmc of the surfactant. In response, a shift in the equilibrium for surfactants between monomeric and micellized state is initiated [1]. Naturally, there will also be a shift in alcohol distribution towards micellar pseudophase [81], as alcohols substitute some of the micellized surfactant. A review of the the general effects of additives on cmc is given by Treiner [43].

Generally, distribution coefficients obtained from this approach are in agreement with literature values determined by other, both direct and indirect methods [83]. It is interesting to observe that the authors apply a stepwise mass action model rather than the pseudophase model for distribution of additive [34, 83], and that the distribution coefficient is determined based on partial molar volume rather than partial molar compressibility, at least in some studies [34, 90, 85]. Micellization is treated according to the pseudophase model.

By concerning the additive-surfactant-water ternary system and surfactant-water binary system, the following equation is derived [1],

$$Y_2 = \alpha_{ma} Y_{2,mic} + (1 - \alpha_{ma}) Y_{2,Aq} + \frac{(m^*_{S,Aq} - m_{S,Aq})\Delta Y_m}{m_2} \tag{A.1}$$

where

$$\alpha_{ma} = \frac{K_b m_{S,mic}}{1 + K_b m_{S,mic}} \tag{A.2}$$

and ΔY_m is micellization property at cmc,

$$\Delta Y_m = Y_{S,mic} - Y_{S,Aq} \tag{A.3}$$

$m^*_{S,Aq}$: Unmicellized surfactant concentration in absence of additive.

$m_{S,Aq}$: Unmicellized surfactant concentration in presence of additive.

$m_{S,mic}$: Micellized surfactant concentration.

K_b: Binding constant (mass action model).

$Y_{S,mic}$: Partial molar property of micellized surfactant.

$Y_{S,Aq}$: Partial molar property of unmicellized surfactant.

The shift of micellization equilibrium is represented by the last term in Equation A.1. Concerning molal concentrations in this term, the following modification is valid at standard condition [2],

$$\lim_{m_2 \to 0} \frac{(m^*_{S,Aq}(cmc) - m_{S,Aq})}{m_2} = \left(\frac{cmc}{1+\nu} [2.3K_S + (1+\beta)K_b] \right)(1-\alpha_{ma}) = A_{cdc}(1-\alpha_{ma}) \quad \text{(A.4)}$$

where K_S is Setchenov's salting-out constant, and ν and β represent the degree of dissociation of unmicellized and micellized surfactant, respectively. Inserting Equation A.4 into Equation A.1 revels their final expression, which is a linear function of the fraction of additive solubilized in the aqueous phase, similar to $(1-\alpha)$ under the pseudophase approximation.

$$Y^o_2 = Y^o_{2,mic} - [(Y^o_{2,mic} - Y^o_{2,Aq}) - A_{cdc}\Delta Y_m](1-\alpha_{ma}) \quad \text{(A.5)}$$

where

$$A_{cdc} = \frac{cmc}{1+\nu}[2.3K_S + (1+\beta)K_b] \quad \text{(A.6)}$$

A_{cdc} can be readily calculated from Equation A.6 if the cmc, the degree of dissociation of surfactant in monomeric and micellized state and Setchenov's constant is known [91]. K_S is known to be negative (i.e. salting-in effect) for surfactant in presence of organic additives [43]. $Y_{2,Aq}$ can be correlated to the corresponding property in pure water $Y_{2,w}$ through the McMillan-Mayer approach [1], where only the interaction parameter between additive and surfactant $Y_{2/1}$ have been considered,

$$Y_{2,Aq} = Y_{2,w} + 2Y_{2/1}m_{S,Aq} \quad \text{(A.7)}$$

Higher ordered interaction terms can be included in this expression if necessary.

Equation A.5 is valid as it is stated for properties which are first derivative of Gibb's free energy, such as volume,

$$V_2^o = V_{2,mic}^o - [(V_{2,mic}^o - V_{2,Aq}^o) - A_{cdc}\Delta V_m](1 - \alpha_{ma}) \tag{A.8}$$

For properties that are second derivatives of Gibb's free energy, like isothermal compressibility, additional terms appear in the second derivative of Equation A.5.

$$\begin{aligned} K_2^T = K_{2,mic}^T + \left[(K_{2,Aq}^T - K_{2,mic}^T) + \Delta V_m \frac{\delta A_{cdc}}{\delta P} + A_{cdc}\Delta K_m^T\right](1 - \alpha_{ma}) \\ + \left[A_{cdc}\Delta V_m + V_{2,Aq}^o - V_{2,mic}^o\right](1 - \frac{\delta \alpha_{ma}}{\delta P}) \end{aligned} \tag{A.9}$$

Høiland et al. [81] highlights the relaxation term, $(\frac{\delta \alpha_{ma}}{\delta P})$, representing pressure effects on the amount additive solubilized in micellar pseudophase. This term is difficult to calculate due to the isentropic condition [81]. This term, along with the rest of the additional terms in Equation A.9, are believed to be negligible with respect to the total experimental error.

B Experimental Procedures

All glassware are washed and successively flushed with distilled water before used. The following procedure was developed and applied for all measurements of liquids.

B.1 Density Measurements

1. Rinse the inner part of a small syringe with sample to be introduced to the measuring cell.

2. Withdraw sample via the syringe. Remove air bubbles from the syringe and use care to avoid introducing air bubbles in the measuring cell.

3. Introduce the sample slowly and continuously until the first of the sample introduced is discharged at the outlet. Make sure the meniscus at the front is convex and vertically symmetric throughout the filling. Do not remove syringe prior to reading.

4. Let the sample reach thermal equilibrium with the thermostatting jacket for a couple of minutes until convergence of the output period is reached. The period is noted as an average of 3 readings within a interval of $\pm 10^{-6}$.

5. Remove syringe and flush tube with distilled water and thereafter ethanol. Let the tube dry in continuous flow of applied air for a minimum of 10 minutes.

Only step 4 (and step 5 prior to 4) was executed for determination of density of air. A was determined at the start of series of measurements and was regularly checked with distilled water after a sequence of 6 solutions or less.

B.2 Sound Velocity Measurements

1. Rinse the inner part of 10 mL syringe with sample to be introduced to the measuring cell.

2. Rinse the inner parts of the measuring cell with sample.

3. Introduce sample slowly to the measuring cell, starting from the silicon tube and upwards until approximately half of the sample chamber is filled with sample. Make sure no bubbles of air are present in the tube, and remove any if necessary. The best way to

observe bubbles is by submerging the silicon tube in a glass container filled with water and inspect visually through the glass container.

4. Fill the rest of the sample chamber. Remove possible air bubbles from the chamber wall by slowly and carefully swiping the syringe needle against the wall of the sample chamber in a rotating fashion. Successively remove air bubbles at the top of the sample by carefully swiping the long side of the needle across the top of the sample chamber. Apply some more sample to the chamber if necessary until the meniscus at the top is convex.

5. Carefully assemble the two parts of the cell.

6. Turn the cell upside down and back to get rid of excess pressure created during the assembly of the cell.

7. Recheck for air bubbles present in the silicon tube.

8. Connect the cell to the instrumentation and submerge the cell in the precision thermostat.

9. Perform a quick test measurement with 25 successive replicates of time determination to confirm that the cell is adequately filled and the instrument setting is appropriate for the measurement.

10. Let the sample reach thermal equilibrium with the thermostatting jacket for 30 minutes prior to performing measurements.

11. Perform three successive measurements each with 150 successive replicates of time determination. The three measurements are used to check for drift and consistency in values.

12. Remove cell from the precision thermostat. Disconnect and disassemble the cell. Rinse thoroughly with ethanol and thereafter distilled water.

Steps 1-12 were repeated for every successive sample to be measured. Calibration with distilled water was performed prior to measurements at least once within 24 hours of measurements. Calibration was also performed if any temperature adjustments were made or drift of more than $\pm 0.002^{o}C$ was observed from relative to the temperature of calibration.

C Error Analysis

y is a function of n independent variables x_1, x_2, ... , x_n, the absolute random error in y, Δy, can generally be expressed as

$$\Delta y = \sqrt{\sum_{i=1}^{n} \left(\frac{\delta y}{\delta x_i} \right)^2 \Delta x_i^2} \tag{C.1}$$

Equation C.1 can be simplified for special cases. For addition and subtraction the following are valid for estimation of error,

$$\Delta y = \sqrt{\sum_{i=1}^{n} \Delta x_i^2} \tag{C.2}$$

For multiplication and division, relative errors are used,

$$\frac{\Delta y}{y} = \sqrt{\sum_{i=1}^{n} \left(\frac{\Delta x_i}{x_i} \right)^2} \tag{C.3}$$

D Least Squares Analysis

If A is $m \times n$ and $\mathbf{b}$ is in $\Re^m$, a least-squares solution of $A\mathbf{x} = \mathbf{b}$ is an in $\Re^n$ such that

$$\|\mathbf{b} - A\| \leq \|\mathbf{b} - A\mathbf{x}\| \tag{D.1}$$

for all $\mathbf{x}$ in $\Re^n$.

$A\mathbf{x}$ is an approximation to $\mathbf{b}$ and the distance between the two is minimized to obtain a most approximate solution to $A\mathbf{x} = \mathbf{b}$. Under the condition that $\hat{\mathbf{x}}$ satisfies $A\hat{\mathbf{x}} = \hat{\mathbf{b}}$, the projection $\hat{\mathbf{b}}$ have the property that $\mathbf{b} - \hat{\mathbf{b}}$ is orthogonal to $Col\ A$, so $\mathbf{b} - A\hat{\mathbf{x}}$ is orthogonal to each column of A. The condition

$$A^T(\mathbf{b} - A\hat{\mathbf{x}}) = \mathbf{0} \tag{D.2}$$

$$A^T A\mathbf{x} = A^T\mathbf{b} \tag{D.3}$$

is satisfied and is a set of equations called normal equations, to which an approximate solution $\hat{\mathbf{x}}$ exists.

E Residuals of Linear Models of Density versus Alcohol Concentration

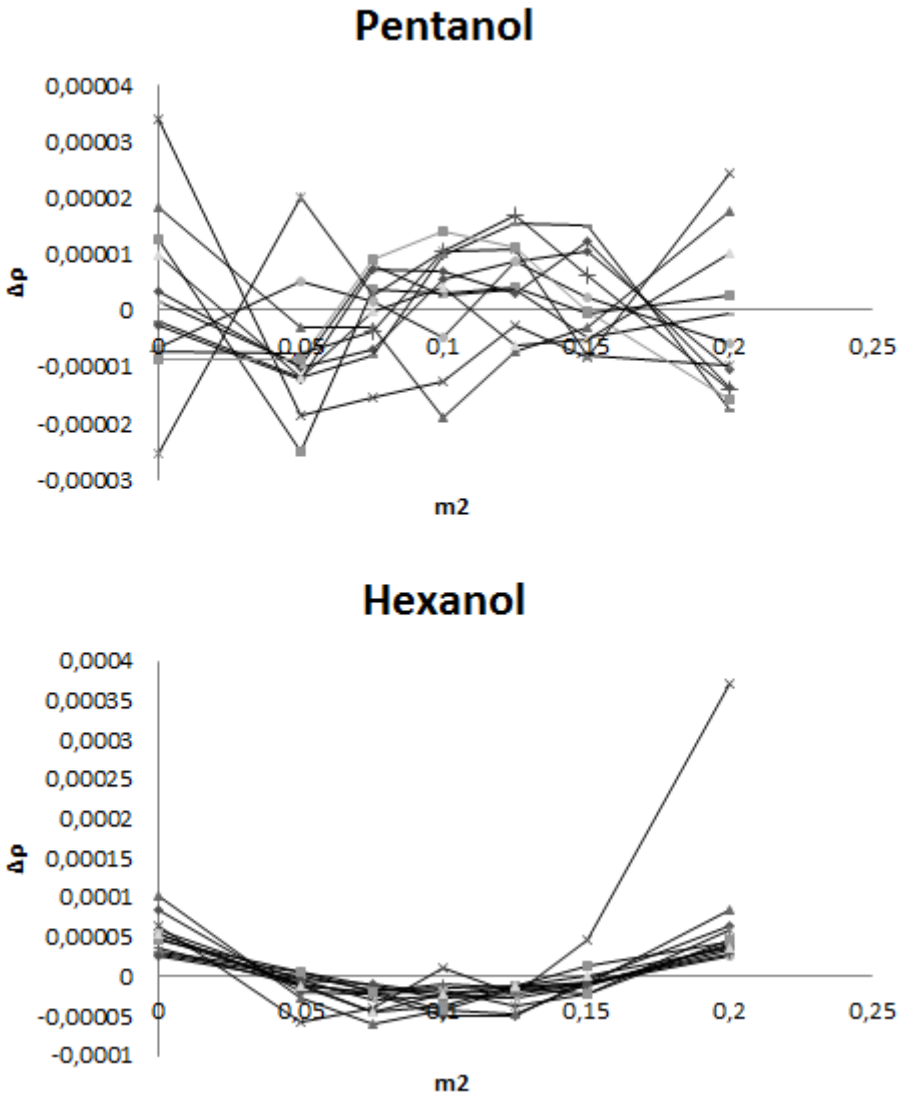

Figure E.1: Plot of residuals of density versus approximate alcohol concentration for pentanols (upper) and hexanols (lower) in IOS 1923. Make note of the obvious trends for hexanols, and also in instances for pentanols. This discards the proposal of using linear functions for modelling density versus alcohol concentration.

F Data and Models

Table F.1: **1-Pentanol in 0.0590 m IOS 1923:** Measured density ρ and sound velocity u, calculated adiabatic compressibility coefficient κ_S, gradients $(\frac{\delta\rho}{\delta m})$, $(\frac{\delta\kappa_S}{\delta m})$, partial and apparent molar volume and compressibility. Regression models for determination of partial molar volume and compressibility given at the lower end.

m	ρ	u	$\kappa_S \cdot 10^4$	$(\frac{\delta\rho}{\delta m_2})$	V_ϕ	V_2	$(\frac{\delta\kappa_S}{\delta m}) \cdot 10^4$	$K_\phi \cdot 10^4$	$K_2 \cdot 10^4$
$molkg^{-1}$	gcm^{-3}	ms^{-1}	bar^{-1}		cm^3mol^{-1}	cm^3mol^{-1}		$cm^3mol^{-1}bar^{-1}$	$cm^3mol^{-1}bar^{-1}$
0.0000	0.999396	1498.70	44.548	-0.0152	-	103.4_3	-2.5532	-	20.5_3
0.0470	0.998701	1501.10	44.437	-0.0151	103.0_5	103.5_0	-2.2432	22.1_2	23.4_4
0.0621	0.998472	1501.84	44.404	-0.0151	103.1_9	103.5_2	-2.1439	22.4_9	24.3_8
0.0950	0.997965	1503.36	44.336	-0.0151	103.4_4	103.5_8	-1.9275	23.5_4	26.4_5
0.1207	0.997575	1504.46	44.289	-0.0150	103.5_0	103.6_2	-1.7581	24.2_9	28.0_8
0.1474	0.997170	1505.54	44.243	-0.0150	103.5_5	103.6_6	-1.5816	25.1_0	29.8_0
0.2086	0.996271	1507.63	44.160	-0.0149	103.5_2	103.7_5	-1.1784	27.1_0	33.7_7
±0.0001	±0.000005	±0.03	±0.004	±0.0001	±0.2	±0.2	±0.0001	±0.3	±0.2

Regression Models

$\rho = 0.000766m^2 - 0.015203m + 0.999404$

$\kappa_S \cdot 10^4 = 3.295m^2 - 2.553m + 44.549$

Table F.2: **1-Pentanol in 0.1188 m IOS 1923:** Measured density ρ and sound velocity u, calculated adiabatic compressibility coefficient κ_S, gradients $(\frac{\delta\rho}{\delta m})$, $(\frac{\delta\kappa_S}{\delta m})$, partial and apparent molar volume and compressibility. Regression models for determination of partial molar volume and compressibility given at the lower end.

m	ρ	u	κ_S	$(\frac{\delta\rho}{\delta m_2})$	V_ϕ	V_2	$(\frac{\delta\kappa_S}{\delta m})$	K_ϕ	K_2
$molkg^{-1}$	gcm^{-3}	ms^{-1}	$\cdot 10^4\ bar^{-1}$		cm^3mol^{-1}	cm^3mol^{-1}	$\cdot 10^4$	$cm^3mol^{-1}bar^{-1}$	$cm^3mol^{-1}bar^{-1}$
0.0000 †	1.001647	1500.32	44.352	-0.0158	-	103.7_6	-1.6035	-	30.0_1
0.0678 †	1.000602	1502.69	44.259	-0.0159	103.4_7	104.0_7	-1.2205	31.9_8	33.7_9
0.0830 †	1.000330	1503.23	44.239	-0.0159	103.9_5	104.1_5	-1.1345	32.3_8	34.6_5
0.1186 †	0.999763	1504.25	44.204	-0.0160	104.0_4	104.3_2	-0.9334	33.5_2	36.6_8
0.1289 †‡	0.999598	1504.58	44.192	-0.0160	104.0_7	104.3_6	-0.8755	33.5_6	37.2_6
0.1595 †‡	0.999113	1505.37	44.167	-0.0160	104.1_0	104.5_1	-0.6981	34.4_1	39.0_7
0.2309 ‡	0.997970	1506.80	44.134	-0.0161	104.2_6	104.8_5	-0.2398	36.5_7	43.8_2
±0.0001	±0.000005	±0.03	±0.004	±0.0001	±0.2	±0.2	±0.0001	±0.3	±0.2

Regression Models

$\rho = -0.000678m^2 - 0.015808m + 1.001653$

$\dagger\kappa_S \cdot 10^4 = 2.511m^2 - 1.560m + 44.352$

$\ddagger\kappa_S \cdot 10^4 = 3.211m^2 - 1.723m + 44.360$

Table F.3: **1-Pentanol in 0.1769 m IOS 1923:** Measured density ρ and sound velocity u, calculated adiabatic compressibility coefficient κ_S, gradients $(\frac{\delta\rho}{\delta m})$, $(\frac{\delta\kappa_S}{\delta m})$, partial and apparent molar volume and compressibility. Regression models for determination of partial molar volume and compressibility given at the lower end.

m	ρ	u	$\kappa_S \cdot 10^4$	$(\frac{\delta\rho}{\delta m_2})$	V_ϕ	V_2	$(\frac{\delta\kappa_S}{\delta m}) \cdot 10^4$	$K_\phi \cdot 10^4$	$K_2 \cdot 10^4$
$molkg^{-1}$	gcm^{-3}	ms^{-1}	bar^{-1}		cm^3mol^{-1}	cm^3mol^{-1}		$cm^3mol^{-1}bar^{-1}$	$cm^3mol^{-1}bar^{-1}$
0.0000 †	1.003723	1501.81	44.173	-0.0159	-	103.6_6	-0.9586	-	36.2_4
0.0542 †	1.002854	1503.24	44.127	-0.0162	103.8_3	104.0_5	-0.7418	37.3_7	38.4_8
0.0792 †‡	1.002443	1503.85	44.109	-0.0163	104.0_0	104.2_4	-0.6417	37.8_9	39.5_3
0.1166 †‡	1.001845	1504.66	44.088	-0.0164	104.0_1	104.5_2	-0.4398	38.6_4	41.6_5
0.1391 ‡	1.001464	1505.07	44.081	-0.0165	104.1_8	104.6_9	-0.3163	39.3_5	42.9_5
0.1589 ‡	1.001134	1505.42	44.075	-0.0160	104.2_7	104.8_4	-0.2075	39.8_3	44.1_1
0.2375 ‡	0.999822	1506.39	44.076	-0.0169	104.5_4	105.4_4	0.2241	42.0_1	48.7_6
±0.0001	±0.000005	±0.03	±0.004	±0.0001	±0.2	±0.2	±0.0001	±0.3	±0.2

Regression Models

$\rho = -0.002027m^2 - 0.015949m + 1.003723$

$\dagger\kappa_S \cdot 10^4 = 2.001m^2 - 0.959m + 44.173$

$\ddagger\kappa_S \cdot 10^4 = 2.745m^2 - 1.080m + 44.178$

Table F.4: **1-Pentanol in 0.2370 m IOS 1923:** Measured density ρ and sound velocity u, calculated adiabatic compressibility coefficient κ_S, gradients $(\frac{\delta\rho}{\delta m})$, $(\frac{\delta\kappa_S}{\delta m})$, partial and apparent molar volume and compressibility. Regression models for determination of partial molar volume and compressibility given at the lower end.

m	ρ	u	$\kappa_S \cdot 10^4$	$(\frac{\delta\rho}{\delta m_2})$	V_ϕ	V_2	$(\frac{\delta\kappa_S}{\delta m}) \cdot 10^4$	$K_\phi \cdot 10^4$	$K_2 \cdot 10^4$
$molkg^{-1}$	gcm^{-3}	ms^{-1}	bar^{-1}		cm^3mol^{-1}	cm^3mol^{-1}		$cm^3mol^{-1}bar^{-1}$	$cm^3mol^{-1}bar^{-1}$
0.0000 †	1.005833	1503.33	43.991	-0.0160	-	103.4_9	-0.6595	-	38.9_7
0.0631 †	1.004820	1504.61	43.961	-0.0165	103.6_1	104.1_8	-0.3085	40.7_4	42.7_1
0.0646 †	1.004792	1504.73	43.955*	-0.0165	103.6_8	104.2_0	-0.3002*	39.9_5^*	42.8_0^*
0.0967 †‡	1.004248	1505.16	43.954	-0.0168	104.0_1	104.5_6	-0.0779	41.8_3	45.1_7
0.1293 ‡	1.003687	1505.57	43.954	-0.0170	104.2_7	104.9_3	0.0856	42.9_6	46.9_8
0.1723 ‡	1.002966	1505.98	43.962	-0.0174	104.3_8	105.4_2	0.3015	44.1_9	49.3_9
0.2147 ‡	1.002217	1506.24	43.980	-0.0177	104.6_6	105.9_0	0.5142	45.4_8	51.8_0
±0.0001	±0.000005	±0.03	±0.004	±0.0001	±0.2	±0.2	±0.0001	±0.3	±0.2

Regression Models

$\rho = -0.003866m^2 - 0.016033m + 1.005837$

$\dagger\kappa_S \cdot 10^4 = 2.782m^2 - 0.659m + 43.991$

$\ddagger\kappa_S \cdot 10^4 = 2.507m^2 - 0.563m + 43.985$

$*$ - Not included in regression modelling

Table F.5: **2-Pentanol in 0.0581 m IOS 1923:** Measured density ρ and sound velocity u, calculated adiabatic compressibility coefficient κ_S, gradients $(\frac{\delta\rho}{\delta m})$, $(\frac{\delta\kappa_S}{\delta m})$, partial and apparent molar volume and compressibility. Regression models for determination of partial molar volume and compressibility given at the lower end.

m	ρ	u	$\kappa_S \cdot 10^4$	$(\frac{\delta\rho}{\delta m_2})$	V_ϕ	V_2	$(\frac{\delta\kappa_S}{\delta m}) \cdot 10^4$	$K_\phi \cdot 10^4$	$K_2 \cdot 10^4$
$molkg^{-1}$	gcm^{-3}	ms^{-1}	bar^{-1}		cm^3mol^{-1}	cm^3mol^{-1}		$cm^3mol^{-1}bar^{-1}$	$cm^3mol^{-1}bar^{-1}$
0.0000	0.999339	1498.64	44.555	-0.0147	-	102.9_8	-3.3604	-	12.2_6
0.0490	0.998594	1501.97	44.390	-0.0145	103.5_0	102.9_2	-3.2091	12.3_4	13.4_1
0.0782	0.998195	1503.72	44.305	-0.0144	102.9_7	102.8_8	-3.1191	13.6_6	14.1_2
0.1058	0.997794	1505.55	44.215	-0.0143	102.9_9	102.8_5	-3.0341	13.3_7	14.7_8
0.1319	0.997420	1507.15	44.137	-0.0142	102.9_7	102.8_1	-2.9534	13.7_9	15.4_2
0.1732	0.996850	1509.62	44.018	-0.0140	102.8_5	102.7_6	-2.8260	14.2_9	16.4_5
0.2274	0.996079	1512.76	43.870	-0.0138	102.9_0	102.6_8	-2.6589	15.0_0	17.8_2
±0.0001	±0.000005	±0.03	±0.004	±0.0001	±0.2	±0.2	±0.0001	±0.3	±0.2

Regression Models

$\rho = 0.002099m^2 - 0.014749m + 0.999330$

$\kappa_S \cdot 10^4 = 1.543m^2 - 3.360m + 44.554$

Table F.6: **2-Pentanol in 0.1176 m IOS 1923:** Measured density ρ and sound velocity u, calculated adiabatic compressibility coefficient κ_S, gradients $(\frac{\delta\rho}{\delta m})$, $(\frac{\delta\kappa_S}{\delta m})$, partial and apparent molar volume and compressibility. Regression models for determination of partial molar volume and compressibility given at the lower end.

m	ρ	u	$\kappa_S \cdot 10^4$	$(\frac{\delta\rho}{\delta m_2})$	V_ϕ	V_2	$(\frac{\delta\kappa_S}{\delta m}) \cdot 10^4$	$K_\phi \cdot 10^4$	$K_2 \cdot 10^4$
$molkg^{-1}$	gcm^{-3}	ms^{-1}	bar^{-1}		cm^3mol^{-1}	cm^3mol^{-1}		$cm^3mol^{-1}bar^{-1}$	$cm^3mol^{-1}bar^{-1}$
0.0000	1.001892	1500.64	44.323	-0.0154	-	103.3_0	-2.5392	-	20.4_4
0.0611	1.000951	1503.88	44.174	-0.0153	103.4_2	103.4_0	-2.3514	21.3_3	22.0_6
0.0678	1.000853	1504.22	44.158	-0.0153	103.3_5	103.4_1	-2.3307	21.4_1	22.2_4
0.0927	1.000481	1505.50	44.099	-0.0152	103.2_9	103.4_5	-2.2543	21.4_9	22.9_0
0.1235	0.999999	1507.00	44.032	-0.0152	103.4_5	103.5_0	-2.1595	22.0_8	23.7_4
0.1323	0.999871	1507.40	44.015	-0.0152	103.4_0	103.5_1	-2.1324	22.2_7	23.9_8
0.2185	0.998570	1511.36	43.841	-0.0150	103.4_7	103.6_5	-1.8676	23.3_7	26.3_8
±0.0001	±0.000005	±0.03	±0.004	±0.0001	±0.2	±0.2	±0.0001	±0.3	±0.2

Regression Models

$\rho = 0.000777m^2 - 0.015373m + 1.001892$

$\kappa_S \cdot 10^4 = 1.537m^2 - 2.539m + 44.323$

Table F.7: **2-Pentanol in 0.1772 m IOS 1923:** Measured density ρ and sound velocity u, calculated adiabatic compressibility coefficient κ_S, gradients $(\frac{\delta\rho}{\delta m})$, $(\frac{\delta\kappa_S}{\delta m})$, partial and apparent molar volume and compressibility. Regression models for determination of partial molar volume and compressibility given at the lower end.

m	ρ	u	$\kappa_S \cdot 10^4$	$(\frac{\delta\rho}{\delta m_2})$	V_ϕ	V_2	$(\frac{\delta\kappa_S}{\delta m}) \cdot 10^4$	$K_\phi \cdot 10^4$	$K_2 \cdot 10^4$
$molkg^{-1}$	gcm^{-3}	ms^{-1}	bar^{-1}		cm^3mol^{-1}	cm^3mol^{-1}		$cm^3mol^{-1}bar^{-1}$	$cm^3mol^{-1}bar^{-1}$
0.0000	1.004168	1502.29	44.125	-0.0162	-	103.8_4	-1.9272	-	26.6_3
0.0542	1.003310	1504.69	44.022	-0.0160	103.5_8	103.8_6	-1.7616	26.7_1	28.0_8
0.0666	1.003110	1505.23	43.999	-0.0160	103.6_6	103.8_7	-1.7239	26.8_2	28.4_2
0.0951	1.002644	1506.29	43.958	-0.0159	103.8_4	103.8_8	-1.6367	28.1_6	29.2_0
0.1248	1.002167	1507.48	43.909	-0.0158	103.8_9	103.8_9	-1.5460	28.4_0	30.0_2
0.1514	1.001756	1508.55	43.865	-0.0157	103.8_3	103.9_0	-1.4647	28.4_5	30.7_6
0.2357	1.000441	1511.58	43.747*	-0.0155	103.8_5	103.9_2	-1.2072	29.4_5^*	33.1_4^*
±0.0001	±0.000005	±0.03	±0.004	±0.0001	±0.2	±0.2	±0.0001	±0.3	±0.2

Regression Models

$\rho = 0.001459m^2 - 0.016190m + 1.004174$

$\kappa_S \cdot 10^4 = 1.527m^2 - 1.927m + 44.124$

$*$ - Not included in regression modelling

Table F.8: **2-Pentanol in 0.2348 m IOS 1923:** Measured density ρ and sound velocity u, calculated adiabatic compressibility coefficient κ_S, gradients $(\frac{\delta\rho}{\delta m})$, $(\frac{\delta\kappa_S}{\delta m})$, partial and apparent molar volume and compressibility. Regression models for determination of partial molar volume and compressibility given at the lower end.

m	ρ	u	$\kappa_S \cdot 10^4$	$(\frac{\delta\rho}{\delta m_2})$	V_ϕ	V_2	$(\frac{\delta\kappa_S}{\delta m}) \cdot 10^4$	$K_\phi \cdot 10^4$	$K_2 \cdot 10^4$
$molkg^{-1}$	gcm^{-3}	ms^{-1}	bar^{-1}		cm^3mol^{-1}	cm^3mol^{-1}		$cm^3mol^{-1}bar^{-1}$	$cm^3mol^{-1}bar^{-1}$
0.0000	1.006281	1503.69	43.951	-0.0163	-	103.7_3	-1.5322	-	30.3_6
0.0544	1.005405	1505.69	43.872	-0.0163	103.5_9	103.9_0	-1.3771	31.0_4	31.8_2
0.0810	1.004953	1506.68	43.834	-0.0163	103.9_2	103.9_9	-1.3013	31.2_7	32.5_4
0.1078	1.004522	1507.58	43.801	-0.0163	103.9_0	104.0_7	-1.2250	31.6_7	33.2_7
0.1364	1.004054	1508.46	43.770	-0.0163	103.9_5	104.1_6	-1.1435	32.3_3	34.0_7
0.1428	1.003958	1508.68	43.761	-0.0163	103.9_0	104.1_8	-1.1251	32.2_8	34.2_4
0.2085	1.002882	1510.68	43.692	-0.0163	104.0_5	104.3_9	-0.9379	33.1_5	36.0_9
±0.0001	±0.000005	±0.03	±0.004	±0.0001	±0.2	±0.2	±0.0001	±0.3	±0.2

Regression Models

$\rho = 0.000109m^2 - 0.016332m + 1.006283$

$\kappa_S \cdot 10^4 = 1.425m^2 - 1.532m + 43.950$

Table F.9: **3-Pentanol in 0.0594 m IOS 1923:** Measured density ρ and sound velocity u, calculated adiabatic compressibility coefficient κ_S, gradients $(\frac{\delta\rho}{\delta m})$, $(\frac{\delta\kappa_S}{\delta m})$, partial and apparent molar volume and compressibility. Regression models for determination of partial molar volume and compressibility given at the lower end.

m	ρ	u	$\kappa_S \cdot 10^4$	$(\frac{\delta\rho}{\delta m_2})$	V_ϕ	V_2	$(\frac{\delta\kappa_S}{\delta m}) \cdot 10^4$	$K_\phi \cdot 10^4$	$K_2 \cdot 10^4$
$molkg^{-1}$	gcm^{-3}	ms^{-1}	bar^{-1}		cm^3mol^{-1}	cm^3mol^{-1}		$cm^3mol^{-1}bar^{-1}$	$cm^3mol^{-1}bar^{-1}$
0.0000	0.999411	1498.70	44.548	-0.0131	-	101.3_6	-3.7908	-	7.2_2
0.0536	0.998734	1502.58	44.348	-0.0130	100.9_0	101.3_2	-3.6325	7.5_7	8.3_9
0.0684	0.998542	1503.60	44.296	-0.0129	101.0_1	101.3_1	-3.5889	8.0_1	8.7_2
0.1004	0.998114	1505.87	44.182	-0.0128	101.2_6	101.2_9	-3.4943	8.3_0	9.4_3
0.1188	0.997872	1507.39	44.103^*	-0.0127	101.3_2	101.2_8	-3.4400	7.2_8^*	9.8_3^*
0.1396	0.997607	1508.56	44.047	-0.0127	101.3_2	101.2_6	-3.3787	8.7_3	10.3_2
0.2068	0.996780	1512.96	43.827	-0.0125	101.2_1	101.2_0	-3.1803	9.5_0	11.8_7
±0.0001	±0.000005	±0.03	±0.004	±0.0001	±0.2	±0.2	±0.0001	±0.3	±0.2

Regression Models

$\rho = 0.001662m^2 - 0.013143m + 0.999420$

$\kappa_S \cdot 10^4 = 1.476m^2 - 3.791m + 44.548$

$*$ - Not included in regression modelling

Table F.10: **3-Pentanol in 0.1189 m IOS 1923:** Measured density ρ and sound velocity u, calculated adiabatic compressibility coefficient κ_S, gradients $(\frac{\delta\rho}{\delta m})$, $(\frac{\delta\kappa_S}{\delta m})$, partial and apparent molar volume and compressibility. Regression models for determination of partial molar volume and compressibility given at the lower end.

m	ρ	u	$\kappa_S \cdot 10^4$	$(\frac{\delta\rho}{\delta m_2})$	V_ϕ	V_2	$(\frac{\delta\kappa_S}{\delta m}) \cdot 10^4$	$K_\phi \cdot 10^4$	$K_2 \cdot 10^4$
$molkg^{-1}$	gcm^{-3}	ms^{-1}	bar^{-1}		cm^3mol^{-1}	cm^3mol^{-1}		$cm^3mol^{-1}bar^{-1}$	$cm^3mol^{-1}bar^{-1}$
0.0000	1.001680	1500.25	44.355	-0.0137	-	101.6_8	-3.0875	-	14.2_8
0.0573	1.000919	1503.77	44.181	-0.0136	101.3_2	101.6_7	-2.9348	14.4_4	15.4_5
0.0767	1.000639	1504.89	44.128	-0.0135	101.6_4	101.6_8	-2.8833	15.2_8	15.8_6
0.1081	1.000217	1506.75	44.038	-0.0134	101.6_4	101.6_8	-2.7994	15.4_5	16.5_2
0.1428	0.999754	1508.75	43.941	-0.0133	101.6_4	101.6_7	-2.7070	15.7_0	17.2_6
0.1474	0.999684	1509.03	43.928	-0.0133	101.7_1	101.6_7	-2.6949	15.7_3	17.3_6
0.2012	0.998986	1511.96	43.788	-0.0132	101.6_2	101.6_7	-2.5515	16.3_7	18.5_3
±0.0001	±0.000005	±0.03	±0.004	±0.0001	±0.2	±0.2	±0.0001	±0.3	±0.2

Regression Models

$\rho = 0.001369m^2 - 0.013717m + 1.001685$

$\kappa_S \cdot 10^4 = 1.332m^2 - 3.088m + 44.355$

Table F.11: **3-Pentanol in 0.1754 m IOS 1923:** Measured density ρ and sound velocity u, calculated adiabatic compressibility coefficient κ_S, gradients $(\frac{\delta\rho}{\delta m})$, $(\frac{\delta\kappa_S}{\delta m})$, partial and apparent molar volume and compressibility. Regression models for determination of partial molar volume and compressibility given at the lower end.

m	ρ	u	$\kappa_S \cdot 10^4$	$(\frac{\delta\rho}{\delta m_2})$	V_ϕ	V_2	$(\frac{\delta\kappa_S}{\delta m}) \cdot 10^4$	$K_\phi \cdot 10^4$	$K_2 \cdot 10^4$
$molkg^{-1}$	gcm^{-3}	ms^{-1}	bar^{-1}		cm^3mol^{-1}	cm^3mol^{-1}		$cm^3mol^{-1}bar^{-1}$	$cm^3mol^{-1}bar^{-1}$
0.0000	1.003650	1501.70	44.183	-0.0141	-	101.8_6	-2.5354	-	19.7_4
0.0547	1.002901	1504.58	44.047	-0.0139	101.5_0	101.7_8	-2.4282	19.9_2	20.5_0
0.0853	1.002464	1506.18	43.972	-0.0138	101.7_5	101.7_4	-2.3682	20.1_4	20.9_3
0.1169	1.002026	1507.76	43.899	-0.0136	101.7_8	101.6_9	-2.3063	20.4_9	21.3_9
0.1213	1.001970	1507.93	43.892	-0.0136	101.7_6	101.6_8	-2.2978	20.7_3	21.4_5
0.1757	1.001236	1510.63	43.767	-0.0134	101.7_2	101.6_0	-2.1912	20.9_5	22.2_4
0.2022	1.000889	1511.88	43.710	-0.0133	101.6_7	101.5_5	-2.1393	21.1_3	22.6_3
±0.0001	±0.000005	±0.03	±0.004	±0.0001	±0.2	±0.2	±0.0001	±0.3	±0.2

Regression Models

$\rho = 0.002141m^2 - 0.014132m + 1.003655$

$\kappa_S \cdot 10^4 = 0.980m^2 - 2.535m + 44.183$

Table F.12: **3-Pentanol in 0.2362 m IOS 1923:** Measured density ρ and sound velocity u, calculated adiabatic compressibility coefficient κ_S, gradients $(\frac{\delta\rho}{\delta m})$, $(\frac{\delta\kappa_S}{\delta m})$, partial and apparent molar volume and compressibility. Regression models for determination of partial molar volume and compressibility given at the lower end.

m	ρ	u	$\kappa_S \cdot 10^4$	$(\frac{\delta\rho}{\delta m_2})$	V_ϕ	V_2	$(\frac{\delta\kappa_S}{\delta m}) \cdot 10^4$	$K_\phi \cdot 10^4$	$K_2 \cdot 10^4$
$molkg^{-1}$	gcm^{-3}	ms^{-1}	bar^{-1}		cm^3mol^{-1}	cm^3mol^{-1}		$cm^3mol^{-1}bar^{-1}$	$cm^3mol^{-1}bar^{-1}$
0.0000	1.005754	1503.17	44.004	-0.0140	-	101.5_3	-2.0956	-	23.8_4
0.0458	1.005122	1505.23	43.911	-0.0141	101.3_5	101.7_6	-2.0071	24.3_6	24.6_3
0.0820	1.004595	1506.86	43.839	-0.0142	101.7_5	101.9_4	-1.9373	24.6_6	25.2_7
0.0950	1.004405	1507.44	43.814	-0.0143	101.8_3	102.0_1	-1.9122	24.7_2	25.5_0
0.1354	1.003839	1509.17	43.738	-0.0143	101.8_3	102.2_2	-1.8342	25.0_2	26.2_2
0.1763	1.003253	1510.90	43.664	-0.0144	101.9_2	102.4_3	-1.7551	25.3_1	26.9_6
0.1955	1.002965	1511.65	43.633	-0.0145	102.0_4	102.5_3	-1.7181	25.6_4	27.3_1
±0.0001	±0.000005	±0.03	±0.004	±0.0001	±0.2	±0.2	±0.0001	±0.3	±0.2

Regression Models

$\rho = -0.001118m^2 - 0.014041m + 1.005757$

$\kappa_S \cdot 10^4 = 0.966m^2 - 2.096m + 44.004$

Table F.13: **1-Hexanol in 0.0592 m IOS 1923*:** Measured density ρ and sound velocity u, calculated adiabatic compressibility coefficient κ_S, gradients $(\frac{\delta\rho}{\delta m})$, $(\frac{\delta\kappa_S}{\delta m})$, partial and apparent molar volume and compressibility. Regression models for determination of partial molar volume and compressibility given at the lower end.

m	ρ	u	$\kappa_S \cdot 10^4$	$(\frac{\delta\rho}{\delta m_2})$	V_ϕ	V_2	$(\frac{\delta\kappa_S}{\delta m}) \cdot 10^4$	$K_\phi \cdot 10^4$	$K_2 \cdot 10^4$
$molkg^{-1}$	gcm^{-3}	ms^{-1}	bar^{-1}		cm^3mol^{-1}	cm^3mol^{-1}		$cm^3mol^{-1}bar^{-1}$	$cm^3mol^{-1}bar^{-1}$
0.0000	0.999446	1498.78	44.541	-0.0179	-	120.1_5	-1.7950	-	35.5_6
0.0627	0.998293	1500.29	44.503*	-0.0191	120.7_9	121.6_2	0.0151	47.7^*_0	54.2^*_8
0.0709	0.998131	1500.46	44.500*	-0.0192	120.9_6	121.8_2	0.2512	48.0^*_6	56.7^*_4
0.0979	0.997618	1500.75	44.506	-0.0197	121.1_5	122.4_6	1.0302	50.3_0	64.9_3
0.1102	0.997370	1500.75	44.517	-0.0200	121.3_4	122.7_6	1.3863	51.8_2	68.7_1
0.1532	0.996465	1499.56	44.628*	-0.0208	122.0_9	123.8_1	2.6250	60.1_{6^*}	82.0^*_1
0.2228	0.994999	1496.82	44.858	-0.0221	122.7_6	125.5_4	4.6351	69.2_9	104.0_0
±0.0001	±0.000005	±0.03	±0.004	±0.0001	±0.2	±0.2	±0.0001	±0.3	±0.2

Regression Models

$\rho = -0.009457m^2 - 0.017898m + 0.999450$

$\kappa_S \cdot 10^4 = 14.430m^2 - 1.795m + 44.541$

$*$ - Not included in regression modelling

Table F.14: **1-Hexanol in 0.1176 m IOS 1923:** Measured density ρ and sound velocity u, calculated adiabatic compressibility coefficient κ_S, gradients $(\frac{\delta\rho}{\delta m})$, $(\frac{\delta\kappa_S}{\delta m})$, partial and apparent molar volume and compressibility. Regression models for determination of partial molar volume and compressibility given at the lower end.

m	ρ	u	$\kappa_S \cdot 10^4$	$(\frac{\delta\rho}{\delta m_2})$	V_ϕ	V_2	$(\frac{\delta\kappa_S}{\delta m}) \cdot 10^4$	$K_\phi \cdot 10^4$	$K_2 \cdot 10^4$
$molkg^{-1}$	gcm^{-3}	ms^{-1}	bar^{-1}		cm^3mol^{-1}	cm^3mol^{-1}		$cm^3mol^{-1}bar^{-1}$	$cm^3mol^{-1}bar^{-1}$
0.0000	1.001697	1500.45	44.343	-0.0184	-	120.3_1	-0.6711	-	46.6_5
0.0503	1.000744	1500.97	44.354*	-0.0193	121.0_1	121.4_8	0.4535	55.9^*_1	58.4^*_4
0.0882	1.000016	1501.19	44.373	-0.0200	121.2_0	122.3_7	1.3023	57.2_5	67.4_4
0.1052	0.999666	1501.11	44.393	-0.0203	121.4_9	122.7_8	1.6828	58.7_6	71.5_2
0.1330	0.999081	1500.57	44.451	-0.0209	121.9_2	123.4_5	2.3053	62.3_6	78.2_6
0.1544	0.998627	1498.73	44.581*	-0.0213	122.2_0	123.9_7	2.7832	69.9^*_0	83.5^*_8
0.1885	0.997910	1498.71	44.614	-0.0219	122.4_9	124.8_0	3.5466	69.0_3	91.9_0
±0.0001	±0.000005	±0.03	±0.004	±0.0001	±0.2	±0.2	±0.0001	±0.3	±0.2

Regression Models

$\rho = -0.009343m^2 - 0.018370m + 1.001697$

$\kappa_S \cdot 10^4 = 11.188m^2 - 0.671m + 44.343$

$*$ - Not included in regression modelling

Table F.15: **1-Hexanol in 0.1759 m IOS 1923:** Measured density ρ and sound velocity u, calculated adiabatic compressibility coefficient κ_S, gradients $(\frac{\delta\rho}{\delta m})$, $(\frac{\delta\kappa_S}{\delta m})$, partial and apparent molar volume and compressibility. Regression models for determination of partial molar volume and compressibility given at the lower end.

m	ρ	u	$\kappa_S \cdot 10^4$	$(\frac{\delta\rho}{\delta m_2})$	V_ϕ	V_2	$(\frac{\delta\kappa_S}{\delta m}) \cdot 10^4$	$K_\phi \cdot 10^4$	$K_2 \cdot 10^4$
$molkg^{-1}$	gcm^{-3}	ms^{-1}	bar^{-1}		cm^3mol^{-1}	cm^3mol^{-1}		$cm^3mol^{-1}bar^{-1}$	$cm^3mol^{-1}bar^{-1}$
0.0000	1.003840	1501.95	44.159	-0.0183	-	119.9_1	-0.0443	-	52.5_1
0.0641	1.002627	1502.26	44.195	-0.0198	120.7_1	121.7_7	1.1368	58.8_1	65.2_3
0.0710	1.002515	1502.22	44.202	-0.0200	120.4_7	121.9_7	1.2628	59.2_4	66.6_0
0.1083	1.001715	1501.82	44.261	-0.0209	121.5_1	123.0_8	1.9506	63.1_1	74.1_7
0.1307	1.001250	1501.32	44.311	-0.0215	121.7_6	123.7_6	2.3638	65.5_0	78.7_6
0.1587	1.000625	1500.52	44.386	-0.0222	122.2_8	124.6_1	2.8788	68.5_0	84.5_4
0.2182	0.999286	1498.13	44.587	-0.0236	123.0_6	126.4_3	3.9746	74.4_0	97.0_3
±0.0001	±0.000005	±0.03	±0.004	±0.0001	±0.2	±0.2	±0.0001	±0.3	±0.2

Regression Models

$\rho = -0.012285m^2 - 0.018262m + 1.003848$

$\kappa_S \cdot 10^4 = 9.210m^2 - 0.044m + 44.159$

Table F.16: **1-Hexanol in 0.2355 m IOS 1923:** Measured density ρ and sound velocity u, calculated adiabatic compressibility coefficient κ_S, gradients $(\frac{\delta\rho}{\delta m})$, $(\frac{\delta\kappa_S}{\delta m})$, partial and apparent molar volume and compressibility. Regression models for determination of partial molar volume and compressibility given at the lower end.

m	ρ	u	$\kappa_S \cdot 10^4$	$(\frac{\delta\rho}{\delta m_2})$	V_ϕ	V_2	$(\frac{\delta\kappa_S}{\delta m}) \cdot 10^4$	$K_\phi \cdot 10^4$	$K_2 \cdot 10^4$
$molkg^{-1}$	gcm^{-3}	ms^{-1}	bar^{-1}		cm^3mol^{-1}	cm^3mol^{-1}		$cm^3mol^{-1}bar^{-1}$	$cm^3mol^{-1}bar^{-1}$
0.0000	1.005969	1503.44	43.979	-0.0189	-	120.2_9	0.3951	-	56.8_3
0.0527	1.004986	1503.54	44.016	-0.0202	120.1_0	121.7_5	1.2634	59.8_9	66.2_3
0.0848	1.004296	1503.16	44.069	-0.0209	121.2_8	122.6_6	1.7913	63.9_9	72.0_5
0.1130	1.003651	1502.53	44.134	-0.0216	122.1_2	123.4_8	2.2565	67.5_7	77.2_4
0.1309	1.003310	1504.02	44.061*	-0.0220	121.9_7	123.9_8	2.5513	60.0_2^*	80.4_0^*
0.1759	1.002297	1500.78	44.296	-0.0230	122.6_4	125.3_0	3.2935	72.2_8	88.9_5
0.2047	1.001370*	1499.64	44.405	-0.0237	124.3_5^*	126.1_8^*	3.7667	75.9_2	94.4_3
±0.0001	±0.000005	±0.03	±0.004	±0.0001	±0.2	±0.2	±0.0001	±0.3	±0.2

Regression Models

$\rho = -0.011658m^2 - 0.018944m + 1.005982$

$\kappa_S \cdot 10^4 = 8.237m^2 + 0.395m + 43.977$

$*$ - Not included in regression modelling

Table F.17: **2-Hexanol in 0.0596 m IOS 1923:** Measured density ρ and sound velocity u, calculated adiabatic compressibility coefficient κ_S, gradients $(\frac{\delta\rho}{\delta m})$, $(\frac{\delta\kappa_S}{\delta m})$, partial and apparent molar volume and compressibility. Regression models for determination of partial molar volume and compressibility given at the lower end.

m	ρ	u	$\kappa_S \cdot 10^4$	$(\frac{\delta\rho}{\delta m_2})$	V_ϕ	V_2	$(\frac{\delta\kappa_S}{\delta m}) \cdot 10^4$	$K_\phi \cdot 10^4$	$K_2 \cdot 10^4$
$molkg^{-1}$	gcm^{-3}	ms^{-1}	bar^{-1}		cm^3mol^{-1}	cm^3mol^{-1}		$cm^3mol^{-1}bar^{-1}$	$cm^3mol^{-1}bar^{-1}$
0.0000	0.999430	1498.81	44.541	-0.0166	-	118.8_2	-2.4584	-	28.3_2
0.0607	0.998394	1501.81	44.409	-0.0174	119.4_3	119.8_8	-1.9461	31.3_1	33.6_3
0.0813	0.998031	1502.71	44.372	-0.0177	119.6_2	120.2_5	-1.7722	32.3_2	35.4_5
0.0985	0.997716	1503.58	44.334	-0.0179	119.8_5	120.5_6	-1.6272	32.1_9	36.9_8
0.1307	0.997154	1504.69	44.294	-0.0183	119.9_4	121.1_4	-1.3560	34.2_1	39.8_8
0.1750	0.996334	1505.70	44.271*	-0.0189	120.3_2	121.9_5	-0.9818	37.8_5^*	43.9_6^*
0.2278	0.995297	1505.42	44.333*	-0.0196	120.9_0	122.9_3	-0.5364	44.4_9^*	48.9_8^*
±0.0001	±0.000005	±0.03	±0.004	±0.0001	±0.2	±0.2	±0.0001	±0.3	±0.2

Regression Models

$\rho = -0.006716m^2 - 0.016561m + 0.999426$

$\kappa_S \cdot 10^4 = 4.218m^2 - 2.458m + 44.541$

$*$ - Not included in regression modelling

Table F.18: **2-Hexanol in 0.1193 m IOS 1923:** Measured density ρ and sound velocity u, calculated adiabatic compressibility coefficient κ_S, gradients $(\frac{\delta\rho}{\delta m})$, $(\frac{\delta\kappa_S}{\delta m})$, partial and apparent molar volume and compressibility. Regression models for determination of partial molar volume and compressibility given at the lower end.

m	ρ	u	$\kappa_S \cdot 10^4$	$(\frac{\delta\rho}{\delta m_2})$	V_ϕ	V_2	$(\frac{\delta\kappa_S}{\delta m}) \cdot 10^4$	$K_\phi \cdot 10^4$	$K_2 \cdot 10^4$
$molkg^{-1}$	gcm^{-3}	ms^{-1}	bar^{-1}		cm^3mol^{-1}	cm^3mol^{-1}		$cm^3mol^{-1}bar^{-1}$	$cm^3mol^{-1}bar^{-1}$
0.0000	1.001687	1500.49	44.341	-0.0176	-	119.5_8	-1.4244	-	38.8_0
0.0492	1.000804	1502.12	44.284	-0.0180	119.9_9	120.2_0	-1.0397	41.5_5	42.7_9
0.0644	1.000540	1502.64	44.265	-0.0182	119.9_0	120.4_0	-0.9212	41.3_0	44.0_3
0.0894	1.000075	1503.32	44.245	-0.0184	120.1_7	120.7_2	-0.7256	42.4_8	46.0_9
0.1196	0.999514	1504.07	44.226	-0.0186	120.3_7	121.1_1	-0.4891	43.6_5	48.6_1
0.1568	0.998821	1504.78	44.215	-0.0190	120.5_6	121.6_0	-1.1983	45.3_0	51.7_5
0.2042	0.997910	1505.16	44.232*	-0.0193	120.9_0	122.2_3	0.1718	48.1_8^*	55.8_2^*
±0.0001	±0.000005	±0.03	±0.004	±0.0001	±0.2	±0.2	±0.0001	±0.3	±0.2

Regression Models

$\rho = -0.004201m^2 - 0.017633m + 1.001686$

$\kappa_S \cdot 10^4 = 3.909m^2 - 1.424m + 44.341$

$*$ - Not included in regression modelling

Table F.19: **2-Hexanol in 0.1782 m IOS 1923:** Measured density ρ and sound velocity u, calculated adiabatic compressibility coefficient κ_S, gradients $(\frac{\delta\rho}{\delta m})$, $(\frac{\delta\kappa_S}{\delta m})$, partial and apparent molar volume and compressibility. Regression models for determination of partial molar volume and compressibility given at the lower end.

m	ρ	u	$\kappa_S \cdot 10^4$	$(\frac{\delta\rho}{\delta m_2})$	V_ϕ	V_2	$(\frac{\delta\kappa_S}{\delta m}) \cdot 10^4$	$K_\phi \cdot 10^4$	$K_2 \cdot 10^4$
$molkg^{-1}$	gcm^{-3}	ms^{-1}	bar^{-1}		cm^3mol^{-1}	cm^3mol^{-1}		$cm^3mol^{-1}bar^{-1}$	$cm^3mol^{-1}bar^{-1}$
0.0000	1.003831	1501.99	44.157	-0.0182	-	119.8_8	-0.8059	-	44.9_1
0.0476	1.002970	1503.17	44.126	-0.0186	119.8_3	120.4_4	-0.4626	46.3_1	48.5_1
0.0802	1.002355	1503.80	44.116	-0.0188	120.2_2	120.8_4	-0.2271	47.8_9	51.0_2
0.0991	1.001983	1504.11	44.114	-0.0190	120.5_1	121.0_7	-0.0910	48.8_3	52.4_9
0.1410	1.001189	1504.72	44.114	-0.0193	120.7_0	121.5_8	0.2110	50.1_5	55.7_7
0.1688	1.000651	1504.94	44.125	-0.0195	120.8_7	121.9_3	0.4114	51.3_9	57.9_8
0.2266	0.999512	1504.88	44.178*	-0.0199	121.2_2	122.6_5	0.8289	54.4_7^*	62.6_7^*
±0.0001	±0.000005	±0.03	±0.004	±0.0001	±0.2	±0.2	±0.0001	±0.3	±0.2

Regression Models

$\rho = -0.003791m^2 - 0.018227m + 1.003836$

$\kappa_S \cdot 10^4 = 3.607m^2 - 0.806m + 44.157$

$*$ - Not included in regression modelling

Table F.20: **2-Hexanol in 0.2367 m IOS 1923:** Measured density ρ and sound velocity u, calculated adiabatic compressibility coefficient κ_S, gradients $(\frac{\delta\rho}{\delta m})$, $(\frac{\delta\kappa_S}{\delta m})$, partial and apparent molar volume and compressibility. Regression models for determination of partial molar volume and compressibility given at the lower end.

m	ρ	u	$\kappa_S \cdot 10^4$	$(\frac{\delta\rho}{\delta m_2})$	V_ϕ	V_2	$(\frac{\delta\kappa_S}{\delta m}) \cdot 10^4$	$K_\phi \cdot 10^4$	$K_2 \cdot 10^4$
$molkg^{-1}$	gcm^{-3}	ms^{-1}	bar^{-1}		cm^3mol^{-1}	cm^3mol^{-1}		$cm^3mol^{-1}bar^{-1}$	$cm^3mol^{-1}bar^{-1}$
0.0000	1.005887	1503.48	43.980	-0.0185	-	119.8_9	-0.4942	-	47.8_1
0.0400	1.005161	1504.16	43.972	-0.0189	119.6_2	120.4_6	-0.1562	50.6_4	51.4_1
0.0598	1.004796	1504.49	43.969	-0.0191	119.7_5	120.7_5	0.0109	50.7_9	53.2_0
0.1111	1.003777	1505.07	43.979	-0.0196	120.6_0	121.5_1	0.4449	52.9_6	57.9_2
0.1326	1.003353	1505.19	43.991	-0.0199	120.7_7	121.8_3	0.6268	53.9_3	59.9_2
0.1505	1.002985	1505.28	44.002	-0.0200	120.9_8	122.1_0	0.7779	54.6_7	61.6_0
0.2468	1.001027	1504.76	44.119	-0.0210	121.6_3	123.5_7	1.5922	59.2_3	70.8_2
±0.0001	±0.000005	±0.03	±0.004	±0.0001	±0.2	±0.2	±0.0001	±0.3	±0.2

Regression Models

$\rho = -0.005032m^2 - 0.018523m + 1.005901$

$\kappa_S \cdot 10^4 = 4.226m^2 - 0.494m + 43.982$

Table F.21: **3-Hexanol in 0.0605 m IOS 1923:** Measured density ρ and sound velocity u, calculated adiabatic compressibility coefficient κ_S, gradients $(\frac{\delta\rho}{\delta m})$, $(\frac{\delta\kappa_S}{\delta m})$, partial and apparent molar volume and compressibility. Regression models for determination of partial molar volume and compressibility given at the lower end.

m	ρ	u	$\kappa_S \cdot 10^4$	$(\frac{\delta\rho}{\delta m_2})$	V_ϕ	V_2	$(\frac{\delta\kappa_S}{\delta m}) \cdot 10^4$	$K_\phi \cdot 10^4$	$K_2 \cdot 10^4$
$molkg^{-1}$	gcm^{-3}	ms^{-1}	bar^{-1}		cm^3mol^{-1}	cm^3mol^{-1}		$cm^3mol^{-1}bar^{-1}$	$cm^3mol^{-1}bar^{-1}$
0.0000	0.999456	1498.77	44.542	-0.0152	-	117.4_6	-3.2581	-	19.7_2
0.0494	0.998675	1501.81	44.396	-0.0157	118.1_6	118.1_7	-2.8520	22.9_5	23.7_6
0.0786	0.998216	1503.65	44.308	-0.0160	118.1_7	118.5_9	-2.6116	22.6_2	26.1_7
0.1035	0.997825	1504.96	44.248	-0.0163	118.2_0	118.9_5	-2.4068	23.9_2	28.2_6
0.1182	0.997578	1505.67	44.217	-0.0165	118.3_6	119.1_7	-2.2859	24.8_6	29.5_0
0.1691	0.996736	1507.61	44.141*	-0.0170	118.6_6	119.9_3	-1.8669	28.6_5^*	33.8_8^*
0.2056	0.996090	1508.15	44.138*	-0.0174	119.0_2	120.4_8	-1.5667	32.8_8^*	37.1_2^*
±0.0001	±0.000005	±0.03	±0.004	±0.0001	±0.2	±0.2	±0.0001	±0.3	±0.2

Regression Models

$\rho = -0.005319m^2 - 0.015208m + 0.999450$

$\kappa_S \cdot 10^4 = 4.113m^2 - 3.258m + 44.543$

$*$ - Not included in regression modelling

Table F.22: **3-Hexanol in 0.1190 m IOS 1923:** Measured density ρ and sound velocity u, calculated adiabatic compressibility coefficient κ_S, gradients $(\frac{\delta\rho}{\delta m})$, $(\frac{\delta\kappa_S}{\delta m})$, partial and apparent molar volume and compressibility. Regression models for determination of partial molar volume and compressibility given at the lower end.

m	ρ	u	$\kappa_S \cdot 10^4$	$(\frac{\delta\rho}{\delta m_2})$	V_ϕ	V_2	$(\frac{\delta\kappa_S}{\delta m}) \cdot 10^4$	$K_\phi \cdot 10^4$	$K_2 \cdot 10^4$
$molkg^{-1}$	gcm^{-3}	ms^{-1}	bar^{-1}		cm^3mol^{-1}	cm^3mol^{-1}		$cm^3mol^{-1}bar^{-1}$	$cm^3mol^{-1}bar^{-1}$
0.0000	1.001653	1500.30	44.354	-0.0160	-	117.9_6	-2.2115	-	30.2_4
0.0670	1.000549	1503.33	44.223	-0.0166	118.5_5	118.8_2	-1.6770	33.0_4	35.6_7
0.0781	1.000367	1503.75	44.207	-0.0167	118.5_7	118.9_6	-1.5890	33.6_7	36.5_8
0.0979	1.000045	1504.53	44.175	-0.0169	118.5_7	119.2_1	-1.4314	34.1_8	38.2_1
0.1300	0.999497	1505.68	44.132	-0.0172	118.7_9	119.6_3	-1.1751	35.3_9	40.8_8
0.1553	0.999062	1506.42	44.108	-0.0174	118.9_5	119.9_7	-0.9739	36.6_6	43.0_1
0.2035	0.998204	1507.10	44.106*	-0.0178	119.3_1	120.6_1	-0.5890	40.4_6^*	47.1_7^*
±0.0001	±0.000005	±0.03	±0.004	±0.0001	±0.2	±0.2	±0.0001	±0.3	±0.2

Regression Models

$\rho = -0.004437m^2 - 0.016006m + 1.001650$

$\kappa_S \cdot 10^4 = 3.986m^2 - 2.212m + 44.354$

$*$ - Not included in regression modelling

Table F.23: **3-Hexanol in 0.1711 m IOS 1923:** Measured density ρ and sound velocity u, calculated adiabatic compressibility coefficient κ_S, gradients $(\frac{\delta\rho}{\delta m})$, $(\frac{\delta\kappa_S}{\delta m})$, partial and apparent molar volume and compressibility. Regression models for determination of partial molar volume and compressibility given at the lower end.

m	ρ	u	$\kappa_S \cdot 10^4$	$(\frac{\delta\rho}{\delta m_2})$	V_ϕ	V_2	$(\frac{\delta\kappa_S}{\delta m}) \cdot 10^4$	$K_\phi \cdot 10^4$	$K_2 \cdot 10^4$
$molkg^{-1}$	gcm^{-3}	ms^{-1}	bar^{-1}		cm^3mol^{-1}	cm^3mol^{-1}		$cm^3mol^{-1}bar^{-1}$	$cm^3mol^{-1}bar^{-1}$
0.0000	1.003524	1501.61	44.193	-0.0160	-	117.7_5	-1.6816	-	35.2_8
0.0514	1.002669	1503.45	44.123	-0.0167	118.4_3	118.6_1	-1.2612	38.6_8	39.6_9
0.0754	1.002275	1504.31	44.090	-0.0170	118.4_2	119.0_2	-1.0656	38.5_5	41.7_6
0.0927	1.001996	1504.84	44.071	-0.0172	118.3_7	119.3_1	-0.9238	39.0_6	43.2_8
0.1217	1.001462	1505.62	44.049	-0.0176	118.9_0	119.8_2	-0.6875	40.5_7	45.8_3
0.1473	1.001022	1506.15	44.037	-0.0180	118.9_9	120.2_6	-0.4778	41.8_3	48.1_1
0.2155	0.999764	1506.81	44.054*	-0.0188	119.6_0	121.4_6	0.0791*	46.2_3^*	54.3_2^*
±0.0001	±0.000005	±0.03	±0.004	±0.0001	±0.2	±0.2	±0.0001	±0.3	±0.2

Regression Models

$\rho = -0.006494m^2 - 0.016041m + 1.003522$

$\kappa_S \cdot 10^4 = 4.086m^2 - 1.682m + 44.195$

$*$ - Not included in regression modelling

Table F.24: **3-Hexanol in 0.2377 m IOS 1923:** Measured density ρ and sound velocity u, calculated adiabatic compressibility coefficient κ_S, gradients $(\frac{\delta\rho}{\delta m})$, $(\frac{\delta\kappa_S}{\delta m})$, partial and apparent molar volume and compressibility. Regression models for determination of partial molar volume and compressibility given at the lower end.

m	ρ	u	$\kappa_S \cdot 10^4$	$(\frac{\delta\rho}{\delta m_2})$	V_ϕ	V_2	$(\frac{\delta\kappa_S}{\delta m}) \cdot 10^4$	$K_\phi \cdot 10^4$	$K_2 \cdot 10^4$
$molkg^{-1}$	gcm^{-3}	ms^{-1}	bar^{-1}		cm^3mol^{-1}	cm^3mol^{-1}		$cm^3mol^{-1}bar^{-1}$	$cm^3mol^{-1}bar^{-1}$
0.0000	1.005863	1503.24	43.995	-0.0166	-	118.0_3	-1.1998	-	40.0_0
0.0513	1.005005	1504.74	43.945	-0.0173	118.2_3	118.8_8	-0.7663	42.2_1	44.5_8
0.0751	1.004609	1505.30	43.929	-0.0176	118.2_3	119.2_7	-0.5646	43.2_2	46.7_3
0.1027	1.004092	1505.92	43.916	-0.0179	118.8_3	119.7_3	-0.3318	44.5_3	49.2_4
0.1345	1.003508	1506.45	43.911	-0.0183	119.1_6	120.2_7	-0.0627	46.0_7	52.1_8
0.1558	1.003113	1506.65	43.916*	-0.0186	119.3_6	120.6_4	0.1168*	47.3_7^*	54.1_6^*
0.2128	1.002054	1506.91	43.947*	-0.0193	119.7_2	121.6_2	0.5990*	50.3_8^*	59.5_6^*
±0.0001	±0.000005	±0.03	±0.004	±0.0001	±0.2	±0.2	±0.0001	±0.3	±0.2

Regression Models

$\rho = -0.006264m^2 - 0.016646m + 1.005871$

$\kappa_S \cdot 10^4 = 4.226m^2 - 1.200m + 43.995$

$*$ - Not included in regression modelling

Table F.25: **1-Pentanol in 0.0616 m IOS 2024:** Measured density ρ and sound velocity u, calculated adiabatic compressibility coefficient κ_S, gradients $(\frac{\delta\rho}{\delta m})$, $(\frac{\delta\kappa_S}{\delta m})$, partial and apparent molar volume and compressibility. Regression models for determination of partial molar volume and compressibility given at the lower end.

m	ρ	u	$\kappa_S \cdot 10^4$	$(\frac{\delta\rho}{\delta m_2})$	V_ϕ	V_2	$(\frac{\delta\kappa_S}{\delta m}) \cdot 10^4$	$K_\phi \cdot 10^4$	$K_2 \cdot 10^4$
$molkg^{-1}$	gcm^{-3}	ms^{-1}	bar^{-1}		cm^3mol^{-1}	cm^3mol^{-1}		$cm^3mol^{-1}bar^{-1}$	$cm^3mol^{-1}bar^{-1}$
0.0000	0.999777	1500.11	44.448	-0.0150	-	103.1_4	-2.8463	-	17.3_8
0.0560	0.998925	1503.25	44.300	-0.0152	103.5_0	103.5_1	-2.4421	19.4_7	21.2_9
0.0658	0.998773	1503.80	44.275	-0.0152	103.5_3	103.5_8	-2.3708	19.5_5	21.9_8
0.0943	0.998345	1505.18	44.212	-0.0153	103.5_1	103.7_6	-2.1651	20.7_9	24.0_1
0.1200	0.997957	1506.42	44.156	-0.0154	103.5_4	103.9_3	-1.9795	21.4_3	25.8_5
0.1554	0.997419	1507.88	44.095	-0.0155	103.6_0	104.1_7	-1.7235	22.9_6	28.4_2
0.1830	0.996996	1509.05	44.047	-0.0156	103.8_3	104.3_6	-1.5242	23.8_1	30.4_3
±0.0001	±0.000005	±0.03	±0.004	±0.0001	±0.2	±0.2	±0.0001	±0.3	±0.2

Regression Models

$\rho = -0.001698m^2 - 0.014967m + 0.999773$

$\kappa_S \cdot 10^4 = 3.612m^2 - 2.846m + 44.448$

$*$ - Not included in regression modelling

Table F.26: **1-Pentanol in 0.1122 m IOS 2024:** Measured density ρ and sound velocity u, calculated adiabatic compressibility coefficient κ_S, gradients $(\frac{\delta\rho}{\delta m})$, $(\frac{\delta\kappa_S}{\delta m})$, partial and apparent molar volume and compressibility. Regression models for determination of partial molar volume and compressibility given at the lower end.

m	ρ	u	$\kappa_S \cdot 10^4$	$(\frac{\delta\rho}{\delta m_2})$	V_ϕ	V_2	$(\frac{\delta\kappa_S}{\delta m}) \cdot 10^4$	$K_\phi \cdot 10^4$	$K_2 \cdot 10^4$
$molkg^{-1}$	gcm^{-3}	ms^{-1}	bar^{-1}		cm^3mol^{-1}	cm^3mol^{-1}		$cm^3mol^{-1}bar^{-1}$	$cm^3mol^{-1}bar^{-1}$
0.0000	1.001907	1502.55	44.209	-0.0159	-	103.8_2	-2.0494	-	25.4_4
0.0503	1.001093	1504.74	44.116	-0.0159	104.1_8	104.0_3	-1.6879	27.5_3	28.9_6
0.0787	1.000646	1505.85	44.071	-0.0160	104.0_8	104.1_6	-1.4840	28.3_3	30.9_7
0.1107	1.000137	1507.03	44.025	-0.0160	104.0_9	104.2_9	-1.2537	29.2_0	33.2_6
0.1316	0.999802	1507.66	44.003	-0.0160	104.1_4	104.3_8	-1.1039	30.1_7	34.7_6
0.1430	0.999629	1508.00	43.990	-0.0160	104.0_9	104.4_3	-1.0219	30.5_1	35.5_9
0.2152	0.998456	1509.66	43.945*	-0.0161	104.3_2	104.7_5	-0.5030	33.6_0^*	40.9_0^*
±0.0001	±0.000005	±0.03	±0.004	±0.0001	±0.2	±0.2	±0.0001	±0.3	±0.2

Regression Models

$\rho = -0.000484m^2 - 0.015894m + 1.001902$

$\kappa_S \cdot 10^4 = 3.593m^2 - 2.049m + 44.210$

$*$ - Not included in regression modelling

Table F.27: **1-Pentanol in 0.1508 m IOS 2024:** Measured density ρ and sound velocity u, calculated adiabatic compressibility coefficient κ_S, gradients $(\frac{\delta\rho}{\delta m})$, $(\frac{\delta\kappa_S}{\delta m})$, partial and apparent molar volume and compressibility. Regression models for determination of partial molar volume and compressibility given at the lower end.

m	ρ	u	$\kappa_S \cdot 10^4$	$(\frac{\delta\rho}{\delta m_2})$	V_ϕ	V_2	$(\frac{\delta\kappa_S}{\delta m}) \cdot 10^4$	$K_\phi \cdot 10^4$	$K_2 \cdot 10^4$
$molkg^{-1}$	gcm^{-3}	ms^{-1}	bar^{-1}		cm^3mol^{-1}	cm^3mol^{-1}		$cm^3mol^{-1}bar^{-1}$	$cm^3mol^{-1}bar^{-1}$
0.0000	1.003441	1504.34	44.037	-0.0158	-	103.5_3	-1.5236	-	30.4_1
0.0601	1.002472	1506.42	43.958	-0.0162	103.9_6	104.1_2	-1.0943	32.5_9	34.8_0
0.1048	1.001741	1507.69	43.916	-0.0165	104.1_4	104.5_7	-0.7750	34.2_1	38.1_2
0.1124	1.001645	1507.83	43.912	-0.0165	103.9_1	104.6_4	-0.7209	34.5_6	38.6_8
0.1219	1.001461	1508.10	43.904	-0.0166	104.1_9	104.7_4	-0.6534	34.9_1	39.3_9
0.1484	1.001021	1508.71	43.888	-0.0168	104.3_0	105.0_1	-0.4639	35.7_8	41.3_9
0.1670	1.000710	1509.04	43.882	-0.0169	104.3_7	105.2_0	-0.3306	36.5_9	42.8_1
±0.0001	±0.000005	±0.03	±0.004	±0.0001	±0.2	±0.2	±0.0001	±0.3	±0.2

Regression Models

$\rho = -0.003293m^2 - 0.015787m + 1.003439$

$\kappa_S \cdot 10^4 = 3.571m^2 - 1.524m + 44.037$

$*$ - Not included in regression modelling

Table F.28: **1-Pentanol in 0.1773 m IOS 2024:** Measured density ρ and sound velocity u, calculated adiabatic compressibility coefficient κ_S, gradients $(\frac{\delta\rho}{\delta m})$, $(\frac{\delta\kappa_S}{\delta m})$, partial and apparent molar volume and compressibility. Regression models for determination of partial molar volume and compressibility given at the lower end.

m	ρ	u	$\kappa_S \cdot 10^4$	$(\frac{\delta\rho}{\delta m_2})$	V_ϕ	V_2	$(\frac{\delta\kappa_S}{\delta m}) \cdot 10^4$	$K_\phi \cdot 10^4$	$K_2 \cdot 10^4$
$molkg^{-1}$	gcm^{-3}	ms^{-1}	bar^{-1}		cm^3mol^{-1}	cm^3mol^{-1}		$cm^3mol^{-1}bar^{-1}$	$cm^3mol^{-1}bar^{-1}$
0.0000	1.004476	1505.50	43.923	-0.0170	-	104.5_9	-1.1207	-	34.7_8
0.0619	1.003438	1507.31	43.864	-0.0168	104.4_9	104.6_0	-0.7404	36.2_0	38.4_6
0.0958	1.002856	1508.06	43.845	-0.0167	104.6_8	104.6_0	-0.5318	37.7_6	40.5_2
0.1103	1.002632	1508.37	43.837	-0.0166	104.5_1	104.6_0	-0.4425	38.0_2	41.4_0
0.1303	1.002289	1508.76	43.830	-0.0165	104.6_1	104.6_0	-0.3196	38.7_0	42.6_2
0.1550	1.001885	1509.19	43.822	-0.0165	104.6_0	104.6_0	-0.1680	39.3_4	44.1_4
0.2057	1.001057	1509.69	43.829*	-0.0163	104.5_9	104.6_0	0.1434*	41.2_8^*	47.3_0^*
±0.0001	±0.000005	±0.03	±0.004	±0.0001	±0.2	±0.2	±0.0001	±0.3	±0.2

Regression Models

$\rho = 0.001709m^2 - 0.016985m + 1.004477$

$\kappa_S \cdot 10^4 = 3.073m^2 - 1.121m + 43.923$

$*$ - Not included in regression modelling

Table F.29: **3-Pentanol in water:** Measured density ρ and sound velocity u, calculated adiabatic compressibility coefficient κ_S, gradients $(\frac{\delta\rho}{\delta m})$, $(\frac{\delta\kappa_S}{\delta m})$, partial and apparent molar volume and compressibility. Regression models for determination of partial molar volume and compressibility given at the lower end. Values at infinite alcohol dilution are not measured.

m	ρ	u	$\kappa_S \cdot 10^4$	$(\frac{\delta\rho}{\delta m_2})$	V_ϕ	V_2	$(\frac{\delta\kappa_S}{\delta m}) \cdot 10^4$	$K_\phi \cdot 10^4$	$K_2 \cdot 10^4$
$molkg^{-1}$	gcm^{-3}	ms^{-1}	bar^{-1}		cm^3mol^{-1}	cm^3mol^{-1}		$cm^3mol^{-1}bar^{-1}$	$cm^3mol^{-1}bar^{-1}$
0.0000	0.997048	1496.69	44.773	-0.0128	-	101.2_4	-4.6744	-	-1.5_5
0.0484	0.996436	1500.99	44.545	-0.0124	101.1_8	101.0_2	-4.5765	-2.3_0	-1.1_3
0.0792	0.996059	1503.61	44.407	-0.0122	101.0_8	100.8_7	-4.5144	-1.6_3	-0.8_5
0.0964	0.995855	1504.99	44.334	-0.0121	100.9_8	100.7_9	-4.4796	-1.0_3	-0.6_8
0.1741	0.994933	1511.57	43.989	-0.0115	100.8_5	100.4_1	-4.3227	-0.9_1	0.0_6
0.2426	0.994163	1517.21	43.697	-0.0110	100.6_7	100.0_7	-4.1843	-0.6_5	0.7_4
± 0.0001	± 0.000005	± 0.03	± 0.004	± 0.0001	± 0.2	± 0.2	± 0.0001	± 0.3	± 0.2

Regression Models

$\rho = 0.003541m^2 - 0.012750m + 0.997047$

$\kappa_S \cdot 10^4 = 1.010m^2 - 4.674m + 44.772$

Table F.30: **3-Hexanol in water:** Measured density ρ and sound velocity u, calculated adiabatic compressibility coefficient κ_S, gradients $(\frac{\delta\rho}{\delta m})$, $(\frac{\delta\kappa_S}{\delta m})$, partial and apparent molar volume and compressibility. Regression models for determination of partial molar volume and compressibility given at the lower end. Values at infinite alcohol dilution are not measured.

m	ρ	u	$\kappa_S \cdot 10^4$	$(\frac{\delta\rho}{\delta m_2})$	V_ϕ	V_2	$(\frac{\delta\kappa_S}{\delta m}) \cdot 10^4$	$K_\phi \cdot 10^4$	$K_2 \cdot 10^4$
$molkg^{-1}$	gcm^{-3}	ms^{-1}	bar^{-1}		cm^3mol^{-1}	cm^3mol^{-1}		$cm^3mol^{-1}bar^{-1}$	$cm^3mol^{-1}bar^{-1}$
0.0000	0.997048	1496.69	44.773	-0.0146	-	117.1_6	-5.4968	-	-2.6_7
0.0526	0.996289	1501.98	44.492	-0.0141	117.0_8	116.8_3	-5.2441	-1.5_5	-0.9_4
0.0781	0.995942	1504.55	44.356	-0.0139	116.8_5	116.6_7	-5.1213	-1.7_8	-0.0_8
0.1083	0.995519	1507.39	44.208	-0.0136	116.8_6	116.4_8	-4.9762	-0.7_6	0.9_5
0.1364	0.995146	1510.06	44.068	-0.0133	116.7_3	116.2_9	-4.8416	-0.5_3	1.9_2
$\pm$0.0001	$\pm$0.000005	$\pm$0.03	$\pm$0.004	$\pm$0.0001	$\pm$0.2	$\pm$0.2	$\pm$0.0001	$\pm$0.3	$\pm$0.2

Regression Models

$\rho = 0.004760m^2 - 0.014595m + 0.997048$

$\kappa_S \cdot 10^4 = 2.402m^2 - 5.497m + 44.774$